Regulation and function of the Na+/H+ exchanger NHE1 in endothelial cells

Dissertation

To Fulfill the Requirements for the Degree of

"Doctor of Philosophy" (Ph.D.)

Submitted to the Council of the Faculty of Medicine of the

Friedrich Schiller University Jena

by

Master of Pharmacy **Nderim Kryeziu**

born on 03.05 1987, in Prishtina, Kosova

Jena, February 2016

Gutachter:

1. Prof. Dr. Regine Heller, Friedrich-Schiller-Universität, Jena

2. Prof. Dr. Christian Hübner, Friedrich-Schiller-Universität, Jena

3. Prof. Dr. Heimo Ehmke, UNI-Klinikum Hamburg-Eppendorf, Hamburg

Tag der öffentlichen Verteidigung: 04.10.2016

List of contents

List of abbreviations

AE	Anion exchanger
AKT	Protein kinase B
AMPK	AMP-activated protein kinase
bFGF	Basic fibroblast growth factor
BSA	Bovine serum albumin
CsiR	scRNA transfected HUVEC
DLL4	Delta-like protein 4
DMEM	Dulbecco`s modified Eagle`s Medium
DTT	DL-Dithiothreitol
ECL	Enhanced chemiluminescence technique
ECM	Extracellular matrix
EM	Endothelial mitogen
eNOS	Endothelial nitric oxide synthase
ERM	Ezrin, radixin, moesin proteins
FAK	Focal adhesion kinase
FCS	Fetal calve serum
HBSS	Hank`s balanced salt solution
HEPES	4-(2-hydroxyethyl)-1-piperazine ethane sulfonic acid
HIF	Hypoxia-inducible factors
HSA	Human serum albumin
HUVEC	Human umbilical vein endothelial cells
M199	Medium 199
MAPK	Mitogen-activated proteinkinase
MLEC	Mouse lung endothelial cells
NBC	Na^+/HCO_3^- cotransporter
NBCn1	Na^+/HCO_3^- cotransporter NBCn1
NCBE	Na^+-driven Cl^-/HCO_3^- exchanger
NHE	Na^+/H^+ exchanger
NHE1	Na^+/H^+ exchanger isoform 1
***Nhe1*$^{-/-}$**	*Nhe1* knockout
NO	Nitric oxide
NsiR	NHE1 siRNA transfected HUVEC
PAI-1	Plasminogen activator inhibitor-1
pH_e	Extracellular pH
pH_i	Intracellular pH
ROS	Reactive oxygen species
S1P	Sphingosine-1-phosphate
Saint-Red	Synthetic, Amphiphilic, Interactive – RNAi-Enhanced Delivery
SDS	Sodium dodecyl sulfate
SDS-PAGE	SDS-Polyacrylamide gel electrophoresis
SEM	Standard Error of the Mean
siRNA	Small interfering RNA
TEMED	N,N,N,N-Tetraethyl ethylene diamine
TGFα	Transforming growth factor α
Tris	Tris(hydroxymethyl)aminomethane
VEGF	Vascular endothelial growth factor
VEGFR2	VEGF receptor 2
EIPA	5-(N-Ethyl-N-isopropyl)amiloride

Summary

Na^+/H^+ exchanger NHE1 is a ubiquitously expressed plasma membrane protein that maintains intracellular pH and cell volume by exchanging extracellular Na^+ for intracellular H^+. Moreover, NHE1 is a scaffold protein that anchors actin filaments and modulates a variety of cellular functions. It is described to play role in proliferation, survival and migration of different cell types, but its role in endothelial function is not completely understood. To study NHE1 in endothelial and vascular functions, appropriate mice models are required. However, the use of the constitutive *Nhe1* knockout (*Nhe1*$^{-/-}$) mice for *in vivo* studies is limited since they grow slowly after birth and develop neurological disorders that lead to early death within 3-4 weeks.

The current work was aimed to examine NHE1's involvement in endothelial cell proliferation, survival and migration, and particularly to analyze if these integrate into complex endothelium functions such as angiogenesis. *In vitro* experiments were performed with primary human umbilical vein endothelial cells after silencing NHE1 with small interfering RNA, as well as with primary *Nhe1*$^{-/-}$ mouse lung endothelial cells. To obtain an appropriate model for *in vivo* studies, endothelial cell-specific *Nhe1*$^{-/-}$ mice were generated using the Cre/loxP-system by mating *Nhe1*-floxed mice with the *VE-Cadherin-Cre*-recombinase transgenic mice. The efficiency and specificity of the knockout was confirmed by western blot and flow cytometry analysis of cultured mouse lung endothelial cells. Angiogenesis was studied *in vivo* in endothelial cell-specific as well as in constitutive *Nhe1*$^{-/-}$ mice employing the Matrigel plug assay.

Intracellular pH measurements confirmed that NHE1 is the most important acid-extruder responsible for the pH recovery after cytoplasmic acidification of endothelial cells even in bicarbonate-buffered solution. Accordingly, when NHE1 was knocked out, steady-state pH_i and recovery after cytoplasmic acidification were drastically reduced in bicarbonate-free buffered solutions, and pH_i recovery was significantly decreased even in the presence of bicarbonate.

Knockdown of NHE1 reduced endothelial cell proliferation by 35% probably by arresting cells in the G_0/G_1 phase of the cell cycle, whereas survival of endothelial cells was not affected. Silencing of NHE1 inhibited endothelial cell migration induced by sphingosine-1-phosphate by 32% probably due to impaired motility and ability to orient towards the gradient of the stimulant. In line with this, NHE1 was localized at plasma membrane protrusions in migrating endothelial cells suggesting a role in cell migration.

In agreement with a proliferative and migratory role of NHE1, its involvement in VEGF-induced angiogenesis was demonstrated *in vitro* and *in vivo*. Downregulation of NHE1 significantly impaired VEGF-induced spheroid sprouting by 56%. Moreover, a Matrigel plug assay in constitutive *Nhe1*$^{-/-}$ mice revealed an inhibition of VEGF-induced angiogenesis by 22% compared to wild type littermates.

However, follow-up experiments with endothelial cell-specific *Nhe1*$^{-/-}$ mice were not conclusive due to unexpected variations in the VEGF-induced angiogenesis in control animals and shall be further investigated.

Together, these findings portray NHE1 as a player in angiogenesis. Results of this thesis also show that NHE1 is upregulated during hypoxia (1% O_2) through HIF2α-dependent mechanisms, which could potentiate NHE1's role in ischemia-induced angiogenesis. Therefore, *in vivo* models like hind limb ischemia could yet highlight the role of NHE1 in angiogenesis. The generated endothelial cell-specific *Nhe1*$^{-/-}$ mice are a valuable tool for future *in vivo* studies.

Zusammenfassung

Der Na^+/H^+-Austauscher NHE1 ist ein ubiquitär exprimiertes Plasmamembranprotein, das den intrazellulären pH-Wert (pH_i) und das Zellvolumen reguliert, in dem es intrazelluläres H^+ durch extrazelluläres Na^+ ersetzt. Des Weiteren ist NHE1 ein *Scaffold*-Protein, das Aktinfilamente verankert und dadurch eine Vielzahl zellulärer Funktionen reguliert. NHE1 spielt in verschiedenen Zelltypen eine Rolle bei Proliferation, Überleben und Migration, aber seine Rolle in Endothelzellen ist noch nicht vollständig verstanden. Um NHE1 im Zusammenhang mit endothelialen und vaskulären Funktionen untersuchen zu können, sind geeignete Mausmodelle vonnöten. Die Verwendung von konstitutiven *Nhe1-knockout* (*Nhe1*$^{-/-}$)-Mäusen für *in-vivo*-Studien ist allerdings begrenzt, da sie nach der Geburt langsam wachsen und neurologische Funktionsstörungen ausbilden, die innerhalb von 3-4 Wochen zu einem frühen Tod führen.

Ziel der vorliegenden Arbeit war es, die Bedeutung von NHE1 für endotheliale Funktionen wie Proliferation, Überleben und Migration zu untersuchen und dabei insbesondere zu analysieren, ob komplexe Prozesse wie die Angiogenese beeinflusst werden. *In-vitro*-Experimente wurden mit primären *human umbilical vein endothelial cells* (HUVEC), in denen NHE1 mit *small interfering* RNA (siRNA) herunterreguliert wurde, und in primären Nhe1$^{-/-}$ Endothelzellen aus der Mauslunge durchgeführt. Um ein geeignetes Modell für *in-vivo*-Studien zu erhalten, wurden mit Hilfe des Cre/loxP-Systems endothelzellspezifische *Nhe1*$^{-/-}$-Mäuse generiert, indem *Nhe1*-gefloxte Mäuse mit *VE-Cadherin-Cre*-Rekombinase-transgenen Mäusen verpaart wurden. Die Effizienz und Spezifität des *knockouts* wurde in Western-Blot- und Durchflusszytometrie-Analysen von aus den Mäusen präparierten primären Endothelzellen bestätigt. Die Angiogenese wurde *in vivo* mit Hilfe des Matrigel-Plug-Assays sowohl in endothelzellspezifischen als auch in konstitutiven *Nhe1*$^{-/-}$-Mäusen untersucht.

Messungen des pH_i bestätigten, dass NHE1 der wichtigste Protonen-Exporter für die Erholung des pH-Werts nach zytoplasmatischer Ansäuerung von Endothelzellen ist, unabhängig davon, ob Bicarbonat im Puffersystem vorhanden ist. Wurde NHE1 depletiert, waren sowohl der basale pH_i als auch die Erholung des pH_i-Werts nach Ansäuerung in Bicarbonat-freien Pufferlösungen drastisch reduziert. Die pH_i-Erholung war auch in Anwesenheit von Bicarbonat noch signifikant vermindert.

Der *knockdown* von NHE1 verminderte die endotheliale Proliferation um 35 %, vermutlich aufgrund eines Zellzyklusarrests in der G_0/G_1-Phase. Dagegen war das Überleben der Endothelzellen nicht beeinflusst. Die Sphingosin-1-Phosphat (S1P)-induzierte Endothelzellmigration wurde durch die Herunterregulierung von NHE1 um 32 % reduziert, was auf einer eingeschränkten Zellmotilität und der verminderten Fähigkeit, sich entlang des Stimulus-Gradienten auszurichten, beruht. NHE1 ist an Fortsätzen der Plasmamembran migrierender Zellen lokalisiert, was für eine Beteiligung an der Migration spricht.

In Übereinstimmung mit der Rolle von NHE1 bei der Proliferation und Migration konnte die Beteiligung von NHE1 bei der *vascular endothelial growth factor* (VEGF)-induzierten Angiogenese *in vitro* und *in vivo* gezeigt werden. Die Herunterregulierung von NHE1 hemmte die VEGF-induzierte Sprossbildung signifikant um 56 %. Im Matrigel-Plug-Assay in konstitutiven *Nhe1*$^{-/-}$-Mäusen wurde die VEGF-induzierte Angiogenese im Vergleich zu den Wildtyp-Geschwistern um 22 % gehemmt. Jedoch waren nachfolgende Experimente in endothelzellspezifischen *Nhe1*$^{-/-}$-Mäusen aufgrund unerwarteter Schwankungen der VEGF-induzierten Angiogenese in Kontrolltieren nicht eindeutig und müssen weiter untersucht werden.

Zusammengefasst stellen die Daten dieser Arbeit NHE1 als ein Mediator der Angiogenese dar. Die Ergebnisse zeigen auch, dass NHE1 unter Hypoxie (1 % O_2) in einem HIF2α-abhängigen Weg hochreguliert wird, was auf eine Rolle von NHE1 bei Ischämie-induzierter Angiogenese hindeutet. *In-vivo*-Modelle wie das *hind limb*-Ischämiemodell könnten die Rolle von NHE1 bei der Angiogenese weiter herausstellen. Die generierten endothelzellspezifischen *Nhe1*$^{-/-}$-Mäuse sind ein wertvolles Modell für weitere *in-vivo*-Studien.

Përmbledhje (in albanian)

NHE1 është një transportues jonik që gjendet në membranën qelizore, i cili përmes këmbimit të një joni Na^+ jashtëqelizorë me një jon H^+ brendaqelizorë luan një rol të rëndësishëm në ruajtjen e pH-së dhe vëllimit të qelizës. Gjithashtu, kjo proteinë në sajë të kontaktit fizik me filamentet e aktinës, që janë pjesë e skeletit qelizorë, mund të ndikojë në një mori funksionesh qelizore. Hulumtimet shkencore kanë treguar përfshirjen e tij në shumimin, mbijetesën dhe migrimin e shumë lloje qelizash, por ende nuk njihet mirë funksioni i këtij transportuesi në qelizat endoteliale. Për të kuptuar më shumë rreth rolit të këtij transportuesi në sistemin kardiovaskularë, është i nevojshëm përdorimi i minjve të modifikuara gjenetikisht. Megjithatë, në rastin e transportuesit NHE1, përdorimi i minjve, në të cilët gjeni që kodon këtë protein është i çaktivizuar në të gjitha indet (*Nhe1*$^{-/-}$), është i kufizuar pasi minjtë e këtij tipi karakterizohen me ngecje në zhvillim dhe çrregullime nervore që çojne në vdekje të hershme brenda 3-5 javësh pas lindjes.

Me qëllim të ekzaminimit të rolit të mundshëm të këtij transportuesi jonik në rritjen, mbijetesën, mirgrimin e qelizave endoteliale, si dhe analizimi i proceseve komplekse vaskulare si angiogjeneza, gjatë këtij projekti janë kryer eksperimenteve *in vitro* me qeliza endoteliale të njeriut nga kordoni umbilikal dhe qeliza endoteliale nga mushkritë e minjve. Në rastin e qelizave humane, manipulipi në shprehjen e proteinës është bërë përmes ARN-ve të shkurtra ndërhyrëse, ndërsa në rastin e qelizave nga minjtë, ato origjinojnë direkt nga gjenotipi *Nhe1*$^{-/-}$. Përvec këtyre, për të studiuar përfshirjen e NHE1 në procesin e angjiogjenezës brenda organizmit (*in vivo*) ishte i novojshëm gjenerimi i modelit në minjë, ku gjeni është çaktivizuar specifikisht vetëm në qelizat endoteliale. Kjo u arrit përmes sistemit Cre/loxP pas kryqëzimit të minjëve transgjenik *Nhe1-flox* me minjë *VE-Cadherin-Cre*-recombinase. Më tej, efikasiteti dhe specificiteti i ndryshimit gjenetik të gjenit *Nhe1* u vërtetua përmes metodave Western blot dhe Flow cytometry. Sudimi i procesit të angjiogjenezës brenda organizmit u realizua duke përdorur metodën Matrigel plug assay.

Të dhënat mbi rregullimin pH-së brendaqelizore nxorën në pah rolin e rëndësishëm të këtij transportuesi në qelizat endoteliale. Në mungesë të proteinës NHE1, qelizat e kanë të kufizuar aftësinë për të mbajtur pH-në bazale në vlerat normale, e sidomos aftësinë për të rikuperuar pH-në citoplazmatike pas acidifikimit.

Përmes eksperimenteve *in vitro* gjithashtu u konstatua se mungesa e NHE1 çon në reduktim të shumimit qelizorë për gati 35%, me gjasë për shkak të frenimit të kalimit të qelizave nga faza G_o në fazën G_1 te ciklit qelizorë. Eksperimente të ngjashme treguan se NHE1 nuk ndikon në mbijetesën qelizore, por ai gjithsesi ndikon në lëvizjen ose migrimin qelizorë. Mungesa e proteinës NHE1 u shoqërua me reduktim të migrimit qelizorë për afërsisht 32% nën stimulimin me sfingosinë-

monophosphatit. Në përputhje me këtë, përmes ngjyrimit citokimik me antitrupa, NHE1 u gjet të vendoset tek protruzionet e qelizave migruese.

Marrë parasysh rolin e proteinës NHE1 në shumimin dhe migrimin e qelizave endoteliale, përmes eksperimenteve *in vitro* dhe *in vivo* kjo protein është gjetur të jetë e rëndësishme gjatë angjiogjenezës pas stimulimit me VEGF. Ulja e nivelit të proteinës NHE1 rezultoi në zvogëlim të angjigjenzës për afro 56% *in vitro* (spheroid assay). *In vivo*, mungesa e plotë e NHE1 në të gjitha indet e miut rezultoi në inhibim të angjiogjenzës për rreth 22% (Matrigel plug assay). Megjithatë, angjigjeneza në minjt ku *Nhe1* ishte çaktivizuar specifikisht në qelizat endoteliale duhet të analizohet më tutje, për arsye se VEGF nuk arriti të stimulojë angjiogjenezën as në minjët kontroll (wildtype).

Si përfundim, NHE1 duket të jetë një faktor i rëndësishëm gjatë angjiogjenezës. Eksperimente të tjera gjatë këtij projekti tregojnë se shprehja e NHE1 në nivelin proteinorë rritet në kushte të hipoksisë (1% O_2) përmes mekanizmave të varura nga HIF2α. Prandaj, Hindlimb ischemia si një model më fiziologjik për të studiuar angjiogjenezën *in vivo*, do të mund të nxirrte më shumë në pah rëndësinë e NHE1 gjatë këtij procesi. Në përgjithësi, minjtë e krijuar gjatë këtij projekti, ku *Nhe1* është inaktivizuar specifikisht në qelizat endoteliale, janë një model i vlefshëm për studime të ndryshme *in vivo*.

1 Introduction

1.1 Endothelium and angiogenesis

Endothelial cells [2, 3] form a monolayer, which constitutes the inner lining of blood vessels. The endothelium is attached to the basal lamina in capillaries and is surrounded by smooth muscle cells in arterioles and venules, as well as by connective tissue in larger vessels. It is in direct contact with the circulating blood and acts as a semipermeable barrier that mediates gas and nutrient exchange with the surrounding tissues. Moreover, the endothelium is a major regulator for vascular tone, blood clotting, angiogenesis and inflammation. Dysfunction of endothelial cells results and/or contributes to many pathophysiological processes including ischemia, thrombosis, atherosclerosis, diabetes and hypertension.

Endothelial cells arise from the mesoderm. They differentiate from hemangioblasts, as do hematopoietic cells, and exhibit heterogeneity regarding morphological and physiological characteristics. Endothelial cells display phenotypic variability not only with respect to the individual blood vessels such as arteries, veins, and capillaries, but also with respect to vascular beds of different organs depending on the surrounding tissue. Vascular development starts with *de novo* vasculogenesis *in utero* while the remodeling and expansion into an organized vascular tree from preexisting blood vessels ensues through angiogenesis [93].

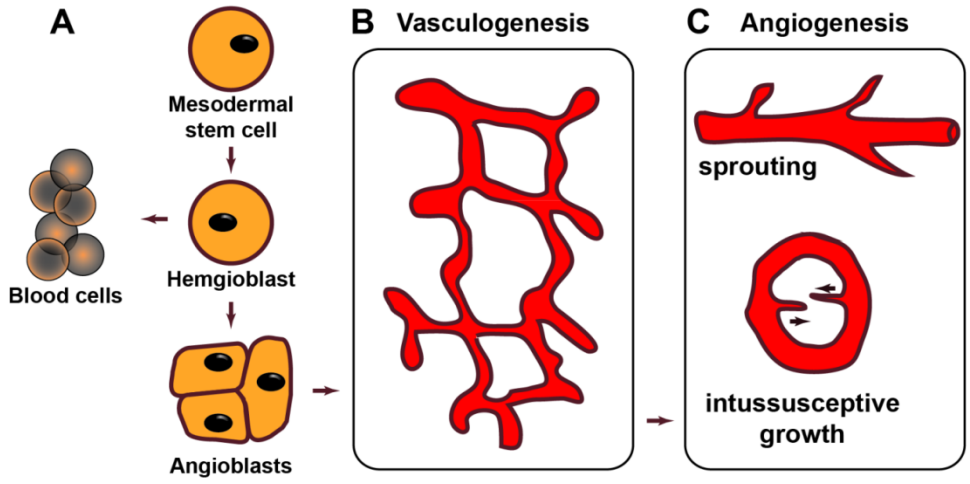

Figure 1-1: Development of the vascular tree
Endothelial cells arise from angioblasts (A), which assemble to form *de novo* primary vascular tree through the process of vasculogenesis during the intrauterine life (B). Angiogenesis is the formation of new blood vessels from preexisting ones and can occur through sprouting or intussesceptive vessel growth (C). Modified from [2].

Angiogenesis occurs throughout life. Physiological angiogenesis maintains tissue´s metabolic needs by ensuring that cells are no more than 50-100 µm distant from capillaries. It is involved in the physiology of development, reproduction, wound healing, and inflammation. Numerous diseases are characterized and/or caused by abnormal, excessive or conversely by insufficient angiogenesis or vessel regression. Therefore, controlling this process is therapeutically important: stimulating angiogenesis improves ischemic conditions and wound healing whereas inhibition of angiogenesis is relevant in cancer, ophthalmic conditions, rheumatoid arthritis, and other diseases.

Angiogenesis can proceed in distinct patterns. Quiescent endothelial cells are activated by angiogenic factors released from the surrounding hypoxic tissue and invade to build a vascular bed into the previously devoid tissue. In this process vascular endothelial growth factor (VEGF) is essential. The sprouting angiogenesis involves selection of an endothelial tip cell that protrudes towards the tissue and digests the extracellular matrix along the way [4]. The tip cell is followed by proliferating endothelial stalk cells that elongate the sprout while the capillary lumen becomes functionally perfusable as opposing tip cells meet each other.

Different to sprouting, intussusceptive (splitting) angiogenesis splits a single vessel in two as the wall extends into the lumen without immediate endothelial proliferation and migration. In both cases, the process is coordinated with pericytes, fibroblasts and smooth muscle cells. Recruitment of the pericytes and deposition of the extracellular matrix stabilizes and maturates the newly formed vessel.

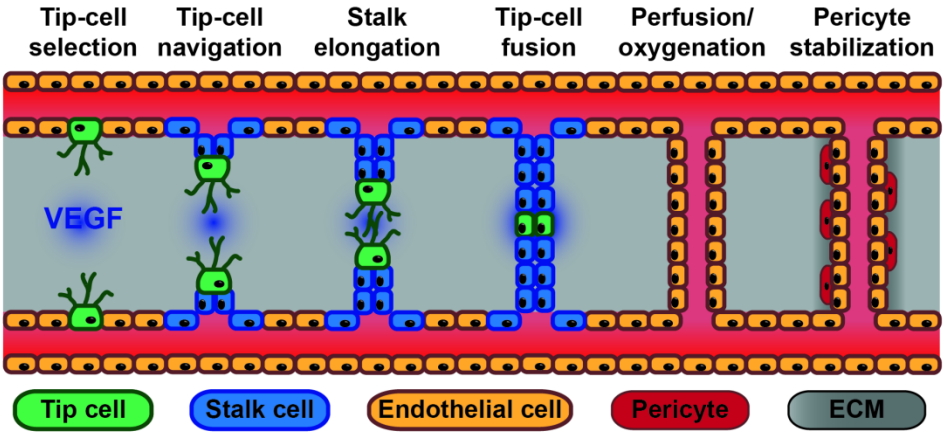

Figure 1-2: Sprouting angiogenesis
VEGF and other growth factors released from the ischemic tissue mediate the selection of the tip cell, which migrates towards the tissue devoided of blood vessels. The stalk cells proliferate and follow the tip cell. The new blood vessel is formed after the different tip cells meet each other while the recruited pericytes and the deposition of extracellular matrix stabilize the newly formed vessel. Modified from [2].

1.1.1 VEGF receptor 2 (VEGFR2) signaling in angiogenesis

VEGF is a central growth factor during angiogenesis. It acts on endothelial cells via three tyrosine receptor kinase receptors (VEGFR1-3) with VEGFR2 being the most important one. VEGF binding to

VEGFR2 leads to receptor homodimerization and autophosphorylation that activates several signaling pathways important for angiogenesis. VEGFR2 signaling promotes cell survival and initiates migration through activation of protein kinase AKT, endothelial nitric oxide synthase (eNOS) and the small GTPase Rac. It also regulates cell metabolism, migration and proliferation via phospholipase Cγ (PLCγ)-dependent activation of AMP-activated protein kinase (AMPK), eNOS and p42/44 mitogen-activated protein kinases (MAPK), respectively. VEGFR2 activation can also initiate cell migration through p38MPAK and activate focal adhesion kinase (FAK).

VEGFR2 signaling enables the tip cell selection, which is a precisely tuned process that allows normal development of vasculature. Tip cells are usually the ones exposed to the highest concentration of VEGF. The membrane of the tip cell develops small projections called filopoida, which are rich in VEGFR2 and can therefore sense the gradient of VEGF. VEGF stimulation of the tip cell induces expression of the Delta-like-4 (DLL4) ligand. Subsequently, direct cell-cell contacts enable DLL4 of the tip cell to bind to the notch receptor of neighbouring cells, thereby reducing VEGFR2 expression and leading to the stalk cell phenotype, which is less migratory and more proliferative and ensures the stability of the new sprout [5, 6].

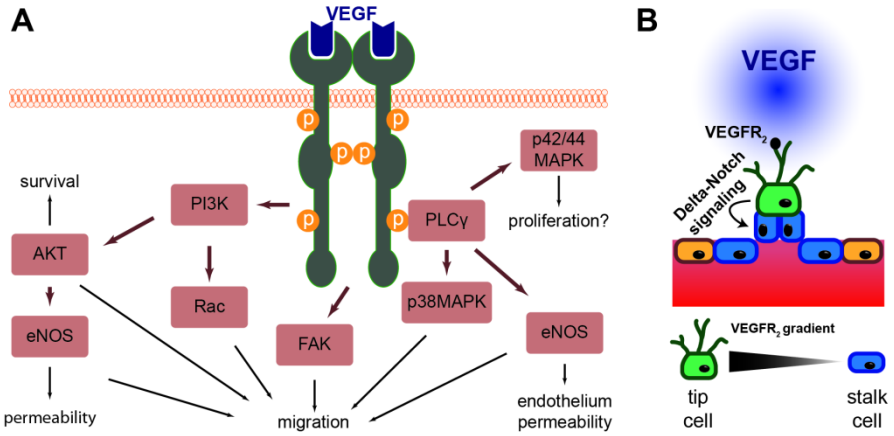

Figure 1-3: Vascular endothelial growth factor (VEGF) in sprouting angiogenesis
Panel (A) shows VEGFR2 signaling pathway in endothelial cells, which leads to tip cell selection and stalk cell induction as depicted in (B). AKT: *protein kinase* B; eNOS: *endothelial nitric oxide synthase*; FAK: *focal adhesion kinase*; MAPK: *mitogen-activated protein kinase*; PI3K*: phosphatidylinositol-3-kinase*; PLCγ: *phospholipase C-γ*. Modified from [2, 5].

1.1.2 Sphingosine-1-phosphate (S1P) in angiogenesis

S1P is an important factor in angiogenesis. It is especially involved in the regulation of endothelial cell migration but also in endothelial survival and proliferation. It is generated from the plasma membrane sphingolipids, and endothelial cells and activated platelets are a major source. Among the five G-protein-coupled S1P receptors (S1P1-5), S1P1 and S1P3 are the most abundant in endothelial cells [7]. S1P receptors trigger downstream activation of Rac and p38MAPK, which regulate cytoskeletal

rearrangements and focal adhesion turnover through FAK and Src activation. In addition, activation of S1P1 induces calcium signaling and calmodulin-mediated activation of eNOS through the phosphoinositide 3-kinase β (PI3Kβ)/PLC pathway. S1P can also activate VEGFR2 in endothelial cells in the absence of VEGF through receptor crosstalk (receptor transactivation) leading to eNOS and Rac activation through PI3Kα/AKT signaling pathway, as well as to activation of CrkII, an adaptor molecule of tyrosine kinases involved in membrane rearrangements and cell motility. Together, focal adhesions turnover, eNOS and Rac activation highlight S1P as an important mediator of endothelial cell migration and angiogenesis [8, 9]. In line with this, S1P strongly potentiated VEGF-induced angiogenesis *in vivo* in mice using the Matrigel plug assay [7]. Of note, S1P might be one of the main migration-inducing-factor in fetal calve serum used in experimental culture conditions [10].

1.2 Homeostasis of intracellular pH and cell volume

The homeostasis of intracellular and extracellular ion concentrations is the basis of physiological processes. Cells maintain ionic gradients across the semi-permeable lipid cell membrane by means of highly specialized proteins: transporters, channels, and pumps. This involves optimal control of the concentration of intracellular protons and osmolyte concentration, i.e. of intracellular pH (pH_i) and cell volume, respectively.

The concentration of hydrogen ions affects the milieu in which metabolic reactions occur. Moreover, the protonation state of weak acid and base moieties defines the conformation and function of all proteins [11]. Consequently, enzymatic reactions are especially sensitive to pH alterations. For instance, a decrease of 0.2-0.3 pH units in the intracellular pH almost completely inhibits the activity of phosphofructokinase-1 (PFK-1) [12] and effectively reduces glycolysis [13]. Other proteins particularly sensitive to slightest changes in pH_i include: ion channels [14], G-protein-coupled receptors [14], and enzymes (*e.g.* eNOS [15-17] and endothelin-converting enzyme [18]). Intracellular pH usually refers to the pH in the cytoplasm, which can be very different from the pH in each cellular organelle [19].

In addition to the intrinsic cell activity that generates mainly acid equivalents, the extracellular surrounding constantly challenges the pH_i. Although drastic deviations of local and systemic extracellular pH are efficiently counteracted, homeostatic mechanisms may become insufficient. For instance, metabolic or respiratory acidosis cause systemic pH disturbances whereas severe ischemia [20] or malignant tumors [21] may result in dramatic local decrease of extracellular pH.

Physiological steady-state intracellular pH (pH_i ~7.2 pH units) is slightly lower than extracellular pH (pH_e ~7.3-7.4 pH units). This is a consequence of acid production during cellular metabolism and the negative plasma membrane potential (~-60 mV, [22]), which drives passive H^+ uptake and efflux of HCO_3^- and OH^-. Intracellular pH follows the changes in extracellular pH in the same direction by

~30% [22] and is more sensitive to respiratory than metabolic extracellular acid-base disturbances [14, 23-25]. Nevertheless, pH_i is much higher than calculated from electrochemical H^+ distribution across the plasma membrane (~6.2 pH units, [26]), which means that acid-extruding processes are very active at steady-state conditions.

Cells maintain optimal pH_i through various mechanisms [22, 27]. Acute perturbations are rapidly buffered by the HCO_3^-/CO_2 buffering system [22], and to some extend by weak acids and bases (*e.g.* side chains of amino acids, phosphate groups). Buffers are able to donate or accept protons and neutralize alkaline or acid load, respectively. Buffering power, however, has no effect on the steady-state pH_i. Various transporters and pumps set and maintain long-term steady-state pH_i by extruding or importing proton equivalents [22] usually by electroneutral ion exchange. Most acid-extruders are secondary active and require Na^+. These include Na^+/H^+ exchangers (NHEs), Na^+/HCO_3^- cotransporters (NBCs) and Na^+ driven Cl^-/HCO_3^- exchanger (NCBEs). On the other hand, Cl^-/HCO_3^- anion exchangers (AEs) use the electrochemical gradient of Cl^- as the driving force to extrude HCO_3^- and indirectly load the cells with acid.

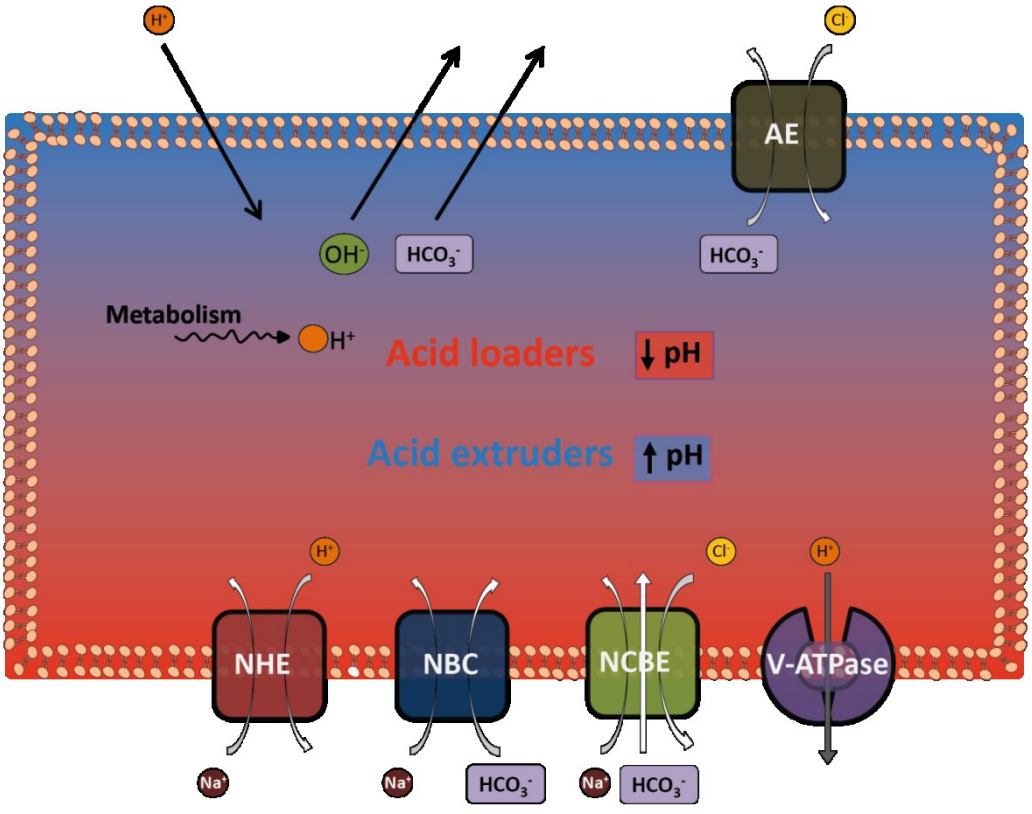

Figure 1-4: Mechanisms involved in cell acid loading and extrusion
Cells are acidified by metabolism and passive movement of ions. The latter includes entry of H^+ and exit of OH^- and HCO_3^- across the lipid membrane. Various transporters, channels and pumps at the plasma membrane regulate pH_i by extruding or loading cells with acid equivalents. NHE: sodium hydrogen exchanger, NBC: sodium bicarbonate cotransporter, NCBE: sodium-driven chloride bicarbonate exchanger, V-ATPase: vacuolar ATP-driven H^+ pump, AE: anion exchanger. Figure modified from [22].

Similar to intracellular pH, cell volume homeostasis is crucial for the integrity and cellular functions. However, cell volume is constantly challenged by changes in the surrounding osmolarity and the intracellular composition, which force water to move in and out of the cell and exert mechanical pressure. The water-permeable plasma membrane forms invaginations upon loss of pressure and can stretch to dampen increased osmotic pressure, but it is fragile to withstand high pressure. Under temporary anisotonic conditions cells activate a number of channels and transporters to avoid excessive alterations of their volume. Shrinkage is countered through regulatory volume increase (RVI) achieved by net influx of NaCl and organic solutes, while swelling triggers regulatory volume decrease (RVD) through net efflux of KCl and organic solutes, and therefore water. The NHE isoform 1 (NHE1) participates in RVI by mediating net NaCl influx when activated in parallel with Cl^-/HCO_3^- anion exchangers (AE) [28, 29].

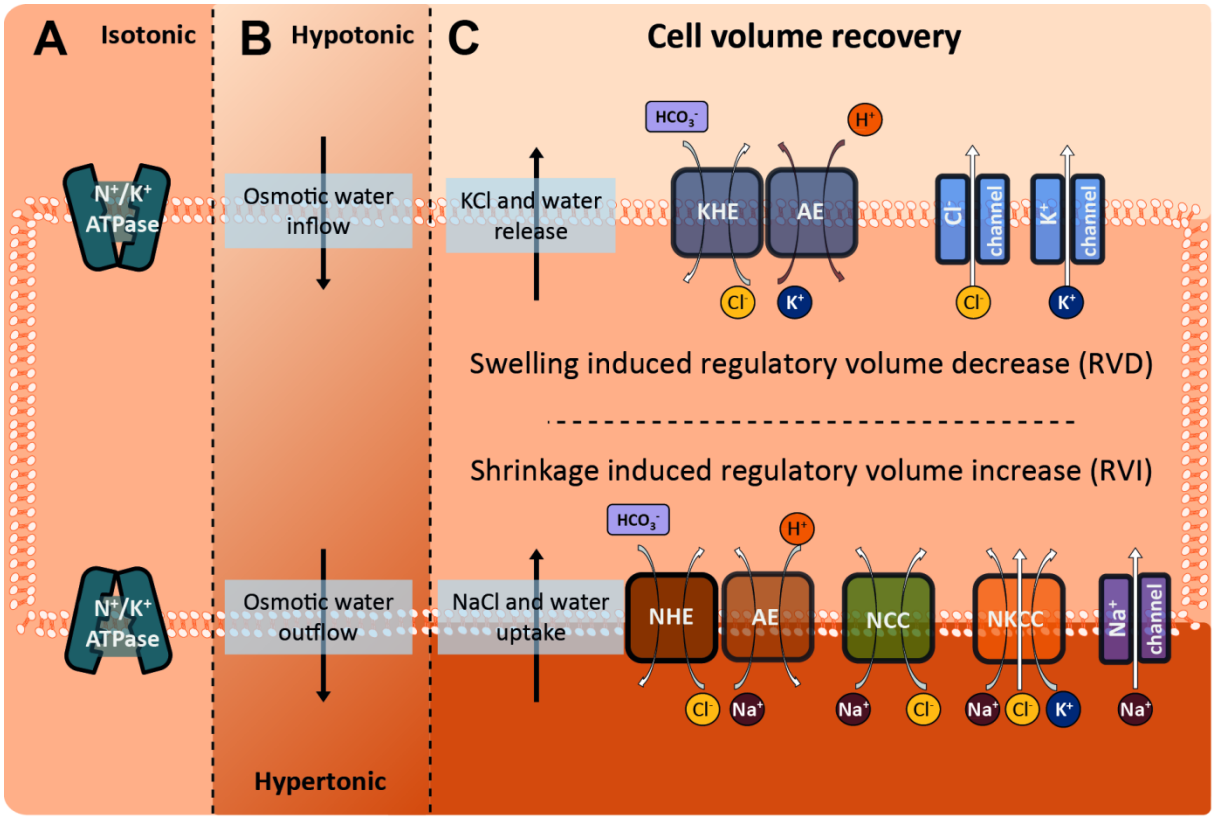

Figure 1-5: Mechanisms involved in cell volume regulation
(A) Under isotonic conditions the Na^+/K^+ ATPase is the most important mechanism that maintains volume homeostasis and the electrochemical gradients of Na^+ and K^+. Changes in extracellular osmolarity (B) disturb cell volume: hypertonicity causes water efflux and shrinking of the cell, whereas hypotonicity leads to water influx and cell swelling. (C) Both stresses are counteracted by mechanisms that lead to NaCl uptake or KCl release respectively. NHE: sodium hydrogen exchanger, AE: anion exchanger, NCC: sodium chloride cotransporter, NKCC: sodium potassium chloride cotransporter, KHE: potassium hydrogen exchanger.

1.3 Sodium/hydrogen exchanger NHE1

The Na^+/H^+ exchanger NHE1 is a ubiquitously expressed plasma membrane protein [30] that catalyses 1:1 electroneutral exchange of intracellular H^+ for extracellular Na^+. As a secondary active transporter, it gains the energy from the inwardly directed Na^+ gradient to extrude H^+ against the concentration gradient. It therefore regulates intracellular pH (pH_i) – important for proper functioning of all proteins – and cell volume by net NaCl influx (and therefore water) when NHE1 acts jointly with Cl^- transporters.

NHE1 has been characterized in several human pathologies. Over-activation is related to ischemia/reperfusion injuries, diabetes-associated vascular dysfunction, and atherosclerosis [31, 32]. Additionally, the putative role of NHE1 in supporting tumor progression has attracted major attention [33]. Inhibition of NHE1 was proven beneficial in animal studies of these pathologies and has therefore many potential pharmacological indications.

Moreover, many processes that endothelial cells undergo during angiogenesis are potentially supported by NHE1, including migration [34], proliferation and ECM degradation. Therefore, it is important to understand the role of NHE1 in endothelial function and angiogenesis, since it may represent a pharmacological target to treat excessive angiogenesis.

1.3.1 NHE1 protein

NHE1 belongs to the SLC9A family of ion transporters [35]. Overall, nine isoforms are described in mammals so far, termed NHE1-9. Isoforms show different tissue distribution and intracellular localization: whereas NHE1-5 locate at the plasma membrane and exchange H^+ for Na^+, NHE6-9 are found at the membranes of intracellular organelles and exchange H^+ for K^+ [19, 36].

The human NHE1 protein comprises 815 amino acids with a molecular mass of approximately 91 kDa. Since functional NHE1 is glycosylated, in SDS-PAGE it runs as a protein of approximately 110 kDa [37]. NHE1 can be separated into two functional domains. The N-terminal domain contains 12 transmembrane α-helices and mediates the ion exchange activity. The hydrophilic intracellular C-terminal domain regulates the exchange activity and has a scaffold function [38]. Importantly, NHE1 can bind to the actin filaments and anchor them to the plasma membrane. This interaction is mediated by actin binding proteins ezrin, radixin, and moesin (ERM) [39].

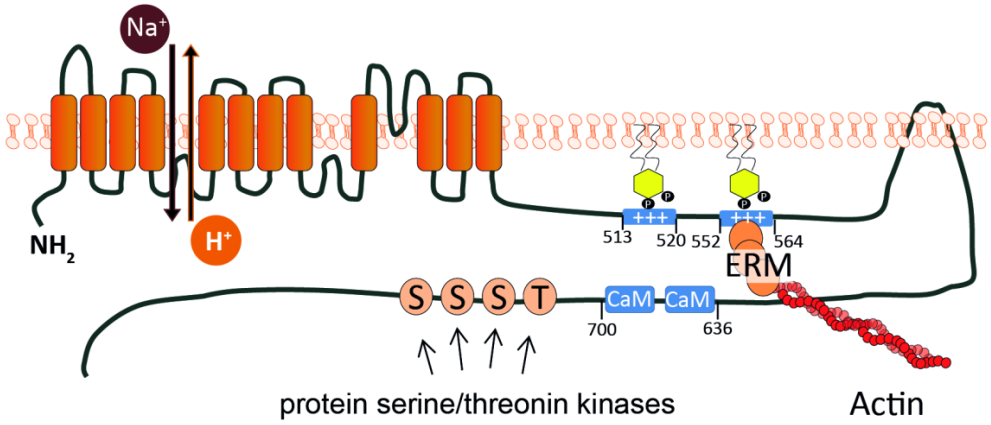

Figure 1-6: Schematic overview of the NHE1 protein
NHE1 protein contains two functional domains: The N-terminal domain containing 12 transmembrane α-helices mediating ion exchange, and the C-terminal cytoplasmic domain that binds several proteins and is phosphorylated at different serine and tyrosine sites. NHE1 can anchor actin through ERM binding (ezrin, radixin, moesin). Modified from [35, 40].

1.3.2 Regulation of NHE1 activity

Two major factors determine the ion exchange rate of NHE1: the intracellular concentration of H^+ ($[H^+]_i$) and changes in cell volume. NHE1's activity can affect both simultaneously, since extrusion of H^+ increases pH_i while the influx of Na^+, if coupled to Cl^- influx, increases intracellular osmolarity and cell volume. Therefore, NHE1 can optimize pH_i and cell volume simultaneously or prioritize one to the expense of the other. Under resting conditions, at physiological steady-state pH_i, bicarbonate-dependend transporters (NBCs and NCBEs) are considered as major long-term regulators of pH_i. If intracellular pH drops below a certain threshold, NHE1 allosterically senses the increase in $[H^+]_i$ and is rapidly activated to recover pH_i to the physiological steady-state range [26]. This threshold is prone to changes, and depends on the affinity of NHE1 for intracellular H^+. Signals from receptor-tyrosine kinases [41], G-protein-coupled receptors [42], and integrin receptors [43, 44] modulate NHE1's affinity for H^+ through phosphorylation, binding of regulatory proteins or inducing other conformational changes in the C-terminal domain. Although NHE1 forms homodimers, it is unclear whether the functional unit is the dimer or rather the monomer [26]. As for the ion exchange activity, it is proposed that monomers are capable of catalyzing ion exchange at acidic pH_i whereas the dimerization is needed for ion exchange at neutral pH_i range [45].

1.4 Cellular functions of NHE1

Co-ordination between ion exchange, actin anchoring and scaffold function enables NHE1 to play crucial role in fundamental cellular processes including cell shape and adhesion [39], migration, proliferation and survival [14].

1.4.1 Migration

Cell migration is a fundamental process in multicellular organisms that among others ensures proper immune response and tissue regeneration. Cells sense and respond to migratory stimuli that are either soluble (chemotaxis), immobilized ligands (haptotaxis), or mechanical (mechanotaxis) [4]. VEGF and basic fibroblast growth factor (bFGF) are strong chemotactic stimuli, while integrins bound to extracellular matrix (ECM) are involved in haptotaxis of endothelial cells. Mechanotaxis triggers mechanotransducion and is therefore important for shear stress induced endothelial cell migration [46].

During directed movement, the cytoskeleton is continuously remodeled and provides the necessary mechanical force that enables cell polarization into dynamic rear and front edge [4, 47]. Filopodia are generated from the membrane and sense motile stimuli. At the front, focal adhesions dynamically form and destabilize allowing lamellipodia and pseudopodia-like protrusions to adhere and pull the cell body forward. Simultaneously, stress fibers lead to destabilization of previous adhesions and retraction at the rear edge.

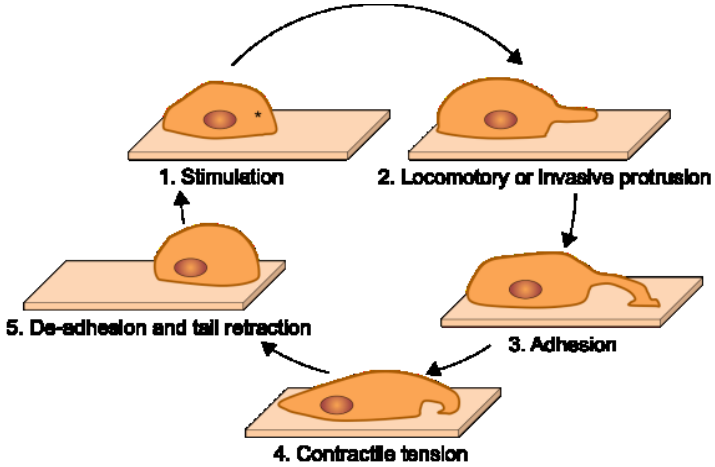

Figure 1-7: The cycle of cell motility
After sensing the migratory stimulus (1), the cell membrane protrudes forward (2) and adheres (3) to pull the cell body forward (4) while the rear end retracts (5). Adapted from [1].

The cell membrane is continuously rearranged throughout migration. It links the cytoskeleton to the extracellular matrix and allows the mechanical changes to occur. Ion transporters participate in anchoring the cytoskeleton to the plasma membrane [48]. In particular, NHE1's ability to anchor actin filaments to the membrane through interaction with ERM proteins makes it an important player in regulating the function and morphology of the moving cell. Through binding to ERM, NHE1 is restricted to primary lamellipodia. Accordingly, an NHE1 mutant unable to bind ERM was distributed diffusely and the cell produced extensions in all directions [49]. Restricting NHE1 at the leading edge enables local pH_i gradients to support scaffolding protein interactions [50-52] while the osmotic activity can provide mechanical force to push protrusions forward [53, 54]. Additionally, NHE1 promotes invasion as local proton extrusion lowers the extracellular pH near the membrane [55] and optimizes metalloproteinase digestion of ECM [56]. Moreover, cytoskeleton anchoring through NHE1 was shown to be required for focal adhesion assembly [39, 52], whereas the ion exchange function of

NHE1 was involved in remodeling focal adhesions. Inability to remodel focal adhesions led to insufficient disassembly of the formed adhesions resulting in elongated tails that failed to retract and slowed down the overall cell movement [49]. NHE1 ion exchange activity was also necessary to disassemble actin stress fibers and to assemble cortical F-actin clusters at focal adhesions [57]. Moreover, polarized ion exchange by NHE1 was able to create whole cell pH_i gradients along the axis of movement [58], which were flattened after inhibiting NHE1 [55, 59].

Taken together, NHE1 supports chemotaxis [53, 60] by regulating cell polarization, pushing protrusions forward, remodeling adhesions both at the rear and front as well as promoting digestion of ECM. NHE1 inhibition may not alter random cell mobility, but may slow down the cell and limit efficient movement towards the stimulus.

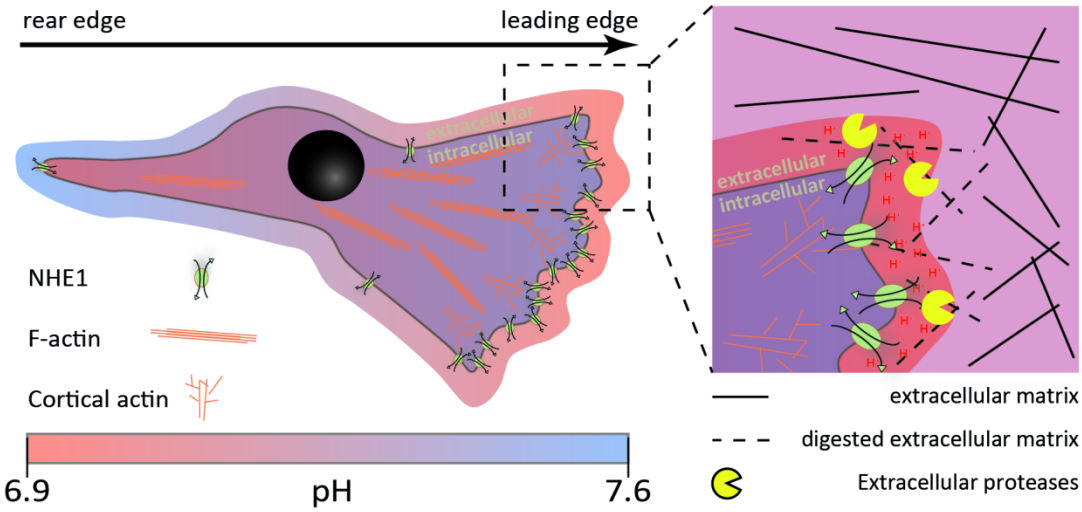

Figure 1-8: Polarization of the cell during migration
(A) NHE1 is translocated to the leading edge, which increases intracellular pH and lowers extracellular pH near the membrane. NHE1 might also be active at the rear edge aiding focal adhesion disassembly. (B) NHE1 activity at the leading edge optimizes the activity of extracellular proteases to digest the extracellular matrix. Modified from [27].

1.4.2 Proliferation and survival

Several studies highlight the importance of NHE1 for cell proliferation not only due to its ion exchange activity that extrudes metabolically-produced protons and mediates the volume increase during mitosis [61], but probably also due to modulating signaling and functional states of cells [30]. In contrast to migration, proliferation is influenced more by global rather than local pH_i changes. NHE1-dependent pH_i regulation is shown to affect G_2/M entry and transition [62] and NHE1 inhibition arrested pulmonary artery smooth muscle cells in G_0/G_1 phase of the cell cycle [63]. Unfortunately, the role of NHE1 in proliferation is often studied under bicarbonate-free conditions [64-66], which blocks other crucial pH_i regulatory mechanisms (*e.g.* NBCs and NCBEs) and

complicates data interpretation. Thus, studies indicate a permissive rather than obligatory role of NHE1 in cell proliferation [66-68].

Similarly, NHE1 promotes survival by simultaneously counteracting the drop in pH_i and cell shrinkage [69, 70], both hallmarks of apoptosis [28, 71], as well as by activating AKT-dependent survival pathways through recruitment of ERM [72].

1.5 NHE1 in endothelium

NHE1 has been described to localize at the basolateral side of the plasma membrane of endothelial cells [73, 74]. It is suggested to be the only relevant NHE isoform expressed in endothelial cells [73, 75] and to represent together with the Na^+/HCO_3^- cotransporter NBCn1 the most important Na^+-dependent acid-extruders regulating pH_i of endothelial cells [17, 68].

In vivo studies have demonstrated NHE1's involvement in complex endothelial cell functions such as endothelium-dependent vessel relaxation, barrier function, and ischemia/reoxygenation damage. Generally, studies suggest that NHE1 exhibits a homeostatic function in endothelial cells under low stress conditions but contributes to dysfunction under severe stress conditions.

1.5.1 NHE1 in endothelial-dependent vasorelaxation

Endothelial cells actively control vascular tone by producing vasoactive factors that change the contraction state of vascular smooth muscle cells. Endothelium-derived nitric oxide (NO) is produced by eNOS and is a well-known inducer of vessel relaxation. Although eNOS activity is regulated by Ca^{2+} signaling and protein phosphorylation, its enzymatic activity is intrinsically sensitive to the surrounding pH. Slight shifts from the physiological pH_i towards higher or lower values significantly reduce NO synthesis [15, 17]. Importantly, NHE1-dependent pH_i regulation of endothelial cells was shown to alter eNOS activity *in vitro* [21] and physiological activation of NHE1 supported NO-mediated vessel relaxation *in vivo* [20]. Surprizingly, constitutive *Nhe1*$^{-/-}$ mice had a lower arterial blood pressure compared to wild type littermates by 25 mmHg [17]. Although arterioles from these mice had thinner walls that produced less contraction force, it is yet to be confirmed if this is the cause or a consequence of reduced arterial blood pressure. Interestingly, constitutive *Nhe1*$^{-/-}$ mice were also protected from hypoxia-induced vascular remodeling and pulmonary hypertension [76].

1.5.2 NHE1 and vascular pathologies

Whereas NHE1 was shown to support physiological endothelium-dependent vessel relaxation, in pathological conditions NHE1 could contribute to tissue damage since genetic inactivation or pharmacological inhibition of NHE1 preserved organ function. Inhibition of NHE1 improved heart functions and endothelium-dependent coronary vessel relaxation in studies with rodents, as shown for

cardiac ischemia [77, 78] and streptozotocin-induced diabetic cardiomyopathy [79, 80]. NHE1 inhibitors failed to produce similar results in clinical trials though, and resulted in increased mortality due to cerebrovascular events [81-84]. Consequently, despite marginal benefits in subgroups of patients, the development of NHE1 inhibitors to treat ischemic cardiomyopathies has been discontinued.

The molecular mechanisms involving NHE1 with these pathologies remain unclear. It has been suggested that overstimulation of NHE activity provokes accumulation of intracellular Na^+, which in turn activates reverse-mode Na^+/Ca^{2+} exchange, leading to an influx of Ca^{2+} into the cells and $[Ca^{2+}]_i$ overload [85]. This in turn would activate several Ca^{2+}-dependent processes contributing to pathological alterations. In line with this, NHE1 inhibition was shown to decrease ICAM-1 expression in hypoxic/reoxygenated coronary microvascular endothelial cells, which could potentially reduce leukocyte-induced tissue damage ([86]). During ischemia, the tissue becomes hypoxic and extracellular pH drops. The acidic microenvironment may inhibit kinetic properties of NHE1. ROS, which are elevated during both hypoxia and reoxygenation, have also been linked to NHE1 regulation. O^{2-} has been shown to increase expression and H_2O_2 to decrease expression of NHE1 [87] and to inhibit the ion exchange activity [75]. Moreover, hypoxia was shown to upregulate NHE1 in endothelial cells [73], possibly through HIF1α-dependent mechanisms [88, 89]. Inhibition by H_2O_2 could serve as a defense mechanism against Ca^{2+} overload mediated by NHE1 during ischemia/reperfustion [14].

Animal models for stroke also show the detrimental situation of active NHE1 during ischemia and after reperfusion. Here, NHE1 was possibly involved in the barrier function of the endothelium by its ability to regulate cell volume. After middle cerebral artery occlusion stroke model in rats, pharmacological inhibition of NHE1 reduced brain edema by preserving the function of the blood brain barrier [90, 91]. Applying the same stroke model, heterozygous *Nhe1* knockout mice developed smaller infarct with preserved neurological function in the brain compared to their wild type littermates [92]. Pharmacological inhibition of NHE1 with cariporide also inhibited induction of microvascular leakage by methylglyoxal, a proinflamatory side-product of metabolism encountered during diabetic angiopathy [93].

1.6 Constitutive *Nhe1* knockout mouse model

Genetic and pharmacological inhibition have been used to study NHE1 in physiological and pathological situations. Constitutive *Nhe1* knockout mouse model (*Nhe1*$^{-/-}$) was first generated in 1999 by *Bell et al. (1999)* [94] and has ever since been a useful model for *in vivo* characterization of NHE1. The constitutive *Nhe1*$^{-/-}$ mice develop normally at first, but after the second postnatal week they grow slowly and are characterized by a severe neurodegeneration. The mice show increased mortality prior

to weaning, likely due to seizures [94]. Therefore, the severe phenotype and early death make the constitutive *Nhe1*$^{-/-}$ mice unsuitable for many *in vivo* studies and tissue-specific knockout models are required to characterize specific functions of NHE1 *in vivo*.

1.7 The aim of the study

NHE1 has been previously suggested to be involved in endothelial cell functions *in vitro* and *in vivo*, although only few data exist about its influence on complex endothelial functions. So far, genetic and pharmacological inhibition have been used to study NHE1 in physiological and pathological situations. However, due to the severe phenotype of the constitutive *Nhe1*$^{-/-}$ mice only a few studies have investigated vascular functions *in vivo*.

The aim of this thesis was to analyze the role of NHE1 in endothelial cells. To this end, an *in vitro* model was established by downregulating NHE1 in cultured endothelial cells using the RNA interference technology. In addition, an endothelial cell-specific *Nhe1*$^{-/-}$ mouse was generated by mating an *Nhe1*-floxed line with an endothelial cell-specific Cre-recombinase mouse line. Using these models together with the constitutive *Nhe1*$^{-/-}$ mice the following questions were addressed:

(I) How does NHE1 affect the intracellular pH regulation in endothelial cells as analyzed by live cell imaging?

(II) Does NHE1 influence endothelial proliferation, survival, migration and angiogenesis *in vitro*?

(III) Does NHE1 control angiogenesis *in vivo* as detected in a Matrigel plug assay?

2 Methods

2.1 Materials

2.1.1 Chemicals

2-Mercaptoethanol	Sigma-Aldrich Chemie GmbH, Germany
Acetic acid	J.T. Baker B.V, Netherlands
Acrylamide 4K-solution 30 % Mix 29:1	AppliChem GmbH, Germany
Amersham ECL	GE Healthcare UK Limited, UK
Ammonium chloride	Sigma-Aldrich Chemie GmbH, Germany
Ammonium persulfate	AppliChem GmbH, Germany
AURION BSA-c (Bovine Serum Albumin)	Aurion Immuno Gold Reagents & Accessories, Netherlands
BCECF-AM	Invitrogen, Molecular Probes, USA
Bio-Rad DC Protein Assay	Bio-Rad Laboratories Inc., Hercules, USA
Bovine serum albumin Fraction V, pH 7,0 (BSA)	AppliChem GmbH, Germany
Bromphenolblue	Sigma-Aldrich Chemie GmbH, Germany
Calcium chloride	AppliChem GmbH, Germany
Complete, EDTA-free Protease inhibitor cocktail tablets (PIC)	Roche Diagnostic GmbH, Germany
Disodium hydrogen phosphate dihydrate	Carl Roth GmbH & Co. KG, Germany
DMSO	Sigma-Aldrich Chemie GmbH, Germany
DTT	Sigma-Aldrich Chemie GmbH, Germany
EDTA	Sigma-Aldrich Chemie GmbH, Germany
EGTA	Sigma-Aldrich Chemie GmbH, Germany
Ethanol	Carl Roth GmbH & Co. KG, Germany
Ethidium bromide	MERCK, Germany
Fibrinogen, Human Plasma	Calbiochem _R
FluoromountG	Southern Biotech, USA
Glucose	Sigma-Aldrich Chemie GmbH, Germany
Glucose (GO) Assay Kit	Sigma-Aldrich Chemie GmbH, Germany
Glycerol	Carl Roth GmbH & Co. KG, Germany
Glycin	AppliChem GmbH, Germany

Goat Serum (Normal)	Dako Deutschland GmbH, Germany
HEPES	Sigma-Aldrich Chemie GmbH, Germany
Human Serum Albumin (HSA)	Bayer Vital GmbH, Germany
Hydrochloric acid 37 % (HCl)	Carl Roth GmbH & Co. KG, Germany
Isopropanol	VEB Jenapharm-Laborchemie, Germany
Kodak GBX developer and replenisher	Sigma-Aldrich Chemie GmbH, Germany
Kodak GBX fixer and replenisher	Sigma-Aldrich Chemie GmbH, Germany
Lactate Assay Kit	Sigma-Aldrich Chemie GmbH, Germany
Magnesium sulfate	Sigma-Aldrich Chemie GmbH, Germany
Methanol	AppliChem GmbH, Darmstadt
Methylcellulose	Sigma-Aldrich Chemie GmbH, Germany
Sodium diphosphate tetrabasic ($Na_4P_2O_7$)	Sigma-Aldrich Chemie GmbH, Germany
Sodium orthovanadate (Na_3VO_4)	Sigma-Aldrich Chemie GmbH, Germany
Nigericin, free acid	Invitrogen, Molecular Probes, USA
N-Methyl-D-Glucamine	Sigma-Aldrich Chemie GmbH, Germany
Paraffin	MerckKGaA, Germany
Paraformaldehyde	AppliChem GmbH, Germany
Phenylmethylsulfonylfluoride (PMSF)	Sigma-Aldrich Chemie GmbH, Germany
Potassium chloride	VEB Jenapharm-Laborchemie, Germany
Potassium dihydrogen phosphate	Riedel-De Haen AG, Germany
Propidium iodide	Sigma-Aldrich Chemie GmbH, Germany
Saponin	E. Merck, Germany
SeaKem LE Agarose	Lonza, USA
Skimmed milk powder	AppliChem GmbH, Germany
Sodium carbonate	MERCK
Sodium chloride	AppliChem GmbH, Germany
Sodium dodecyl sulfate	Sigma-Aldrich Chemie GmbH, Germany
Sodium hydroxide	Carl Roth GmbH & Co. KG, Germany
Spectra Multicolor Protein Ladder (10-260 kDa)	Fermentas GmbH, Germany
Sulfuric acid	Sigma-Aldrich Chemie GmbH, Germany
TEMED	AppliChem GmbH, Darmstadt
Thrombin, Human plasma	Sigma-Aldrich Chemie GmbH, Germany
Tris(hydroxymethyl)aminomethan (Tris)	AppliChem GmbH, Germany

tri-Sodium citrate dihydrate	Fluka Chemie GmbH, Germany
Triton X-100	Ferak Berlin GmbH, Germany
Tween 20	SERVA Electrophoresis GmbH, Germany
Xylol	VWR (BDH) Prolabo Chemicals, France
Zinc Fixative IHC	BD Biosciences, San Diego, USA

2.1.2 General materials

Biofuge pimo R (centrifuge)	Heraeus Holding GmbH, Germany
BP310P (balance)	Sartorius AG, Germany
BP61 (balance)	Sartorius AG, Germany
Fridge +4 °C / Freezer -20 °C	Liebherr-International Deutschland GmbH, Germany
Hamilton-Syringe	Hamilton Bonaduz AG, Switzerland
Heracell 150 (incubator)	Heraeus Holding GmbH, Germany
Heraeus function line (warming incubator)	Heraeus Holding GmbH, Germany
KH-3 (Cooling system - Blotting)	Biometra® Biomedizinische Analytik GmbH, Germany
KS 501 digital	IKA® Werke GmbH 6 Co. KG, Germany
Labofuge 400R	Heraeus Holding GmbH, Germany
Laminarbox Herasafe	Heraeus Holding GmbH, Germany
M6 Lauda (water bath)	MS Laborgeräte, Germany
Magnet stirrer	R3T GmbH, Germany
MC1 Laboratory LC4200 (scale)	Sartorius AG, Germany
mc6® (fume hood)	Waldner Laboreinrichtungen GmbH & Co. KG
Medap (vacuum vessel)	Medizinische Apparate, Med.-Techn. Gasanlagenbau, Austria

2.1.3 General instruments

Biofuge pimo R (centrifuge)	Heraeus Holding GmbH, Germany
BP310P (balance)	Sartorius AG, Germany
BP61 (balance)	Sartorius AG, Germany
Fridge +4 °C / Freezer -20 °C	Liebherr-International Deutschland GmbH, Germany

Hamilton-Syringe	Hamilton Bonaduz AG, Switzerland
Heracell 150 (incubator)	Heraeus Holding GmbH, Germany
Heraeus function line (warming incubator)	Heraeus Holding GmbH, Germany
KH-3 (Cooling system - Blotting)	Biometra® Biomedizinische Analytik GmbH, Germany
KS 501 digital	IKA® Werke GmbH 6 Co. KG, Germany
Labofuge 400R	Heraeus Holding GmbH, Germany
Laminarbox Herasafe	Heraeus Holding GmbH, Germany
M6 Lauda (water bath)	MS Laborgeräte, Germany
Magnet stirrer	R3T GmbH, Germany
MC1 Laboratory LC4200 (scale)	Sartorius AG, Germany
mc6® (fume hood)	Waldner Laboreinrichtungen GmbH & Co. KG
Medap (vacuum vessel)	Medizinische Apparate, Med.-Techn. Gasanlagenbau, Austria
Microprocessor pH meter ph537	WTW Wissenschaftlich-Technische Werkstätten GmbH, Germany
Microwave	Sharp Electronics GmbH, Germany
MP20/System II (membrane vacuum pump)	Biometra® Biomedizinische Analytik GmbH, Germany
OV3 (warming incubator)	Biometra® Biomedizinische Analytik GmbH, Germany
Pharmacia LKB MultiTemp II (cooling system - electrophoresis)	GE Healthcare UK Limited, UK
Power Pac 1000 (electrophoresis)	Bio-Rad Laboratories Inc., USA
Power Pac 200 (blotting)	Bio-Rad Laboratories Inc., USA
Präzitherm Typ PZ 35	Störk-Tronic, Störk GmbH & Co. KG, Germany
Protean® II xi Cell (electrophoresis)	Bio-Rad Laboratories Inc., USA
Shaker	Eppendorf AG, Germany
Thermomixer 5437	Eppendorf AG, Germany
Thermostat Julabo	JULABO Labortechnik GmbH, Germany

Trans-Blot™ Cell (blotting)	Bio-Rad Laboratories Inc., USA
Vortex	IKA® Werke GmbH 6 Co. KG, Germany
WT17 (tumbling shaker)	Biometra® Biomedizinische Analytik GmbH, Germany
centrifuge 5415 C	Eppendorf AG, Germany

2.1.4 Cell culture

BioWhittkaer® human serum	Lonza, Walkersville Inc., USA
BioWhittkaer® medium 199 (M199)	Lonza, Ealkersville Inc., USA
Ciprofloxacin Kabi	Fresenius Kabi Deutschland GmbH, Germany
Collagenase II	Worthington Biochemicals Corporation, USA
Dulbecco`s modified Eagle`s medium (DMEM/F12 1X)	Gibco® Life Technologies Corporation, UK
Dulcecco's modified Eagle medium (high glucose))	PPA Laboratories GmbH,
Endothelial mitogen (EM)	Biomedical Technologies Inc., USA
Fetal calf serum (FCS)	Cambrex Bio Science Verviers SPRL, Belgium
Gelatine	ICN Biomedicals GmbH, Germany
Hank`s balanced salt solution (HBSS)	Cambrex Bio Science Verviers SPRL, Belgium
Heparin-sodium	Hoffmann-La Roche AG,
L-Glutamine	ICN Biomedicals GmbH, Germany
Penicillin/streptomycin	Cambrex Bio Science Verviers SPRL, Belgium
Saint-Red siRNA/RNAi-delivery system	Synvolux Therapeutic B.V., Belgium
Trypsin-EDTA (0,05 % / 0,02 %)	Sigma-Aldrich Chemie GmbH, Germany
Trypsin inhibitor	Sigma-Aldrich Chemie GmbH, Germany
Vitamin C	Sigmal-Aldrich Chemie GmbH, Germany

2.2 Endothelial cells used for *in vitro* experiments

In vitro experiments were done with primary human umbilical vein endothelial cells (HUVEC) prepared from human umbilical cords, and primary mouse lung endothelial cells (MLEC) derived from the mouse lungs.

2.2.1 Preparation of human umbilical vein endothelial cells (HUVEC)

The fresh cords were cleaned with 70% ethanol from the outside. The vein was perfused with sterile washing buffer (see Table 1 for media and buffers composition), and then filled and incubated with 0.01% Collagenase II in M199 for 3 min at 37 °C. Dissociated cells were then collected in a tube with stop medium and centrifuged for 6 min at 500 *g*. The cells were resuspended in stop medium and seeded in a 0.2% gelatine pre-coated 75 cm^2 cell culture flask and incubated at 37 °C, 5% CO_2 and 95% humidity overnight. Afterward, the cells were washed with PBS to remove non-adherend cells, and fresh growth medium was added (supplemented with 0.5% Ciprofloxacin until the first passage). After reaching confluency, the cells were washed with PBS, detached with trypsin-EDTA (0.05%/0.02%) and propagated into new flasks. Each batch of HUVEC was cultured and employed up to a maximum of three passages. Each biological repetition was done with HUVEC obtained from independent preparations.

Table 1: Media and buffers used for HUVEC preparation

Washing buffer (for the umbilical vein)	
NaCl	0.9%
Penicillin	100 U/ml
Streptomycin	100 µg/ml
Stop medium	
FCS	10%
Penicillin	100 U/ml
Streptomycin	100 µg/ml
	in M199
PBS (phosphate buffered saline)	
NaCl	145 mM
KCl	2.7 mM
KH_2PO_4	1.5 mM
Na_2HPO_4	8 mM
pH adjusted to 7.4, autoclaved and stored at 4 °C	
200 mM Vitamin C (stock)	
Freshly prepared in M199 and neutralized with 0.2 M NaOH 1:5 (V/V)	
Gelatine	
0.2% gelatine was dissolved in ddH_2O at 56 °C and sterile-filtered and stored at 4 °C	
Growth medium	
FCS	17.5%
Human serum	2.5%
Penicillin	100 U/ml
Streptomycin	100 µg/ml
L-Glutamine	680 µM
Heparin	25 µg/ml
Endothelial mitogen	7.5 µg/ml
Vitamin C	5 µg/ml
	in M199

2.2.2 Preparation of mouse lung endothelial cells (MLEC)

Lung endothelial cells were prepared from animals of different genotypes (see section 2.9.1). Constitutive *Nhe1*$^{-/-}$ were employed at age of 3 weeks, since they die early in life; wild type littermates of the same age were used as controls. Endothelial cell-specific *Nhe1*$^{-/-}$ mice were processed at the age of two months; mice of *Nhe1*$^{flox/flox}$ genotype without Cre-recombinase were used as controls. All animals were sacrificed by cervical dislocation and the skin was disinfected with 70% ethanol. The lungs were excised and washed in ice-cold DMEM. The tissue was minced and incubated in 0.2% Collagenase II in DMEM for 1 h at 37 °C under gentle mixing every 10 min. The digest was triturated 20-30 times with blunt edge cannula and filtered through a 40 µm cell strainer to remove undigested tissue. (-) Medium (see Table 2 for media composition) was used to wash the strainer and stop the enzymatic activity, and the suspension was centrifuged at 500 *g* for 10 min. The cells were resuspended in (+) medium and seeded in 75 cm^2 culture flasks pre-coated with 0.2% gelatine. On the next day, the mixed culture of lung tissue-derived cells was briefly washed with 2% FCS in PBS and was incubated further in (+) medium. The first positive enrichment for endothelial cells was performed before full confluence of the culture was reached (to prevent non-endothelial cell overgrowth). To this end, magnetic beads coupled to secondary antibody (3 x 10^6 beads per 75 cm^2 flask) (Table 2) were washed with 2 % FCS in PBS and then conjugated with anti-CD102 antibody (4.5 µg per 75 cm^2 flask) for 2 h at 4 °C under slight tumbling. Beads were washed with the help of a magnet (Dynabeads MPC-S; Dynal Biotech ASA). Mixed cell cultures were then incubated with the anti-CD102-conjugated beads for 1 h at 4 °C. Thereafter, culture was trypsinized and transferred into a 15 ml tube, which was filled up to the maximal volume with (-). A second 15 ml tube was placed in the magnet and the cell suspension was pipetted over 4-6 min at the side where the tube contacts the magnet. Thereby, endothelial cells with beads were allowed to stay at the tube wall, whereas other cell types remained suspended. After 10 min incubation - allowing all cells with beads to be dragged by the magnet to the tube wall - the medium containing bead-free cells was poured out and the tube was removed from the magnet. Bead-binding cells were detached from the wall with (+) medium and seeded in new culture flasks. Selection was repeated once after confluence was reached again (to increase culture purity) and cells were seeded for experiments. Medium was changed daily to provide optimal growth conditions yielding 5-10 x 10^6 MLEC per mouse. Culture purity was checked for each preparation by flow cytometry staining CD31 as an endothelial marker (see section 2.10.2.1). It fluctuated between 80–95 %.

Table 2: Antibodies and media used for MLEC preparation

Antigen	Type (IgG)	Cat No	Vendor
Anti-Mouse-CD102	rat anti-Mouse	553326	BD Biosciences
Dynabeads	sheep anti Rat	110.35	Dynal Biotech ASA

(-) Medium	
FCS	20%
Penicillin	100 U/ml
Streptomycin	100 µg/ml
L-Glutamine	2 mM
	in DMEM/F12
(+) Medium	
Heparin	25 µg/ml
EM	75 µg/ml

2.3 Transfection of HUVEC with siRNA

HUVEC were transfected at 50-60% confluency with siRNAs directed against NHE1, HIF1α or HIF2α (Table 3). The Saint-Red siRNA/RNAi-Delivery System (Synvolux Therapeutics B.B.) was used for lipofection. Prior to transfection, the cells were washed twice with pre-warmed Hank's balance salt solution (Cambrex Bio Science Verviers SPRL), and incubated with Saint-Red (15 nmol/ml) and siRNA (0.5 µg/ml or 37 nM) in serum-free medium (0.25% HSA in M199). Growth medium was added four hours later, and the culture was usually used for experiments within 120 h after transfection. In parallel, cells transfected with non-targeting siRNA were used as controls. Downregulation efficiency was verified by western blotting, immunocytochemistry or flow cytometry.

Table 3: siRNAs used for experiments with protein downregulation

Target mRNA	Design	Cat No
Non-targeting (control)	Dharmacon On-Targetplus siCONTROL Non-targeting Pool	D-001810-10
HIF1α	SMARTpool: ON-TARGETplus HIF1A siRNA	L-004018-00
HIF2α (EPAS1)	SMARTpool: ON-TARGETplus EPAS1 siRNA	L-004814-00
NHE1	Dharmacon siGENOME SMARTpool Human SLC9A1	M-005277-00

All siRNAs were purchased from GE Healthcare, Dharmacon RNAi & Gene Expression.

2.4 Cell stimulation

For short-term stimulation of up to 30 min, the cells were starved for four hours in serum-free medium (M199 containing 0.25% HSA). 30 min before stimulation with VEGF (Cat. nr.: 296-VE, R&D Systems) and S1P (Cat. Nr. 567727, Calbiochem), medium was substituted with HEPES-buffered solution containing 0.25% HSA and cells were incubated at 37 °C without CO_2. Stimuli were added to this medium.

For long-term stimulation of 24 to 48 h, the cells were starved in low serum medium (Table 4) for four hours, to which VEGF or 1P was then added.

Table 4: Low serum medium and HEPES-buffered solution used for stimulation experiments

Low serum medium	
FCS	2%
Penicillin	100 U/ml
Streptomycin	100 µg/ml
L-Glutamine	2 mM
Heparin	25 µg/ml
Vitamin C	5 µg/ml
	in M199

HEPES-buffered solution	
NaCl	145 mM
KCl	5 mM
$CaCl_2$	1.5 mM
$MgSO_4$	1 mM
HEPES (buffer substance)	10 mM
Glucose	10 mM

pH adjusted to 7.4, sterile filtered
and stored at 4 °C
Supplemented with 0.25% HSA before use

2.5 Cell proliferation and survival

The cells were transfected with control or NHE1 siRNA. 48 h after transfection, proliferation was either analyzed in growth medium or cells were first reseeded on 35 mm dishes at 1.5 x 10^4 cells/cm^2 for VEGF-induced proliferation experiments. For the second case, the cells were stimulated with 50 ng/ml VEGF the following day after reseeding and counted 24 and 48 h after stimulation. One sample per each siRNA was analyzed at the time of stimulation and denoted as "0 h". In addition to cell counting, cell cycle (see section 2.10.2.2) and viability (see section 2.10.2.2 and 2.10.2.3) were also analyzed.

2.6 Hypoxia

The cells were incubated for up to 72h under hypoxic conditions with 1% O_2, 5% CO_2 and 95% humidity at 37 °C (HERAcell 150i; Thermo Fischer Scientific) for up to 72 h. Medium was first equilibrated in hypoxic conditions before medium changes took place.

2.7 Protein preparation for western blot analysis

The cells were washed with ice-cold wash-lysis buffer and were incubated with lysis buffer on ice for 15 min. The cells were then scraped off the plastic surface and the collected cell lysates were centrifuged (700 *g*, 6 min, 4 °C), and the supernatant was transferred into a new tube. After taking aliquots for determination of protein concentration, 3x Laemmli buffer was added to the lysate and proteins were denaturized for 5 min at 95 °C under gentle shaking. The lysates were stored at -20 °C. Protein concentration was determined using the Lowry method and analyzed spectrophotometrically (Uvikon 930; Tresser Instruments).

For immunoblotting, 30-50 µg protein per lane were separated through a water-cooled and electrode buffer-filled 7.5% SDS-PAGE. The separated proteins were transferred onto polyvinylidene fluoride membranes using a water-cooled and blotting buffer-filled wet blotting technique. The protein-loaded membranes were then blocked with 5% non-fat dry milk in TN-tween buffer for 1 h at RT, followed by an overnight incubation with primary antibodies (see Table 2 for antibodies) at 4 °C. Membranes were washed and incubated with peroxidase-coupled secondary antibody for 1 h at RT. After another washing step, the peroxidase-coupled secondary antibodies were visualized with an enhanced chemiluminescence Kit on autoradiography films. Before probing with another primary antibody, the membranes were treated with stripping buffer for 35 min at 54 °C under gentle shaking to remove the previously bound primary antibody. Between each step, the membranes were washed with TN-Tween buffer, while the last wash before chemiluminescence detection was done with TN-buffer without tween. Finally, the films were scanned, and the protein bands were quantified with the ImageJ software (National Institutes of Health).

Table 5: Buffers and solutions used for protein preparation, SDS-PAGE and western blot analysis

Wash-lysis buffer	
Tris pH 7.4	50 mM
EDTA	2 mM
EGTA	1 mM
NaF	50 mM
	stored at 4 °C
freshly added:	
$Na_4P_2O_7$	100 mM
Na_3VO_4	1 mM
DTT	1 mM
Lysis buffer	
Triton X-100	1%
SDS	0.1%
PMSF	0.2 M
PIC	10 µl/ml
	added freshly to Wash-lysis buffer
Electrode buffer	
Tris	192 mM
Glycine	25 mM
SDS	0.1%
	pH 8.3; stored at RT
Blotting buffer	
Tris	25 mM
Glycine	192 mM
3x Laemmli buffer	
SDS	9%
Glycerol	15%
Tris pH 6.8	186 mM
EDTA	10 mM
2-Mercaptoethanol	6%
Bromphenolblue	0.03%
	stored at -20 °C
TN-buffer	
NaCl	0.15 M
Tris	1 mM
	stored at 4 °C
TN-Tween buffer	
Tween 20 in TN-buffer	0.1%
Protein standard (westernbloting)	
BSA	10 mg
	in 10 ml 0.9 % NaCl solution, stored at 4 °C
Stripping buffer	
Tris	62.5 mM
SDS	2%
pH 6.7, stored at RT, before use warmed to 54 °C	

Table 6: Antibodies used in western blot analysis

Antigen	Phosphorylation site	Type (IgG)	Dilution	Cat No
β-Actin		rabbit, monoclonal	1:5 000	4970
eNOS		mouse, polyclonal	1:2 000	610297[#]
HIF1α		rabbit, polyclonal	1:1 000	3716
HIF2α		rabbit, polyclonal	1:1 000	NB100-122[§]
NHE1		mouse, monoclonal	1:1 000	mab3140*
p44/42 MAPK		mouse, monoclonal	1:2 000	9107
panAkt		rabbit, monoclonal	1:1 000	4691
panAMPK		rabbit, polyclonal	1:1 000	2532
Phospho-Akt	Ser473	rabbit, polyclonal	1:1 000	9271S
Phospho-AMPK	Thr172	rabbit, monoclonal	1:1 000	2535
Phospho-eNOS TypIII	S1177	rabbit, monoclonal	1:1 000	9570S
Phospho-p42/44 MAPK	T202/204	mouse, monoclonal	1:5 000	9106
Phospho-VEGFR2	Y1175	rabbit, monoclonal	1:1 000	2478
Phspho-Akt	Thr308	rabbit, monoclonal	1:1 000	4056
Vinculin		rabbit, monoclonal	1:5 000	4650
Mouse IgG (H+L)		goat polyclonal, peroxidase labeled	1:5 000	074-1806[$]
Rabbit IgG (H+L)		goat polyclonal, peroxidase labeled	1:5 000	074-1506[$]

Primary antibodies were dissolved in 5% BSA in TN-tween buffer (supplemented with 0.02% sodium azide) and stored at 4 °C. Secondary antibodies were dissolved in 5% milk in TN-tween buffer. Antibodies were purchased from Cell Signaling Technology (USA); or * EMD Millipore (USA), [#] BD Biosciences (USA), [$] Kirkegaard & Perry Laboratories (USA), [§] Novus Biological (USA).

2.8 Assays to evaluate endothelial function *in vitro*

2.8.1 Spheroid assay

Groups of endothelial cells can be also grown as spheres. When embedded in a 3D fibrin gel and stimulated with angiogenic factors, the spheres produce sprouts representing capillary-like structures. This assay is used to study *in vitro* angiogenesis by quantifying sprout number and length (see Figure 2-1).

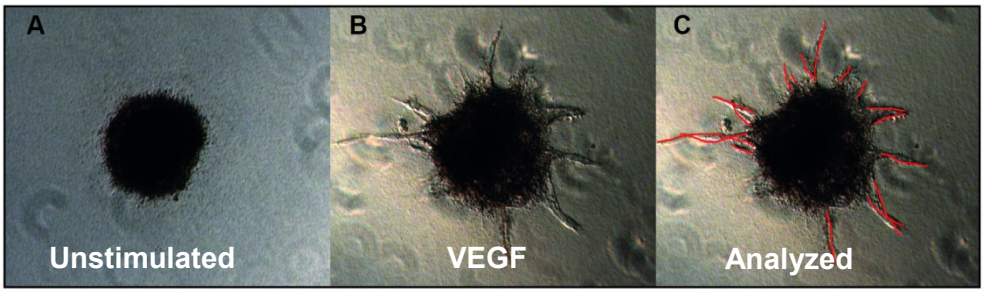

Figure 2-1: Sprouting of spheroids and analysis
Spheroids embedded in 3D fibrin gel (A) sprout with capillary-like structures when stimulated with an angiogenic factor like VEGF (B). The sprout number and average length are analyzed to quantify *in vitro* angiogenesis.

To generate spheroids, trypsinized HUVEC were set to 37,500 cells/ml in growth medium. This cell suspension was mixed with methylcellulose (12 mg/ml) in a 5:1 volume ratio, of which 3,000 cells/well (100 µl) were seeded in round bottom 96-well plates and incubated overnight at 37 °C. The formed spheroids were pooled in tubes and washed twice with HEPES-buffered solution (centrifuged in between for 4 min at 200 *g*). Fibrinogen dissolved in HEPES-buffered solution was sterile-filtered and diluted with the spheroid suspension to a final concentration of 1.8 mg/ml. The mixture was supplemented with 200 U/ml aprotinin to block the degradation of the fibrin gel. 300 µl per well of this suspension were polymerized with 10 µl thrombin (final concentration of 0.66 U/ml) in 24-well-plates for 20 min at 37 °C (without CO_2). Low serum medium was then added and changed three times in 10 min intervals to wash away the thrombin. Finally, the embedded spheroids were incubated in low serum medium (without or with VEGF: 10 ng/ml or 50 ng/ml) for 48 h. Afterward, spheroids were fixed with 4% PFA for 10 min at RT and washed with PBS. Each experiment included technical duplicates (two wells per condition) and approximately 10 spheroids per well were documented (Axio Vert 200; Zeiss) and analyzed with CellD software (Olympus) for sprout number and length.

Preparation of methylcellulose solution: Methylcellulose was autoclaved as powder and then stirred in M199 medium (24 g/l) for 20 min at 60 °C. This solution was further diluted with M199 to 12 g/l and

stirred for one hour at RT and then overnight at 4 °C. The resulting solution was centrifuged for two hours at 4000 *g*, and the supernatant was collected for the experiments.

2.8.2 Transwell migration assay

The transwell assay estimates cell migration through 0.8 µm pores on membrane inserts (FALCON® Transwell insert; Corning Incorporated). Cells were seeded on the upper side and migrate towards the chemoattractant in the lower chamber on the other side of the membrane (Figure 2-2). The cells were starved for three hours in serum-free medium and were then trypsinized. Instead of stop medium, a Trypsin-inhibitor (1 mg/ml; Sigma-Aldrich) was used to stop Trypsin's activity and prevent FCS-stimulation. The detached cells were centrifuged for 6 min at 500 *g* and resuspended in M199 containing 0.25% HSA. Inserts were placed on 24-well-plates and coated with 0.2% gelatine. Immediately after aspirating the gelatine 8 x 10^4 cells were seeded on the upper chamber of each insert. The lower chamber was filled with serum-free medium and supplemented with 50 ng/ml VEGF or 0.1 µM S1P to stimulate migration, whereas no attractants were added to controls. Cells were allowed to migrate for four hours and fixed with 4% PFA in PBS for 10 min at RT. Next, inserts were washed with distilled water four times for 2.5 min each and stained with hematoxylin for 5 min. Membranes were then washed thoroughly with tap water and left for 10 min in tap water for the color to develop. Non-migrated cells on the upper side of the membrane were removed with a cotton swab and membranes were air dried at RT overnight. Membranes were excised from the inserts with a crooked scalpel and embedded with FluoromountG on microscope slides. Each experiment included technical duplicates and five pictures per insert were taken at a 200x magnification. Migrated cells were counted manually with ImageJ software.

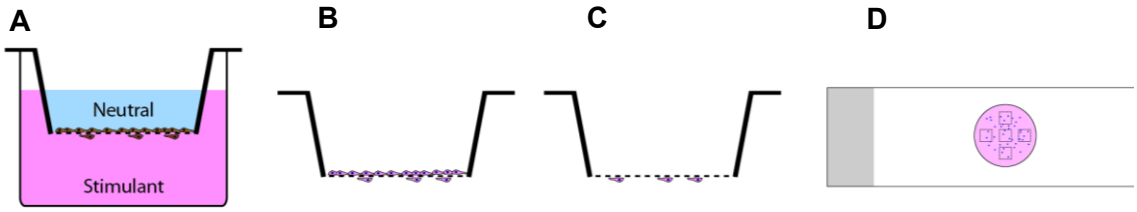

Figure 2-2: Transwell migration assay
Cells were seeded on the upper chamber of the insert while the stimulant was pipetted on the lower chamber. After 4 h migrated cells were positioned on the lower side of the membrane (A). The inserts were fixed and stained (B), and the non-migrated cells on the upper part were removed with a cotton swab (C). The inserts were placed on microscopic slides and imaged at five different positions before analysis (D).

2.8.3 2D Chemotaxis

IbiTreat chemotaxis µ-Slides [95] (µ-Slides Chemotaxis^{3D}; ibidi GmbH) were used to study HUVEC's ability to sense chemotactic gradients *in vitro in* (Figure 2-3). Slides were handled according to the manufacturer´s instructions to study 2D chemotaxis of adherent cells. The HUVEC were trypsinized 72 h after transfection with control or NHE1 siRNA and seeded on the chemotaxis slides at a low

confluency, although a high density suspension of 2-3 x 10^6 cells/ml was needed due to the small height of the observation area. Although cells beca Three hours later, the cells were carefully washed three times and incubated further in low serum medium, which was pre-incubated in 5% CO_2 air for pH equilibration. Three hours later, 50 ng/ml VEGF or 0.1 µM S1P was added to the right chamber, whereas controls were left unstimulated. Slides were immediately placed on the motorized stage of the microscope (Nikon Eclipse Ti) in a chamber warmed at 37 °C and flooded with 5% CO_2 humidified air. A larger area was scanned in 10 min intervals under 200x magnification by automatically stitching 4 x 7 individual images. The Nikon Perfect focus system was used to keep cells in focus. The experiment was stopped after 24 h and migrating cells (cell nuclei) were tracked in ImageJ software using the Manual Tracking plugin. The tables obtained from ImageJ software were analyzed with Chemotaxis and Migration Tool software. Among the parameters analyzed (Figure 2-3), the displacement of the Center of Mass (COM), Forward Migration Index (FMI), and the migration velocity were chosen to describe migrational behaviour of the cells. These parameters were calculated for the parallel axis of the gradient and the perpendicular axis. Theoretically, no net displacement of COM should be observed in the perpendicular axis.

2.8.4 Wound healing

The wound healing assay was used as another approach to study HUVEC migration after NHE1 knockdown. Instead of scratching a confluent cell monolayer, which is usually inhomogenous, a uniform cell free area of approximately 500 µm wide, in which endothelial cells could move in, was created using ibidi Culture inserts in 35 mm µ-Dishes (ibiTreat) as shown in Figure 2-4. The inserts were handeled according to the manufacturer´s manual. HUVEC were trypsinized and seeded on the inserts (4 x 10^4 cells/well) 72 h after transfection . The inserts were removed 3-4 h after seeding, in order to avoid the detachment of the cell monolayer together with the insert. The cells were washed, and low serum medium was added, which was pre-incubated in 5% CO_2 air for pH equilibration. Two to three hours later 50 ng/ml VEGF or 0.1 µM S1P was added, whereas controls were left unstimulated.

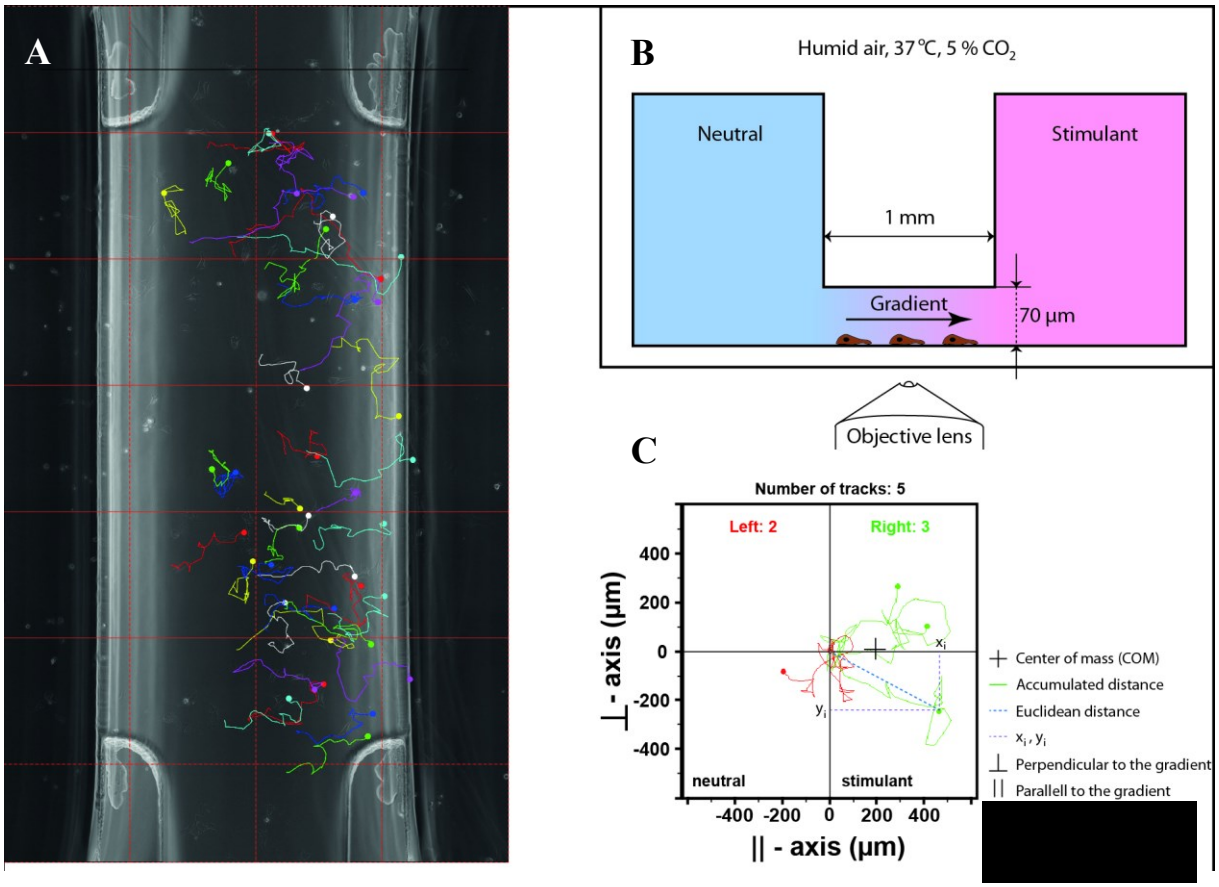

Figure 2-3: Chemotaxis assay

Panel A shows from above the space of the slide in which the cells are seeded and where the gradient forms. In this panel some cell tracking's are also shown as the majority of cells move towards the stimulant on the right. Panel B shows the slide in perpendicular section with two medium pools and the narrow slit where cells are attached and the gradient forms. Panel C shows the analysis of cell trackings with some of the parameters that can be analyzed.

Following the stimulation, the dishes were immediately placed on the motorized stage of the microscope (Nikon Eclipse Ti) in a chamber warmed at 37 ˚C and flooded with 5% CO_2 humidified air. A larger area was scanned in 10 min intervals at 200x magnification by automatically stitching 11 x 4 individual images, while the Nikon Perfect focus system was used to keep the cells in focus over 24 h. Cell nuclei within the wound area were counted with ImageJ software in two hours intervals for six hours, at which point the opposite sides of the wound usually reached each other.

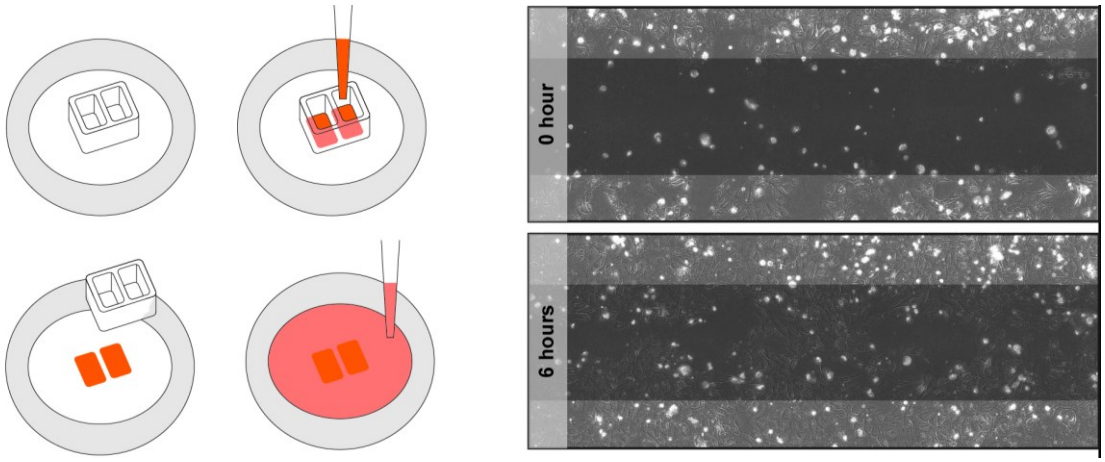

Figure 2-4: Wound healing assay
After attaching the culture inserts to the dish bottom (A), cells were seeded in the insert's wells (B) and 3 h later the insert was removed (C) leaving an empty area between the two monolayers. The dish was filled with low serum medium (D) to which stimulants were added after 2 h of starvation. Cells migration into the wound was tracked within the first 6 h after stimulation (E).

2.9 Molecular biology

2.9.1 Mouse lines

Nhe1-floxed: Exon 2 coding for 4 out of 12 transmembrane domains of NHE1 was flanked by loxP sites as shown in Figure 2-5. After Cre-lox recombination, loss of exon 2 leads to a frameshift and a premature stop codon that results in a destabilized mRNA. The *Nhe1*-floxed line was backcrossed with C57BL/6 and used to generate both the constitutive (ubiquitous Cre deleter [96]) and the endothelial cell-specific *Nhe1*$^{-/-}$ mice (*VE-Cadherin-Cre* [97]). The *Nhe1*-floxed mouse line was generated by Dr. Christopher Hennings.

Table 7: Mouse lines

Mouse line	Modification	Reference
Nhe1-flox	conditional construct	Generated by Dr. Christopher Hennings
VE-Cadherin-Cre (*Cdh5-cre*)	transgene	[97]
Tie2-cre	transgene	[98]
Tomato ROSA-locus	knockin	[99]
Cre-Rekombinase Ubiquitous deleter	transgene	[96]

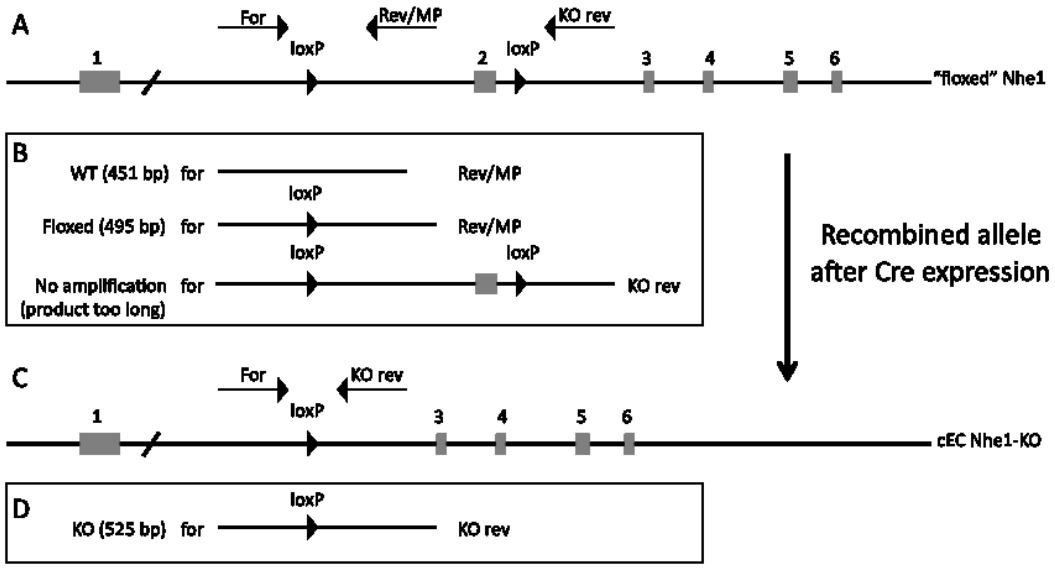

Figure 2-5: The strategy for the conditional knockout of the *Nhe1* allele
Exon 2 of the *Nhe1* allele is flanked by two loxP sites (A) and cre-recombination results in gene knockout since the loss of exon 2 leads to a frameshift and a premature stop codon (D). The binding stie for genotyping primers are also depicted (A, D) as well as the resulting amplicons (B, C).

2.9.2 Phenol/chloroform extraction of genomic DNA

In order to extract genomic DNA, tail biopsies (2-3 mm) were incubated overnight at 55 °C in 500 µl lysis buffer (50 mM Tris 100 mM EDTA, 100 mM NaCl, 1% SDS, pH 8.0) supplemented with 10 µl Proteinase K (14 mg/ml). After cooling, one volume of TE-buffered phenol-chloroform-isoamyl alcohol (25:24:1, Roth) was added, and the lysates were mixed on a rotator for at least 5 min at RT. The samples were then centrifuged at maximal speed over 10,000 *g* for 15 min at 4 °C, and the upper aqueous phase was collected in new tubes. Traces of phenol were removed through two consecutive washes with one volume chloroform-isoamyl alcohol (24:1), and DNA was precipitated with one volume isopropanol (supplemented with 8 mM LiCl). The DNA pellet was washed once with 70% ethanol and air-dried. The pellet was then solubilized in 150 µl low TE buffer (10 mM Tris, 1 mM EDTA, pH 7.4) overnight at 55 °C, and stored at 4 °C or -20 °C for further use. 1-2 µl were used in the PCR for genotyping.

2.9.3 HotSHOT DNA extraction

In a faster alternative for genomic DNA extraction, tail-biopsies (2-3 mm) were incubated in 75 µl alkaline lysis buffer (25 mM NaOH, 0.2 mM EDTA, pH 12.0 – no adjustment) for 30-60 min at 95 °C, cooled on ice and neutralized with acidic buffer (40 mM Tris-HCl, pH 5.0–no adjustment). Extracted DNA was stored at 4 °C or -20 °C. 1-2 µl were used for the PCR reaction for genotyping.

2.9.4 Genotyping

DNA prepared by HotSHOT or Phenol/Chloroform extraction was used for genotyping in a polymerase chain reaction (PCR) using Taq-Polymerase (Invitrogen). The PCR products were separated by horizontal gel electrophoresis (2% agarose in running buffer: 40 mM Tris-Acetate, 1 mM EDTA) and visualized by supplementing the gel with 0.5 µg/ml ethidium bromide. Samples were mixed with 5x DNA loading buffer (30% Glycerin, 0.25% bromophenol blue and 0.25% xylene cyanol), and the fragment sizes were compared to a 1 kb DNA ladder (Gene graft). Amplicons were separated at a constant voltage of 160 V for 30-90 min and visualized under ultraviolet light.

For *Nhe1*-flox genotyping, the PCR was set with three primers to amplify the *Nhe1*-wildtype (451 bp), *Nhe1*-floxed (495 bp), and *Nhe1*-knockout allele (525 bp) (see Figure 2-5 for the genotyping strategy and Table 8 for primer sequences).

Table 8 *Nhe1* genotyping primers

***Nhe1* Primers**	**sequence (5´-3´)**
*Nhe1*_for	TTA GGA GCT GGG AAG GAG AGT
*Nhe1*_revI/MP	CTT CTT GTG CTG AAA AGC TGC C
*Nhe1*_KO	GCA TTC ACA CCT GAA CTA AGC

2.9.5 Quantitative real-time PCR angiogenesis array

To find a link between NHE1 and VEGF-stimulated angiogenesis, we have analyzed the expression of 84 angiogenesis-related genes with the Qiagen qPCR angiogenesis array (RT^2 Profiler™ PCR Array Human Angiogenesis). For this experiment, HUVEC were seeded in 90 mm cell culture dishes and were transfected the next day. 72 h after transfection, the cells were starved for four hours in low serum medium and stimulated with 50 ng/ml VEGF for 4 or 24 h with appropriate unstimulated controls.

The time-points for stimulation were chosen after a careful review of the literature for the VEGF-induced expression kinetics of the array-covered genes. The majority of genes were analyzed at 24 h after VEGF stimulation, whereas the remaining genes were analyzed after four hours including ANGPTL4, CCL11, CXCL10, CXCL9, EDN1, F3, FGFR3, FTL1, IFNA1, IL1B, IL6, IL8, MMP2, MMP9, MMP14, NOS3, PTGS1, S1PR1, SERPINE1, SERPINF1 and TIE1. We have used Qiagen kits for each step of sample preparation and analysis. RNA was isolated with the RNeasy Kit, from which cDNA was synthesized using the RT^2 First Strand Kit. The obtained Ct values from the qPCRs were analyzed using a Qiagen Web-based software. Genes with at least twofold difference were considered further.

2.10 Analysis using fluorescent probes

2.10.1 Live cell imaging for intracellular pH measurements

Intracellular pH (pH_i) in living cells was measured using 2′,7′-Bis(2-carboxyethyl)-5(6)-carboxyfluorescein (BCECF) [100] as a ratiometric fluorescent indicator, it is pH-sensitive when excited with a wavelength of 495 nm and pH insensitive at 440 nm (its isosbestic point). This allows monitoring pH_i independently of dye loading or leakage from the cell, as well as photobleaching [101]. The esterified form BCECF-AM is permeable through the cell membrane and trapped inside the cell after cleavage by intracellular esterases. For these experiments 18 mm-diameter glass coverslips were used, which were pretreated with 1% SDS, 3 x washed for 10 min with distilled water, incubated for 10 min with 70% ethanol and 30 min with 99% ethanol, and finally heat sterilized. Thereafter, coverslips were coated with 0.2% gelatine before HUVEC or MLEC were seeded on them and loaded with 4 µM BCECF-AM in HEPES-buffered solution for 10-15 min at 37 °C. Coverslips were mounted in a perfusion chamber (Chamlide EC; Live Cell Instruments, Korea) with a heated stage (37 °C). The cells were then superfused with 37 °C warmed HEPES-buffered solution at a linear flow rate of 1.5-2.0 ml/s (Peri-Star Pro; World Precision Instruments, USA), which corresponds to approximately four complete buffer changes per minute. Emitted light of 510-535 nm was recorded after alternating excitation at 495 nm and 440 nm and captured through a 10x objective in 30 seconds intervals (to reduce phototoxic effects) or 5 seconds when quick changes were expected with a charge-coupled device camera (AxioCam MRm; Zeiss) on Axio Observer.Z1 microscope (Zeiss). Steady-state pH_i was recorded for at least 10 min before the cells were acid-loaded by the "rebound acidification" technique [102] for 5 min with 10 mM ammonium chloride in HEPES-buffered solution (equimolar substitution of NH_4^+ for Na^+). The cells were then washed with Na^+-free HEPES-buffered solution (equimolar substitution of N-Methyl-D-glucamine for NaCl) for 5 min. Experiments were also done in the presence of bicarbonate in which case solutions were buffered with HCO_3^-/CO_2 instead of HEPES. Upon reintroduction of Na^+, pH_i recovery was observed, and $\delta pH_i/dt$ was determined for the first 40 seconds of recovery. Data from more than three coverslips (>30 cells/coverslip) from at least three independent preparations were averaged. At the end of each experiment, a calibration curve was constructed with a calibration buffer of pH ranging from 6.6-7.4 and supplemented with nigericin as an ionophore. A linear regression was calculated from the multipoint calibration curve, and F_{495}/F_{440} ratio was converted into pH_i values [101].

Table 9: Buffers used for intracellular pH

HEPES-buffered solution	
NaCl	145 mM
KCl	5 mM
$CaCl_2$	1.5 mM
$MgSO_4$	1 mM
HEPES (buffer substance)	10 mM
Glucose	10 mM
pH adjusted to 7.4, sterile filtered stored at 4 °C	

Bicarbonate-buffered solution	
NaCl	119 mM
KCl	5 mM
$CaCl_2$	1.5 mM
$MgSO_4$	1 mM
$NaHCO_3$	26 mM

Calibration buffer	
KCl	135 mM
N-methyl-D-glucamine	20 mM
$MgSO_4$	4 mM
Glucose	10 mM
HEPES (buffer substance)	30 mM
Nigericine	10 nM
pH adjusted to 6.6; 6.8; 7.0 or 7.4 stored at 4 °C	

2.10.2 Flow cytometry

1-5 x 10^4 cells per sample were measured using the BD FACS Canto flow cytometer (BD Biosciences, USA) and analyzed with the FlowJo software. Unstained and single stained controls were used to compensate for spectral overlap in multicolor assays.

2.10.2.1 Analysis of MLEC purity

The efficiency of positive enrichment for mouse lung endothelial cells (MLEC) was determined using flow cytometry. The cell culture was washed with warm PBS and fixed with 0.5% PFA for 2-3 min on ice. The mild fixation protocol maintains the CD31 antigen recognizable and allows trypsinization after which cells are processed in suspension. The cells were washed twice with PBS (centrifuged in between for 6 min at 500 *g*) and blocked with 0.2% BSA-c in PBS for 30 min at RT. The anti-CD31 antibody was added to the suspension and incubated for further 30 min. After washing with PBS, the cells were incubated for 30 min with secondary antibody (diluted in 0.2% BSA-c in PBS). Finally, the cells were washed once and re-suspended in PBS to be analyzed by flow cytometry.

2.10.2.2 Cell cycle analysis with propidium iodide

This method quantifies cell DNA and estimates the fraction of cells in each phase of the proliferation cycle (G_0/G_1; S; G_2/M). G_0 and G_1 or G_2 and M phase cells contain the same amount of DNA and are therefore indistinguishable. Additionally, cells undergoing apoptosis release apoptotic bodies with less DNA than the intact cell and constitute the sub-G_1 population. Cell clumps were excluded from analysis after plotting the height against the width of the signal for propidium iodide fluorescence.

The supernatant was pooled together with the washing fractions and the trypsinized cell suspension. The cells were washed twice with PBS (centrifuged in between for 6 min at 500 *g*). After resuspension in 200 µl PBS, 2 ml of 70% ethanol were added dropwise, and fixation in ethanol was done at 4 °C for

at least 1 h or stored for at least two weeks at -20 °C. The cells were then washed twice with 0.5% Tween-20 in PBS and incubated with 300 µM RNaseA for 15 min at 37 °C. Next, one volume of 200 µM propidium iodide was added, and samples were analyzed by flow cytometry after 10 min incubation in the dark.

2.10.2.3 Annexin V/Propidium iodide apoptosis assay

In healthy cells, the phosphatidylserines of the plasma membrane face the intracellular compartment. Early in apoptosis, they flip towards the extracellular compartment and can, therefore, bind Annexin V (Cat Nr. 31490013, ImmunoTools, Germany). Alternatively, late apoptotic or necrotic cells with damaged plasma membrane are leaky and allow annexin V bind to phosphatidyl serines from the inner side of the membrane as well. The damaged plasma membrane is also permeable to propidium iodide, which stains double stranded nucleotide chains. Therefore, viable cells are neither stained by annexin V nor propidium iodide. Early apoptotic cells are only annexin V positive, whereas apoptotic and necrotic dead cells are positive for both annexin V and propidium iodide.

For this assay, the supernatant was pooled with the washing fractions and the trypsinized cell suspension. The cells were washed twice with PBS (centrifuged in between for 6 min at 500 *g*). 1 x 10^5 cells were resuspended in 100 µl binding buffer (140 mM NaCl, 2.5 mM $CaCl_2$, 10 mM, pH adjusted to 7.4) with 2.5 µl Annexin V-FITC and 2.5 µl Propidium iodide (50 µg/ml) and incubated in the dark for 15 min. Afterward, the suspension was diluted with 300 µl PBS, and the samples were analyzed by flow cytometry.

2.10.2.4 Staining of intracellular proteins for flow cytometry

The cells were washed with warm PBS and fixed with 0.5% PFA for 2-3 min on ice. Afterward, the cells were trypsinized, washed twice with PBS (centrifuged in between for 6 min at 500 *g*) and blocked/permeabilized (in 0.2% BSA-c and 0.06% Saponin in PBS) for 30 min at RT. Primary antibodies were added, and the incubation continued for another 30 min. After a washing step, the cells were incubated with fluorophore-conjugated secondary antibodies (diluted in 0.2% BSA-c and 0.06 Saponin in PBS) for 45 min at RT. After washing away the secondary antibodies, the cells were resuspended in PBS and analyzed by flow cytometry. CD31 was stained in parallel with NHE1, for which cell permeabilization is necessary since the antibody (NHE11-A, Alpha Diagnostik) recognizes an intracellularly located antigen.

2.10.3 Immunocytochemistry and F-actin staining

Cells that were grown on glass coverslips coated with 0.2% gelatine were washed with HEPES-buffered solution and fixed with 4% PFA at RT. Afterward, the cells were washed with PBS and permeabilized for 5 min with 0.1% Triton in PBS and blocked with 0.2% BSA-c and 5% goat serum in PBS with 0.1% Triton for 30 min. Coverslips were incubated with fluorophore-labeled Phalloidin (not

an antibody;Cat No: A12379, Invitrogen) and washed subsequently for 30 min. The incubation with primary antibodies was done for 1 h at RT or overnight at 4 °C. After washing away the primary antibody, the samples were incubated with fluorophore-conjugated secondary antibodies for 45 min at RT. The cells were then stained with 4',6-diamidino-2-phenylindole (DAPI, 1 µg/ml in PBS) for 10 min, embedded with FluoromoutG, and the slides were stored at 4 °C until microscopic analysis. The coverslips were washed with PBS between each step.

Table 10: Antibodies for Immunofluorescence

Antigen	Type (IgG)	Application	Dilution	Cat. Nr.	Vendor
CD31	rat, monoclonal	MLEC purity	1 : 25	550274	BD Pharmingen
CD31	rabbit, polyclonal	Matrigel plug assay	1 : 200	AP06560PU-N	Acris Antibodies
NHE1	mouse, monoclonal	Cytochemistry	1 : 250	Sc136239	Santa Cruz
Rabbit IgG	goat, polyclonal	Alexa Fluor 488	1 : 250	A11034	Molecular Probes
Mouse IgG	goat, polyclonal	Cy3	1 : 200	A10521	Life Technologies
Rat IgG	goat, polyclonal	Cy5	1 : 100	AP136S	Millipore

2.10.4 Staining of Matrigel plugs

Matrigel plugs excised from mice were fixed overnight with IHC Zinc Fixative (Cat No: 550523, BD Pharmingen) and dehydrated in a Hystokinette (MICROM STP 120 Thermo Fischer Scientific) with the following protocol: 2x 1 h in 70% ethanol, 1 h 96% ethanol, 2x 2 h in 96% ethanol, 2x 2 h in 99% ethanol, 1 h in ethanol:xylene 2:1, 1 hour in ethanol:xylene 1:2, 1 h in xylene, 2 h in melted paraffin and another 3 h in a second vessel with melted paraffin. Finally, the plugs were embedded in paraffin blocks using the MICROM EC 350-1&2 (Thermo Fischer Scientific). Afterward, 5 µm sections were prepared from each plug using the MICROM HM 335 (Thermo Fischer Scientific) and Feather blades (R35; Feather Safety Razor CO.) and mounted on polysine-coated microscope slides (Gerhard Menzel GmbH). The slides were stored at RT.

The prepared sections on the slides were deparaffinized in xylene 3x 10 min, and rehydrated in subsequent 99%, 96%, 70% and 50% ethanol steps for 5 min each and finally in distilled water. The sections were then treated for antigen retrieval in pre-warmed citrate-buffered solution (10 mM tri-Sodium citrate dihydrate; pH 6.0) for 12 min in a microwave at 630 W. The sections were cooled to RT, washed with PBS and permeabilized with 0.01% Triton in PBS for 8 min. The slides were then mounted on Shandon cassettes (Thermo Fischer Scientific). After 30 min incubation in blocking solution (0.01% Triton, 10% goat serum, 0.25% BSA-c in PBS), the sections were subjected to immunofluorescence staining with an anti-CD31 antibody for 2 h and an Alexa Fluor 488 labeled

secondary antibody for 30 min at RT. The sections were then embedded with FluoromountG and covered with coverslips (0.17+/- 0.01mm, selektiert; Gerhard Menzel GmbH).

2.10.5 Immunostaining of mouse tissues

Mice were anesthetized by intraperitoneal injection of a fentanyl (0.05 mg/kg) and Medetomidine (0.5 mg/kg) mixture. The chest was then opened, and a cannula was inserted into the left ventricle to perfuse the mouse with 4% PFA for 3 min. Afterward, the mice were left for another 10 min to be fixed with the perfused PFA, and several organs were collected. The organs were washed with PBS and dehydrated in 30% sucrose in PBS overnight at 4 °C. The organs were then embedded with Tissue-Tek (Ref. 4583, Sakura) and stored at -80 °C until further processing. 10 µm thick cryosections were prepared on adhesive slides using the Leica CM 1850 Cryostat (Cat. No. 0810401; Histobond Marienfeld) and stored at -20 °C.

For immunostaining, the sections were dipped in PBS to wash-away the Tissue-Tek and placed on Shandon cassettes. The sections were blocked with 5% normal goat serum and 0.1% Triton-X in PBS for 30 min at RT. Primary and secondary antibodies were diluted in blocking solution as well. After washing with PBS, the sections were incubated with primary antibody overnight at 4 °C, followed by incubation with a fluorophore-conjugated secondary antibody for 45 min at RT, and then stained with DAPI (1 µg/ml PBS) for 10 min at RT. After each step, the sections were washed with PBS. No staining was necessary for Tomato, as the protein retains its fluorescence activity throughout the histochemical procedure. Finally, the sections were covered with coverslips (0.17+/- 0.01mm, selektiert; Gerhard Menzel GmbH, Germany) after embedding with FluoromountG, and imaged with a confocal microscope (Leica TCS SP5; Wetzlar) under a 400x magnification. (David Böhm has helped with the workload during cryosectioning and staining of the mouse tissues)

2.11 *In-vivo* angiogenesis with Matrigel plug assay

Table 11: Preparation of 4% PFA in PBS solution

PBS for paraformaldehyde

Stock I (base)

Na_2HPO_4 anhydrous	1 M
NaCl	1.36 M

Stock II (acid)

NaH_2PO_4 x H_2O	1 M
NaCl	1.36 M

Mixing

Mix 700 ml H_2O with 17.5 ml Stock II
Titrate to pH 7.4 with Stock I
Fill up to 1 L with H_2O

4% Paraformaldehyde (PFA)

Dissolve 40 g PFA in 400 ml H_2O at 60 °C,
clarify soltution with 4 drops of NaOH H_2O
and fill-up to 500 ml H_2O

Mix 500 ml PBS for PFA with 500 ml dissolved PFA, filter and store at -20 °C

Matrigel is extracellular matrix obtained from mouse sarcomas and processed to reduce its growth factor content. It is stored at -20 °C and thawed on ice before use. After subcutaneous injection, the matrigel solidifies at body temperature forming a plug into which blood vessles from the surrounding tissue can grow. Therefore, the matrigel plug assay is used to study angiogenesis *in vivo*.

The Matrigel plug assay was approved by the local administrative institution (Thüringer Landesamt für Verbraucherschutz, Bad Langensalza, Germany) under the application document "Reg.-Nr. 02-028_13_Regulation und Funktion NHE1 in Endothelzellen_Heller" and the experiment was performed according to the guidelines of the animal welfare committee of the State of Thuringia.

Two separate matrigel plug experiments were performed. In the first one angiogenesis was studied with constitutive *Nhe1*$^{-/-}$ mice and wildtype littermates that were 10-16 days old. In the second experiment angiogenesis was studied in 12-15 weeks old endothelial cell-specific *Nhe1*$^{-/-}$ mice of the genotype *Nhe1*$^{flox/flox}$; *VE-Cadherin*-Cre^{+}, while *Nhe1*$^{flox/flox}$ littermates without Cre were used as control animals. All the mice were of mixed 129SvJ/C57BL/6 background, which were backcrossed for ten generations with C57BL/6 mice in case of the constitutive *Nhe1*$^{-/-}$ mice, or three generations for the endothelial cells specific *Nhe1*$^{-/-}$ mice.

Animals were anaesthetized by intraperitoneal injection of a fentanyl (0.05 mg/kg) and Medetomidine (0.5 mg/kg) mixture and ice-cold Matrigel was injected subcutaneously on each flank; supplemented with heparin (400 µg/ml; 12.7 units/ml) and VEGF (400 ng/ml) for the right flank. Less than 250 µl Matrigel could be injected on each flank in the small pups, compared to 500 µl for the older mice. Few minutes later, the mice were injected intraperitoneally with an antidote mixture of Atipamezole (2.5 mg/kg), Flumazenil (0.5 mg/kg) and Naloxone (1.2 mg/kg). Mice were sacrificed after seven days of incubation. Excised plugs were processed as described in section 2.10.4. Sections from the experiment with constitutive *Nhe1*$^{-/-}$ mice were imaged with a confocal microscope (Leica TCS SP5) at a low magnification (50x) in order to capture the whole plug section in one picture. The sections from the experiment with endothelial cell-specific *Nhe1*$^{-/-}$ mice were scanned at a 200x magnification with an epifluorescent microscope (Nikon Eclipse Ti) and single images were stitched automatically. The Nikon Perfect Focus System was used to keep subsequent pictures in focus. To obtain a representative evaluation for each plug, two sections from at least four levels were collected, discarding 100 µm between each level. The images were analyzed in ImageJ software using Otsu automatic threshold and CD31-positive pixels were normalized against the manually defined plug area. The normalized values for each level were used to calculate the final average for the plug.

2.12 Statistical analysis

The information on the number of subjects used and the statistical test applied are included in respective figure legends. Paired two-tailed Student's t-test or two-way repeated measurements

ANOVA were used to calculate significance after analyzing variance with Holm-Sidak correction for multiple comparisons. $p<0.05$ was considered significant. Data in the figures are represented as mean ± SEM of independent experiments performed with cells from separate preparations. Additionally, some figures contain data from individual experiments depicted as gray lines.

3 Results

3.1 NHE1 downregulation in endothelial cells

In order to develop a tool for investigating the functional importance of NHE1 in endothelial cells, downregulation of the protein by applying the RNAi technology was established. The NHE1 protein was detected in MLEC and HUVEC as a band of around 110 kDa after SDS-PAGE separation and western blotting (Figure 3-1A). The antibody (mab3140; EMD Millipore, USA) also recognized a second band at a slightly larger size but this was most likely unspecific, because it was also observed in MLEC from the constitutive *Nhe1*-knockout (*Nhe1*$^{-/-}$) mice. A pool of four different specific siRNA sequences at a total concentration of 0.5 µg/ml (37 nM) was applied while the control cells received the same amount of scRNA. Figure 3-1C shows that the siRNA transfection resulted in efficient knockdown of NHE1 by 75% on average. NHE1 levels were decreased as soon as 24 h and remained low for at least 120 h after transfection. Consequently, the *in vitro* experiments in HUVEC were performed after downregulation of NHE1 by transfection of siRNA and within the described time.

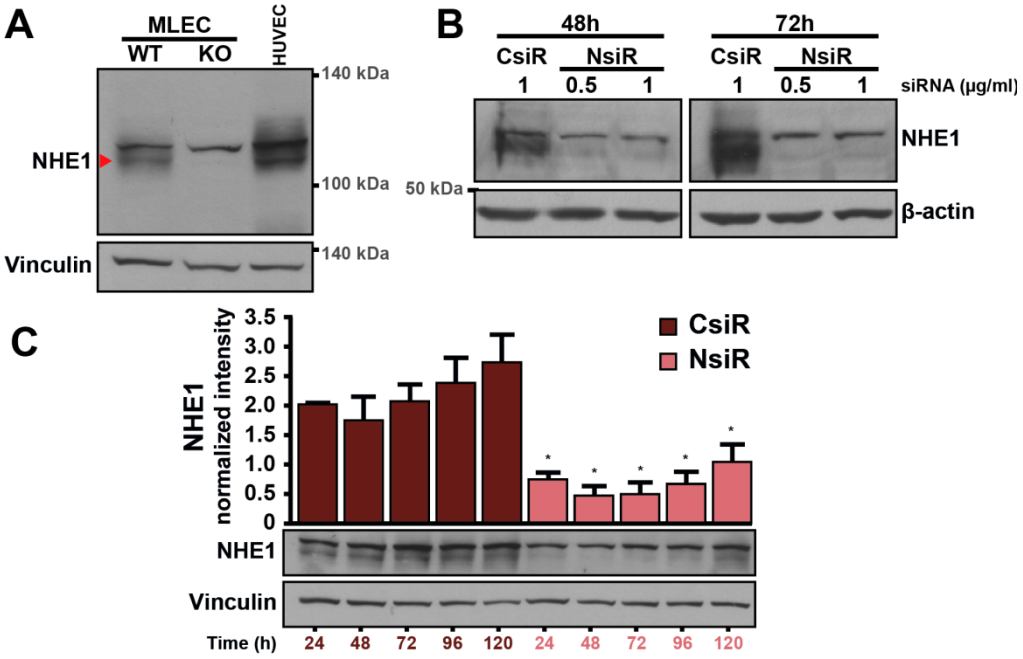

Figure 3-1: Downregulation of NHE1 in HUVEC
NHE1 was detected at approximately 110 kDa with an unspecific band at a slightly larger size recognized by the same antibody (A). Low doses of 0.5 ug/ml siRNA pool (four siRNA sequences) sufficiently downregulated NHE1 (B) for at least 120 h (C), a timeframe used for all experiments. CsiR (scRNA transfected HUVEC), NsiR (NHE1 siRNA transfected HUVEC), n=3 for C, * $p<0.05$ *vs*. CsiR of the respective time point, Student´s t-test.

3.2 NHE1 in regulating pH_i of endothelial cells

NHE1 regulates the intracellular proton concentration. Therefore, the pH_i recovery of acid loaded cells was measured to functionally verify NHE1 knockdown and to study its involvement in endothelial cell pH_i regulation. Cells cultured on glass coverslips were perfused with HEPES-buffered solution to block the contribution of HCO_3^--dependent transporters. HUVEC treated with NHE1 siRNA (NsiR) had a lower basal pH_i than control cells treated with non-targeting siRNA (CsiR) (CsiR: 7.24±0.04; NsiR: 7.09±0.04), and recover their pH_i at a significantly slower rate after cytoplasmic acidification with the ammonium prepulse technique (CsiR: 0.52±0.07 δpH/min; NsiR: 0.22±0.03 δpH/min) (Figure 3-2). The reason for the remaining recovery is unclear, but might be due to maximal activation of residual NHE1 protein since downregulation with siRNA incomplete (see section 3.1).

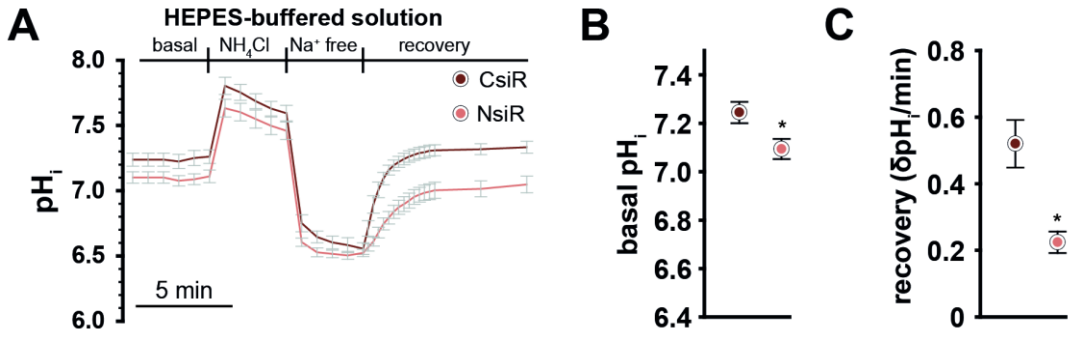

Figure 3-2: Intracellular pH measurements in HUVEC
Traces of pH_i measurements in HEPES-buffered solutions are shown in (A). NHE1 knockdown reduced basal pH_i (B) and pH_i recovery after acidification with ammonium prepulse protocol (B). n=7 for CsiR (scRNA transfected HUVEC), n=10 for NsiR (NHE1 siRNA transfected HUVEC), $p<0.05$, * *vs.* CsiR, Student's t-test.

3.3 In vitro characterization of NHE1 in endothelial cell functions

3.3.1 The role of NHE1 in HUVEC proliferation and survival

Intracellular pH regulation by NHE1 was shown to affect proliferation and survival of different cell types. Therefore, NHE1 knockdown approach was used to evaluate whether the same applies to HUVEC. To this purpose, cell cycle analysis, annexin V and propidium iodide stainings and cell counting were performed in two different sets of experiments. In the first one, HUVEC were cultured in growth medium and analyzed within 48 h after transfection without additional stimulation. In order to mimic similar conditions to the spheroid assay (see section 3.3.3), in the second set HUVEC were transfected, reseeded 48 h later and stimulated with 50 ng/ml VEGF 24 h after reseeding (time 0 h). Further analyses were performed in the next two days (time 24 h and 48 h after stimulation or 96 or 120 h after transfection, respectively).

The first series of experiments showed that downregulation of NHE1 by siRNA repressed cell growth. Alterations in the cell cycle between CsiR and NsiR cells were observed 24 h after transfection. NsiR

cells showed a higher proportion in the G_0/G_1 phase of the cell cycle and a lower proportion in the S plus G_2/M phase (61±1% and 40±3%, respectively) when compared to CsiR cells (42±2% and 57±1%, respectively) suggesting a lower proliferative capacity in NHE1-depleted cells. Consequently, 48 h after transfection the cell number in NsiR samples was significantly reduced by 35%. At the same time point, control cells approached confluence and proliferation decreased, thus no difference was observed anymore in the cell cycle analysis. Since NsiR cells were viable in growth medium over 48 h after transfection, the difference in cell count cannot be explained by cell loss.

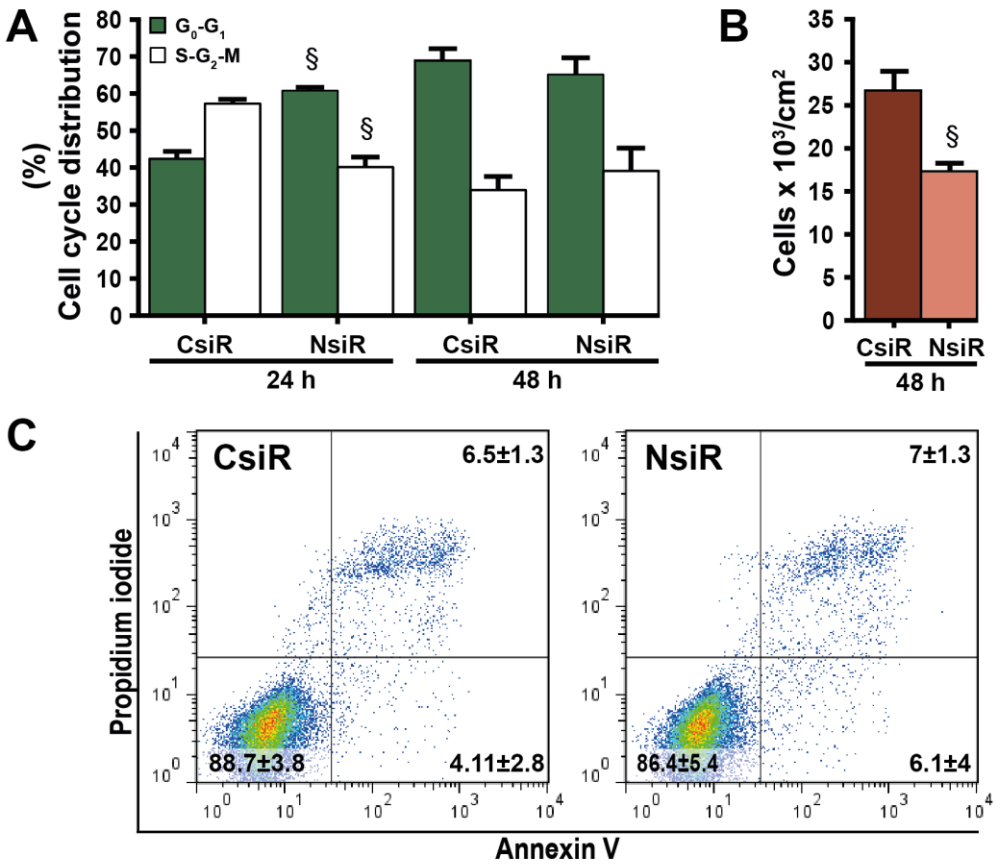

Figure 3-3: HUVEC proliferation in growth medium

Cells were stained with propidium iodide and analyzed by flow cytometry for cell cycle distribution at 24 and 48 h after transfection (A). 48 h after transfection, cells were counted (B) or analyzed for cell death and apoptosis (C). NHE1 knockdown reduced cell cycle progression within 24 h, which was reflected in lower cell count at 48 h after transfection. The number of apoptotic and dead cells was comparable between samples (C). CsiR (scRNA transfected HUVEC), NsiR (NHE1 siRNA transfected HUVEC), n=3 (A, C), n=6 (B); $p<0.05$, § *vs*. CsiR, Student's t-test.

In the second series of experiments, transfected cells were reseeded to determine the cell growth curve after VEGF stimulation in low serum medium (2% FCS). VEGF induced a significant increase in cell number in both control and NHE1 siRNA-treated HUVEC after 48 h. However, NHE1 knockdown reduced VEGF-stimulation HUVEC proliferation after by 24%, while the same trend was observed for unstimulated samples (Two Way RM ANOVA, $p<0.01$ for VEGF, $p=0.053$ for unstimulated).

Evaluation of the sub-G_1 population in cell cycle analysis was used to estimate cell survival. Figure 3-4B shows that VEGF stimulation led to a considerable decrease of particles in the sub-G_1 fraction in control conditions and after downregulating NHE1, which indicates a potent survival effect in both situations. Thus, while VEGF was only a weak stimulus for HUVEC proliferation, it had strong antiapoptotic effects. These effects were seen 24 and 48 h after stimulation, even though the proportion of apoptotic cells was much higher after 48 h. The latter is due to the low serum conditions in this experiments leading to induction of apoptosis. Although the number of dying NHE1-siRNA-treated cells tended to increase compared to control cells, the difference was statistically not significant.

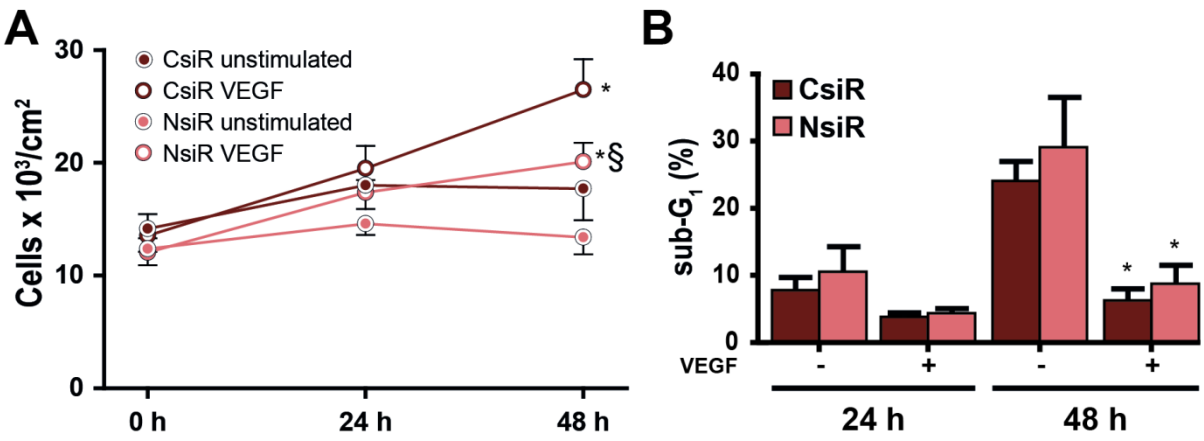

Figure 3-4: VEGF-induced HUVEC proliferation
48 h after transfection with siRNA, cells were reseeded for growth curve (A) and sub-G_1 analysis (B). Cells were starved for 4 h in low serum medium, to which VEGF was added. Samples were analyzed at the time of stimulation (0 h) as well as 24 and 48 h later. HUVEC proliferated less upon VEGF stimulation if NHE1 was downregulated. Additionally, sub-G1 analysis showed that the survival effect of VEGF was comparable between control and NHE1-depleted cells. CsiR (scRNA transfected HUVEC), NsiR (NHE1 siRNA transfected HUVEC), n=7 (A), n=3 (B); $p<0.05$, * *vs.* respective unstimulated control, § *vs.* CsiR VEGF, Two Way RM ANOVA.

Taken together, NHE1 depletion slowed down HUVEC proliferation both in growth medium immediately after transfection and later after VEGF stimulation in low serum medium. The survival effect of VEGF did not seem to be affected by NHE1 knockdown.

3.3.2 The role of NHE1 in HUVEC migration

NHE1 has been shown to be involved in cell migration in different cell types, in which mainly the effect of NHE1 overexpression was observed. In these studies NHE1 was localized at the leading edge of migrating cells [49, 103]. In the current study, similar observations were made. Figure 3-5 shows that NHE1 is co-stained with actin at cell protrusions in a single spontaneously migrating endothelial cell. In a confluent HUVEC monolayer NHE1 is stained at cell-cell contacts.

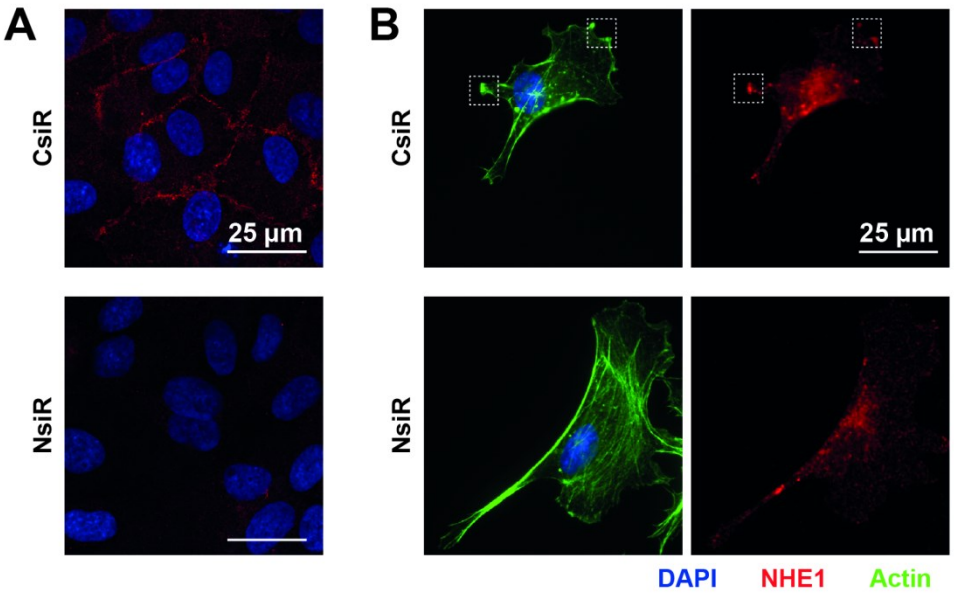

Figure 3-5: Immunocytochemistry of NHE1 in HUVEC
NHE1 is stained at the cell-cell contacts of a confluent endothelial cell culture (A). In a spontaneously migrating cell of a subconfluent culture, NHE1 is co-stained with actin at plasma membrane protrusions (B). CsiR (scRNA transfected HUVEC), NsiR (NHE1 siRNA transfected HUVEC).

Based on this observation, three different assays were used to study the role of NHE1 in HUVEC migration: wound healing, transwell and chemotaxis assay.

3.3.2.1 Transwell migration assay

Cells transfected with siRNA were starved for 3 h in serum-free medium and stimulated with 50 ng/ml VEGF or 0.1 µM S1P for 4 h in a transwell system. Thereafter, cells were fixed, stained and the number of migrated cells was analyzed. Basal migration was similar between CsiR and NsiR cells (Figure 3-6). In contrast to what was expected from literature data [104-106], VEGF did not stimulate HUVEC migration neither in control cells nor in NHE1-depleted cells under the experimental conditions used. However, S1P potently induced migration. The migratory response was significantly reduced by 31% by NHE1 downregulation, suggesting that NHE1 is an important factor for HUVEC migration.

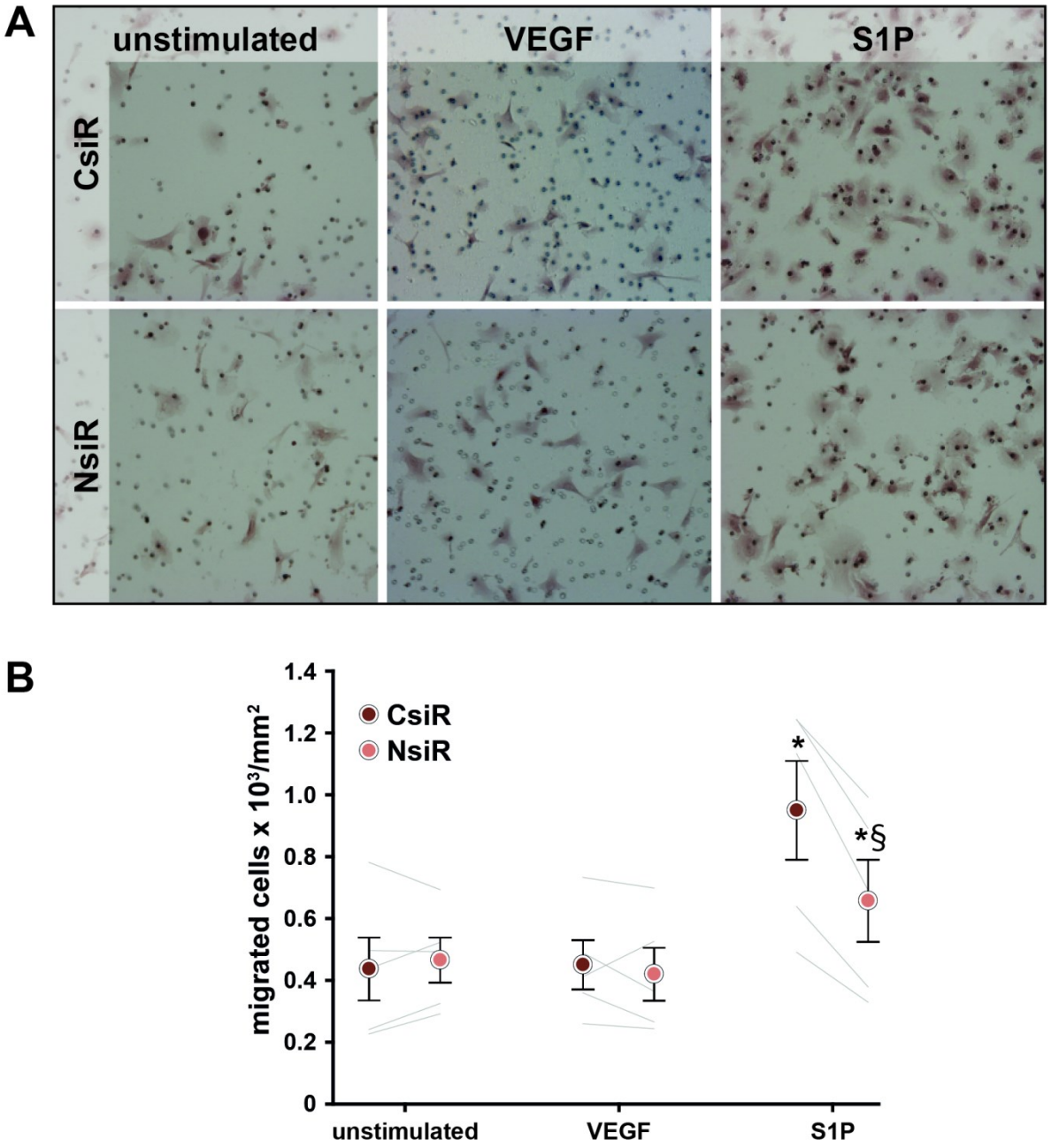

Figure 3-6: Transwell migration assay
HUVEC transfected with siRNA were seeded on transwell inserts and either left to migrate spontaneously, or stimulated with VEGF (50 ng/ml) or S1P (0.1 µM) for 4 h. Representative images are shown in (A). VEGF was unable to induce migration in the conditions used, whereas S1P was a strong stimulus and its effect was dampened when NHE1 was downregulated (B). CsiR (scRNA transfected HUVEC), NsiR (NHE1 siRNA transfected HUVEC), n=5, $p<0.001$, * *vs.* unstimulated, § *vs.* CsiR S1P, Two Way RM ANOVA.

3.3.2.2 Wound healing assay

HUVEC were seeded at high confluency (1.5 x 10^5 cells/cm^2) on ibiTreat culture dishes with inserts. After removing the insert, a cell-free area between two monolayers was created, the so-called wound, into which cells could migrate. After preincubation in low serum medium for 2 h, cells were either left unstimulated or stimulated with VEGF (50 ng/ml) or S1P (0.1 µM). After six hours, migration slowed

down when both sides of the wound reached each other and the wound closed completely within 12-16 h in the stimulated samples. Therefore, the healing was quantified by counting cells in 2 h intervals within 6 h after stimulation. Whereas VEGF only slightly induced wound healing, S1P significantly stimulated healing by twofold (Figure 3-7). Importantly, NHE1 knockdown significantly inhibited wound closure by 21% in S1P-stimulated samples. This further confirms NHE1´s involvement in the migratory process in HUVEC. It was observed though that the unstimulated cells in the very dense monolayer died abundantly under low serum conditions, thus the VEGF and/or S1P effect on wound closure could be partly due to the survival effect as well.

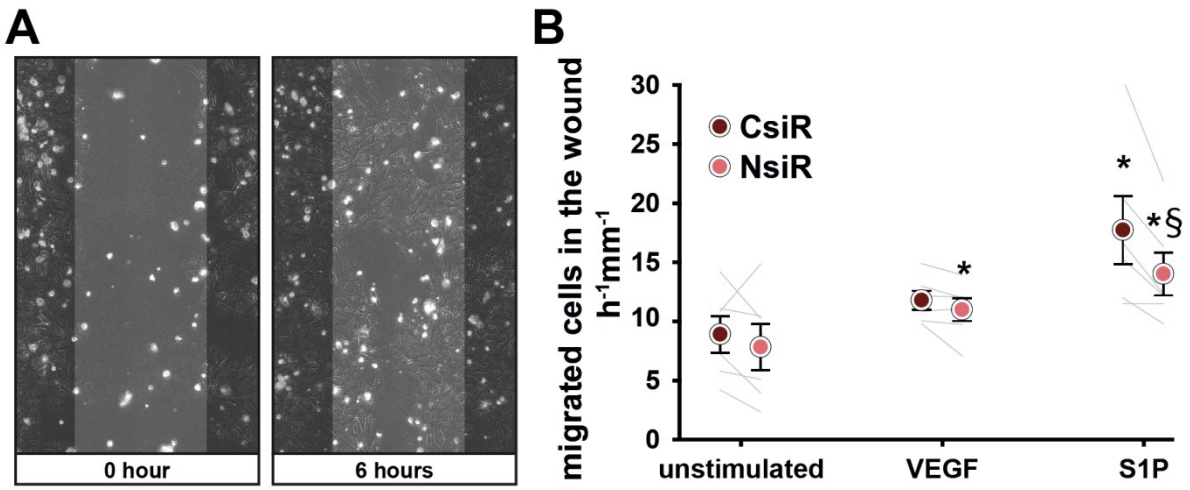

Figure 3-7: Wound healing assay
HUVEC transfected with siRNA were seeded on ibiTreat culture dishes with wound healing inserts. After removing the inserts, cells were starved for 2 h in low serum medium to which VEGF (50 ng/ml) or S1P (0.1 µM) was then added. Subsequently, migration was tracked over 6 h by counting the cell nuclei in the wound area (A). Whereas S1P promoted wound closure, VEGF had only a slight effect (B). NHE1 knockdown significantly slowed down the healing in S1P-stimulated samples (B). CsiR (scRNA transfected HUVEC), NsiR (NHE1 siRNA transfected HUVEC), n=6, $p<0.05$, * *vs.* respective unstimulated control, § *vs.* CsiR S1P, Two Way RM ANOVA.

3.3.2.3 2D chemotaxis assay

As a third approach, 2D chemotaxis slides (ibidi, ibiTreat) were used to test how HUVEC react to gradients of VEGF (50 ng/ml) or S1P (0.1 µM). As expected, net cell movement in the unstimulated samples is close to zero for both the parallel (∥) and transverse axis (⊥). VEGF was unable to induce polarization and movement towards the gradient, while 24 h of S1P stimulation led to cell polarization and ~150 µm net movement towards the stimulus (Figure 3-8). S1P-induced responses regarding velocity and forward migration index (FMI) in the parallel axis were reduced in NHE1-depleted cells although this did not reach statistical significance. However, a 32% significant inhibition of the displacement of center of mass was seen in NHE1 knockdown HUVEC, again indicating negative regulation of migration by NHE1 (Figure 3-9). Overall, the three different approaches suggest that

NHE1 is important in migration of endothelial cells, as its downregulation inhibits S1P-induced migration.

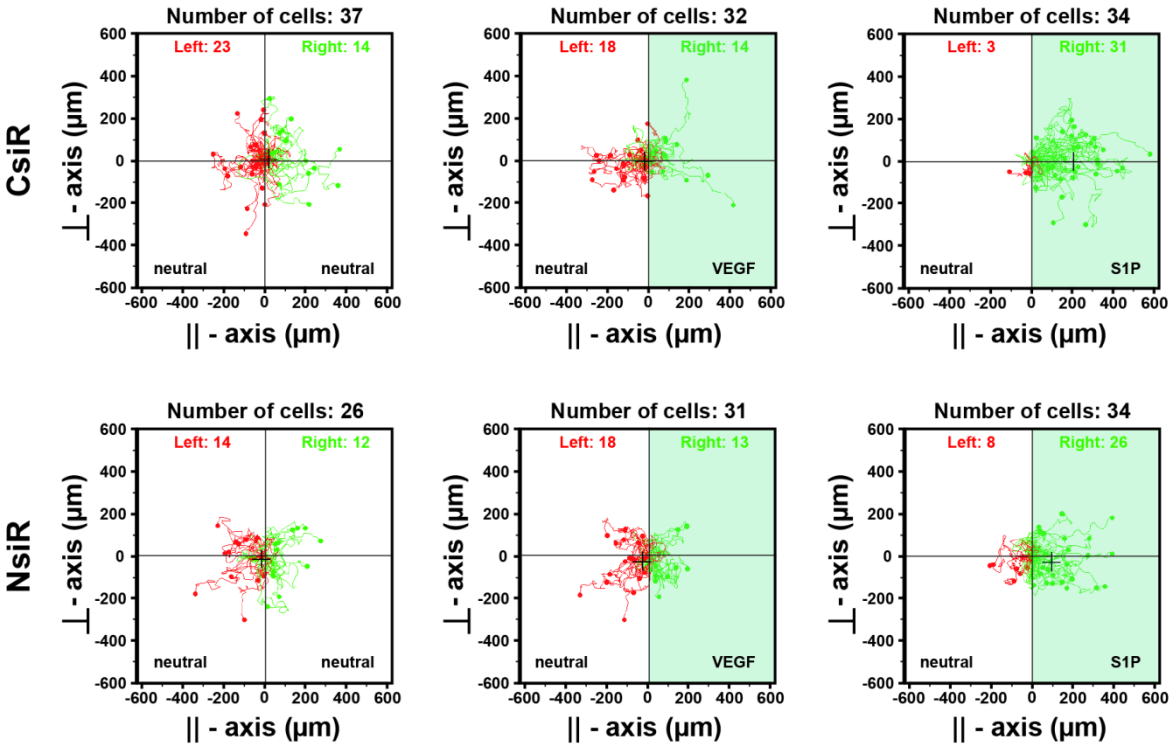

Figure 3-8: Representative traces of 2D chemotaxis
Migrating HUVEC were traced moving within the chemotactic gradient of VEGF (50 ng/ml) or S1P (0.1 µM) or in the absence of a stimulus. Cells migrating to the left of the parallel (∥) axis are labeled in red, whereas cells migrating towards the stimulus in green. S1P, but not VEGF, was able to induce chemotaxis. CsiR (scRNA transfected HUVEC), NsiR (NHE1 siRNA transfected HUVEC).

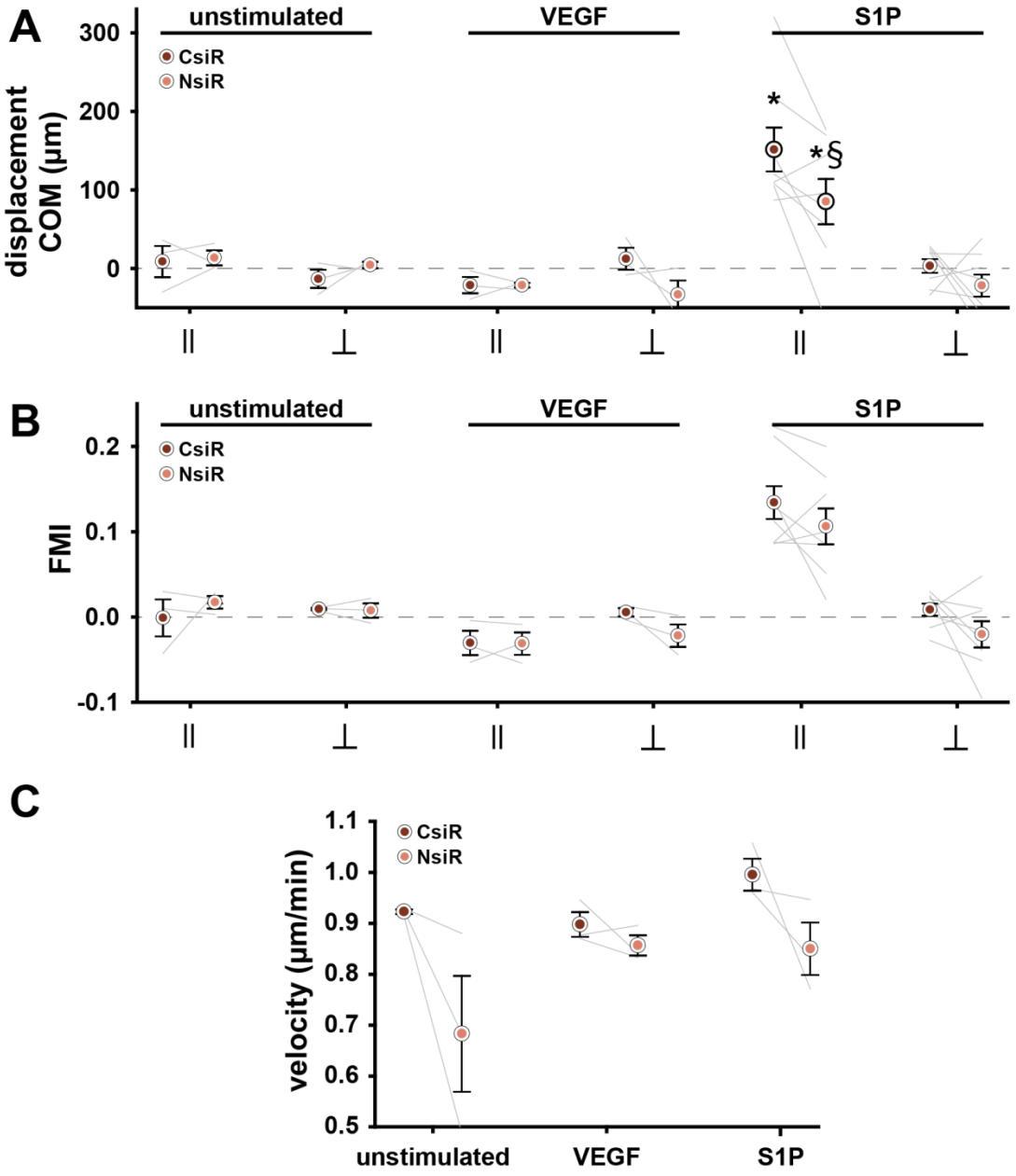

Figure 3-9: 2D chemotaxis assay

HUVEC transfected with siRNA were seeded on ibidi chemotaxis slides (ibiTreat surface) and 4 h later medium was changed to low serum medium. After 2 h VEGF (50 ng/ml) or S1P (0.1 µM) was added on one side of the chamber and migration was tracked within 24 h. Approximately 30 cells per chamber were traced to calculate migration velocity (C) as well as the displacement of Center of Mass (COM) (A) and the Forward Migration Index (FMI) (B) for both the parallel (∥) and the perpendicular (⊥) axis. NHE1 knockdown reduced HUVEC chemotaxis after S1P stimulation as seen for the displacement of COM**.** CsiR (scRNA transfected HUVEC), NsiR (NHE1 siRNA transfected HUVEC), n=3 for unstimulated and VEGF, n=8 for S1P; $p<0.05$, * *vs.* respective unstimulated control, § *vs.* CsiR S1P parallel axis, Student's t-test.

3.3.3 The role of NHE1 for *in vitro* angiogenesis

Based on the data from proliferation and migration experiments, NHE1 was further tested for potentially participating in the complex process of angiogenesis. To this end, endothelial spheroids were embedded in a 3D fibrin gel, where they produce capillary-like sprouts upon angiogenic stimulation, which was quantified as a measure for angiogenesis *in vitro*. Spheroids from control or NHE1-depleted HUVEC were stimulated with two different VEGF concentrations, 10 or 50 ng/ml. After 48 h, sprout number and length were quantified. Unstimulated spheroids did not sprout, while VEGF induced a clearly visible angiogenic response (Figure 3-10). The number of VEGF-stimulated sprouts was significantly reduced by 56% when NHE1 was downregulated (Figure 3-10B). Similarly, the average sprout length was significantly shorter by 20% (Figure 3-10C). Taken together, as hypothesized from proliferation and migration data, NHE1 supported angiogenesis *in vitro* since its downregulation inhibited VEGF-induced sprouting.

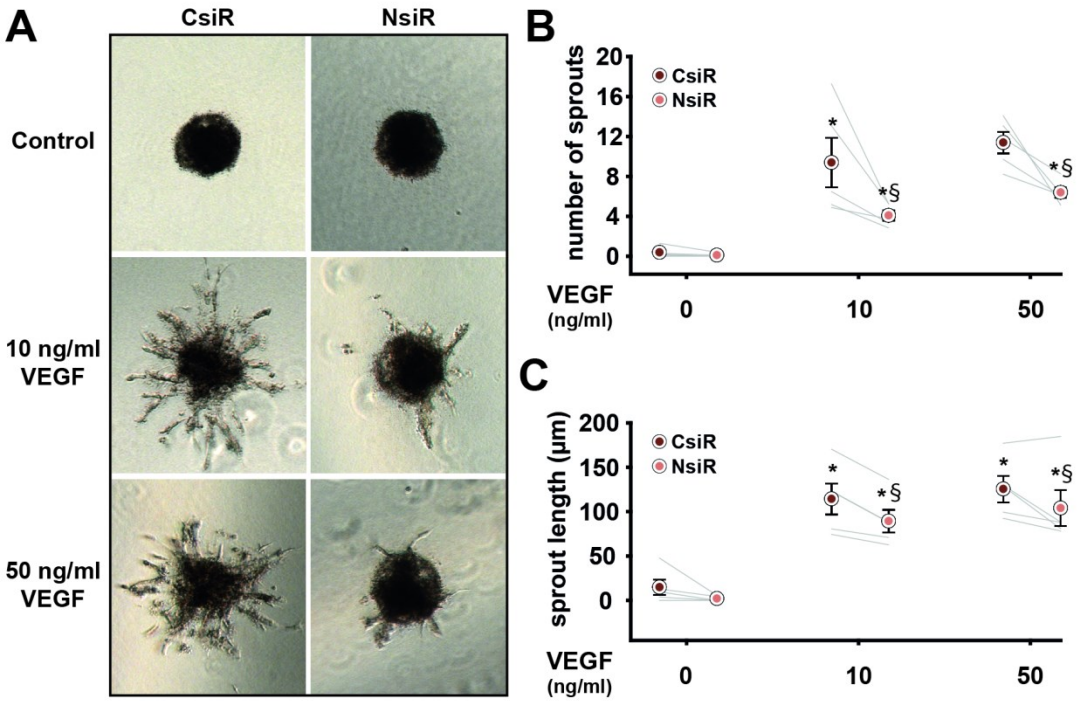

Figure 3-10: Importance of NHE1 in VEGF-induced spheroid sprouting
Spheroids generated from control or NHE1siRNA-transfected HUVEC were left unstimulated in low serum medium or stimulated with two different VEGF concentrations (10 ng/ml or 50 ng/ml) and analyzed after 48 h (A). NHE1 downregulation dampened both VEGF-induced sprout number (B) and length (C). CsiR (scRNA transfected HUVEC), NsiR (NHE1 siRNA transfected HUVEC), n=5, $p<0.05$, * *vs.* respective unstimulated control, § *vs.* CsiR, Two Way RM ANOVA.

3.4 NHE1 in endothelial cell signaling

3.4.1 Interaction between NHE1 and VEGF signaling

In order to understand the cellular mechanisms of how NHE1 may affect VEGF-induced angiogenesis, VEGF-induced signaling and gene expression were analyzed in NHE1-depleted HUVEC using western blot analysis and qPCR, respectively. The analysis of VEGF-induced signaling cascades did not show differences between control cells and NHE1-depleted cells. As seen in Figure 3-11: VEGF-induced VEGFR2 phosphorylation, VEGF-induced VEGFR2 phosphorylation was quantitatively similar in NsiR and CsiR HUVEC (Figure 3-11).

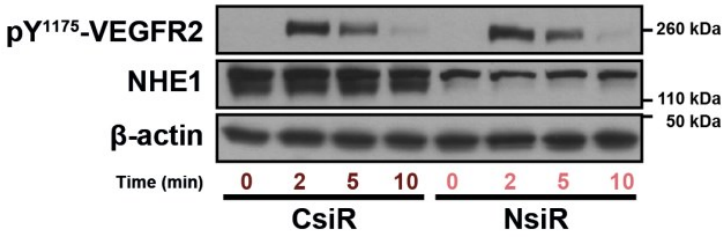

Figure 3-11: VEGF-induced VEGFR2 phosphorylation
HUVEC were starved for 4 h in serum-free medium and then for 30 min in HEPES-buffered solution supplemented with 0.25% HAS. Afterwards, cells were stimulated for the respective time points with 50 ng/ml VEGF. NHE1 downregulation did not alter the quantity or the kinetics of VEGFR2 phosphorylation. CsiR (scRNA transfected HUVEC), NsiR (NHE1 siRNA transfected HUVEC).

Moreover, extent and kinetics of phosphorylation of four downstream enzymes were similar in NsiR and CsiR HUVEC after VEGF stimulation: pT^{172}-AMPK, pS^{1196}-eNOS, $pT^{202/204}$-ERK 1/2 and pS^{473}-AKT (Figure 3-12). Both controls and NHE1-depleted cells showed a clear transient phosphorylation of AMPK, ERK1/2 and eNOS with peaks at two to five minutes after VEGF stimulation. The phosphorylation of AKT showed a maximum at ten to fifteen minutes and was also comparable between NsiR and CsiR HVUEC.

To understand whether NHE1 downregulation in HUVEC alters the expression of angiogenic genes, a qPCR angiogenesis array was performed. The 84 genes included in this array were grouped in quickly induced and slowly induced ones and evaluated after 4 or 24 h of VEGF treatment, respectively. This grouping followed an extensive review of the literature for the kinetics of gene expression in HUVEC after VEGF stimulation. Surprisingly, VEGF induced more than twofold changes in the expression of only 13 genes, which are depicted Figure 3-13A.

A limited number of genes was differentially expressed in HUVEC when NHE1 was downregulated and cells were stimulated with VEGF or kept unstimulated (Figure 3-13B). These include genes for angiopoietin 1 and 2 (ANGPT1, ANGPT2), brain-specific angiogenesis inhibitor 1 (BAI1), tissue

factor (F3), the chemokines CXCL10 and interleukin 8 (IL8), the matrix metalloprotease 9 (MMP9), plasminogen activator inhibitor-1 (PAI-1) and the S1P receptor 1 (S1PR1). For instance, under basal conditions an upregulation in NHE1-depleted cells was seen for ANGPT1 and a downregulation for CXCL10 and PAI-1.

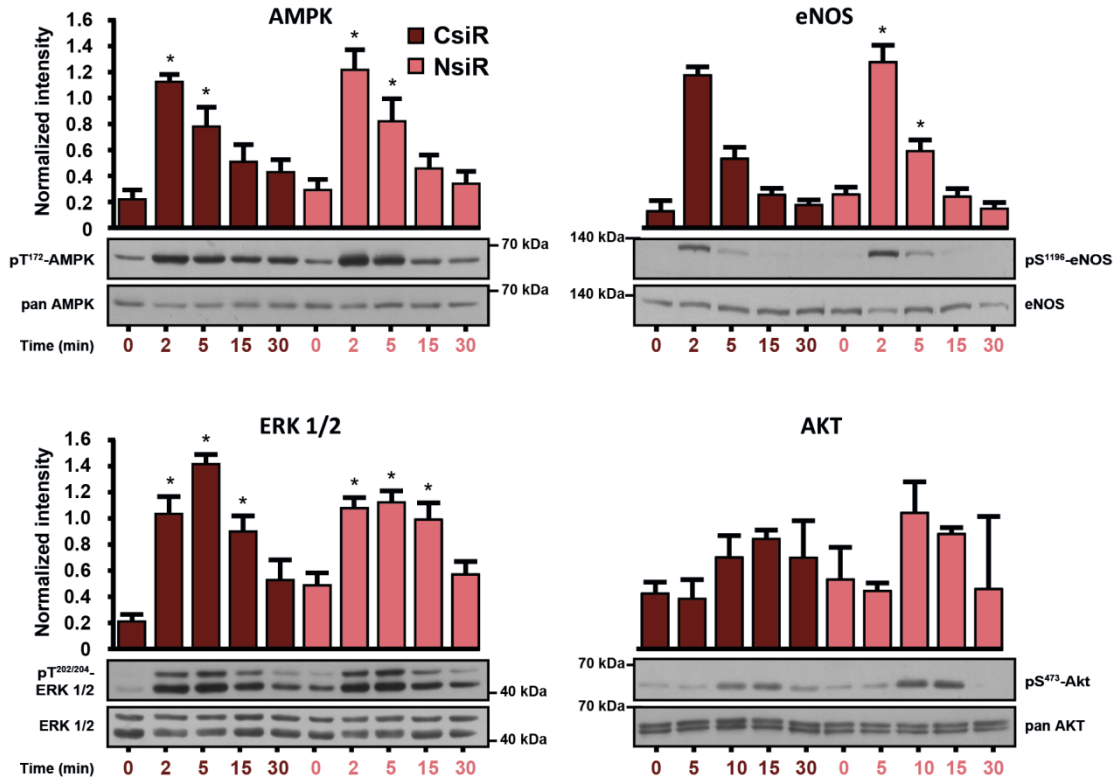

Figure 3-12: VEGF-induced signaling after NHE1 downregulation

Phosphorylation of several downstream targets of VEGFR2 was monitored over 30 min of stimulation with 50 ng/ml VEGF. Cells were first starved in serum-free medium for 4 h and incubated further for 30 min in HEPES-buffered solution supplemented with 0.25% HSA, in which VEGF was then added. NHE1 downregulation did neither alter the quantity nor the kinetics of phosphorylation of AMPK, eNOS , ERK1/2 (all n=4) and AKT (n=2). $p<0.05$, **vs*. respective unstimulated control (0 min), Student´s t-test. pT (phospho threonine), pS (phospho serine). CsiR (scRNA transfected HUVEC), NsiR (NHE1 siRNA transfected HUVEC).
AMPK: *AMP-activated protein kinase*, eNOS: *endothelial nitric oxide synthase*, ERK 1/2: *extracellular signal-regulated kinase 1/2*, AKT: *protein kinase B*.

Differences in VEGF-induced effects between control and NHE1-depleted cells were seen for CXCL10 (stronger inhibition in response to VEGF) and F3, MMP9 and IL8 (lower stimulation in response to VEGF). However, in general, the differences were not striking and most of these genes did not reach the twofold change threshold. The strongest effect was seen for ANGPT1 (twofold), but this result could not be reproduced with different primers (data not shown). Nevertheless, the identified genes could be promising to be analyzed at a different VEGF stimulation time-point and with other cell batches in further experiments.

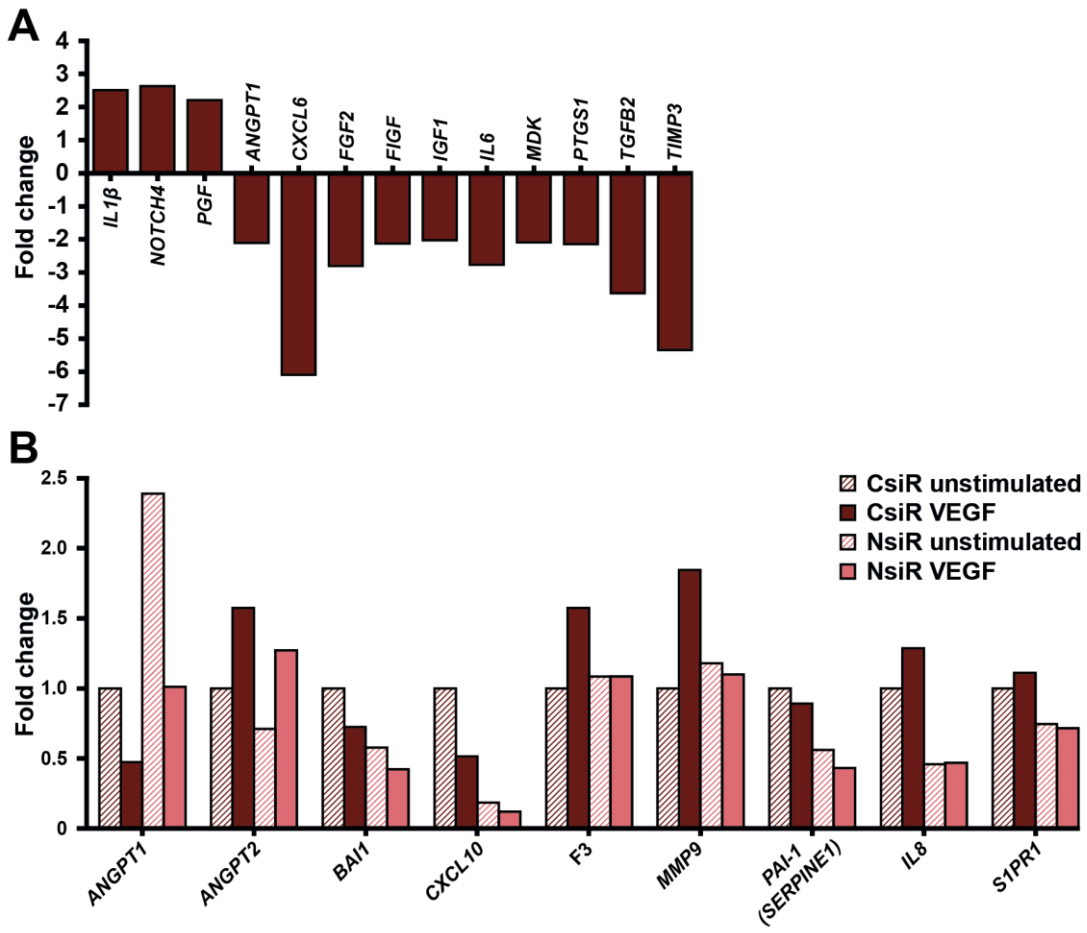

Figure 3-13: VEGF regulation of gene expression during angiogenesis

HUVEC were stimulated with VEGF (50 ng/ml) for 4 or 24 h and the expression of 84 angiogenesis related genes was analyzed with a qPCR angiogenesis array. In the conditions used *in vitro*, VEGF altered 13 genes by more than twofold (A). NHE1 knockdown seems to moderately influence the expression of a number of genes (B). Fold change: (2^(-ΔΔCt)) of the Test *vs.* Control, upregulation >1, downregulation <1. CsiR (scRNA transfected HUVEC), NsiR (NHE1 siRNA transfected HUVEC).

IL1β: interleukin 1β, NOTCH4: *neurogenic locus notch homolog protein 4*, PGF: *placental growth factor*, ANGPT1: *angiopoietin 1*, ANGPT2: *angiopoietin2*, CXCL6: *chemokine (C-X-C motif) ligand 6*, FGF2: *fibroblast growth factor 2*, FIGF: *c-fos induced growth factor*, IGF1: insulin-like growth factor 1, IL6: interleukin 6, MDK: midkine, PTGS1*: prostaglandin-endoperoxide synthase 1*, TGFB2: transforming growth factor beta 2, TIMP3: TIMP metallopeptidase 3, BAI1: *brain-specific angiogenesis inhibitor 1*, CXCL10: *chemokine (C-X-C motif) ligand 10*, F3*: tissue factor*, MMP9: *matrix metalloproteinase-9 precursor*, PAI-1: *plasminogen activator inhibitor-1*, IL8: *interleukin 8*, S1PR1: *sphingosine-1-phosphate receptor 1*.

3.4.2 S1P signaling in NHE1-depleted cells

Since knockdown of NHE1 in HUVEC affected S1P-induced migration, the effect on S1P signaling was also checked. Therefore, cells with normal and downregulated NHE1 were time-dependently stimulated with S1P and the phosphorylation of several downstream targets of S1P receptor was monitored. S1P induced a fast phosphorylation of eNOS, ERK1/2 or AKT reaching maximal values after 2 min (Figure 3-14). NHE1 knockdown did not alter the extent or the dynamics of S1P-induced phosphorylation events.

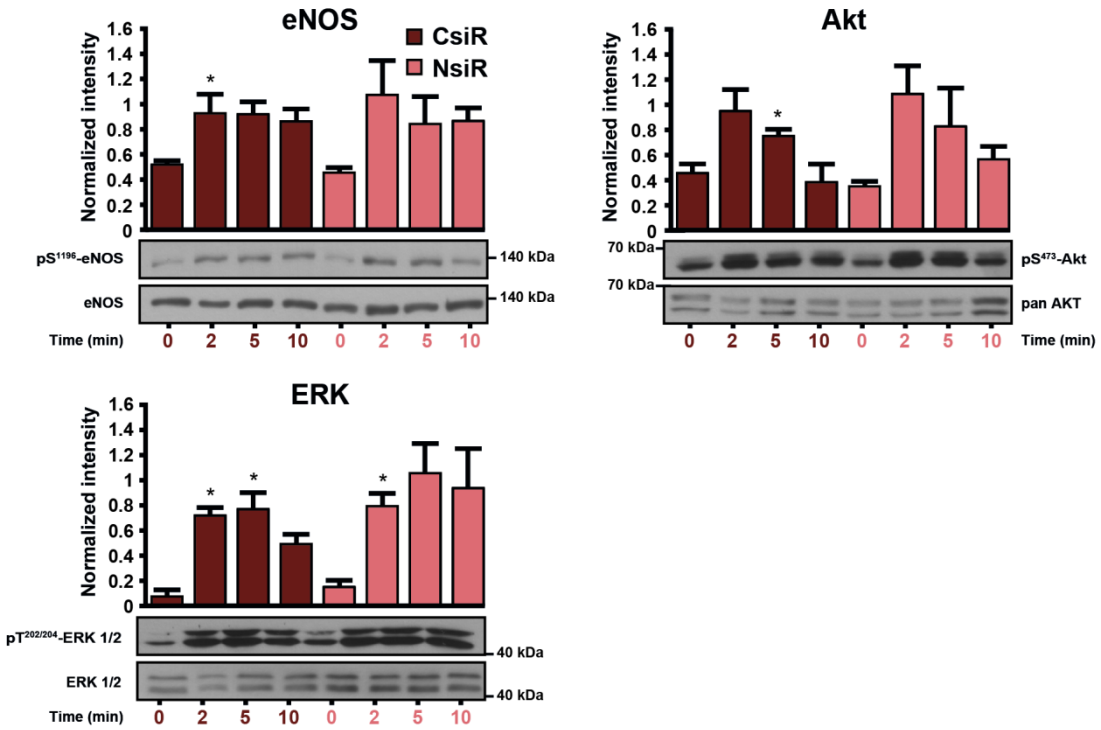

Figure 3-14: S1P-induced signaling after NHE1 downregulation

Phosphorylation of several downstream targets of the S1PR1 was monitored over 30 min of stimulation with 0.1 µg/ml S1P. NHE1 down-regulation did neither alter the quantity nor the kinetics of phosphorylation of eNOS, ERK1/2 (all n=4) and AKT (n=2). pT (phospho threonine), pS (phospho serine). CsiR (scRNA transfected HUVEC), NsiR (NHE1 siRNA transfected HUVEC), $p<0.05$, **vs*. respective unstimulated control (0 min), Student´s t-test.

eNOS: *endothelial nitric oxide synthase*, ERK1/2: *extracellular signal-regulated kinase 1/2*, AKT: *protein kinase B*.

3.5 NHE1 expression under growth factor treatment and hypoxia

In addition to studies of signaling and gene expression, growth factor effects on NHE1 expression were analyzed (Figure 3-15). 50 ng/ml VEGF or 0.1 µM S1P did not increase NHE1 expression after 24 or 48 h of incubation compared to control medium with 2% FCS. However, a moderate increase of NHE1 expression was observed upon serum depletion (comparing medium supplemented with 17.5% FCS, 2.5% human serum and mitogen and medium with 2% FCS, respectively) (not significant).

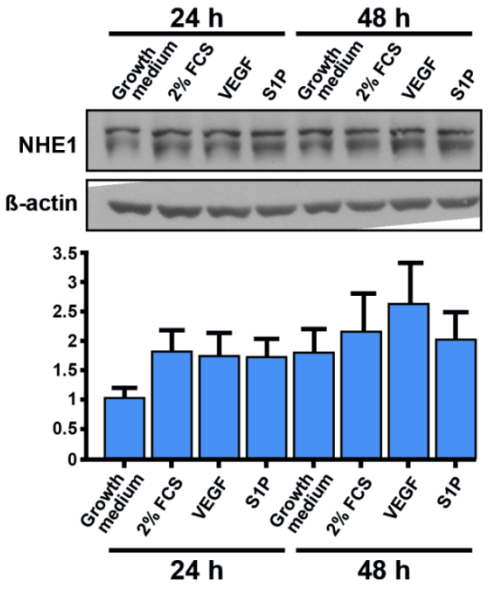

Figure 3-15: The effect of growth factors on NHE1 protein levels

HUVEC were cultured in low serum medium (2% FCS) only or supplemented with VEGF (50 ng/ml) or S1P (0.1 uM) for 24 and 48 h. Growth medium (containing 17.5% FCS, 2.5% human serum, and mitogen) was used as an additional control. Neither VEGF nor S1P increased NHE1 expression compared to 2% FCS medium. Under growth factor rich conditions NHE1 expression was slightly lower compared to low serum medium. n=3.

Endothelial cells undergo hypoxic stress, for instance when sprouting into hypoxic areas, and respond with changes in gene regulation mediated by HIF1α or HIF2α. Therefore, the effect of hypoxia (1% O_2 experimentally) on NHE1 expression in HUVEC was investigated. Figure 3-16 shows that HUVEC accumulate both HIF1α and HIF2α after 8 h of hypoxia and maintain the expression of both transcription factors for up to 72 h. During this time, HIF1α expression decreased while HIF2α remained equally high. An increased HIF1α/2α expression was also seen after incubating HUVEC with $CoCl_2$, a chemical inducer of HIF. Importantly, hypoxia led to a slow increase of NHE1 expression (Figure 3-16). After 72 h NHE1 protein was significantly doubled in hypoxic samples compared to normoxic controls. In addition, $CoCl_2$ had the same effect like hypoxia.

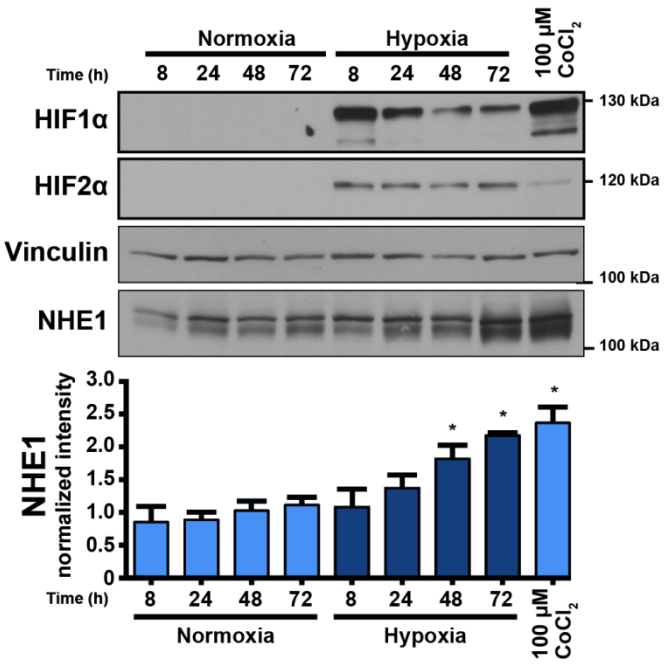

Figure 3-16: NHE1 expression in HUVEC under hypoxia (1% O_2)
NHE1 expression increased over time, reaching twofold higher levels in hypoxic samples compared to normoxic controls after 72 h. Chemical hypoxia using 100 µM $CoCl_2$ also increased the amount of NHE1 protein. HIF1α and HIF2α were both detectable in hypoxia and during chemical hypoxia. Whereas HIF1α levels dropped after 8 h, HIF2α stayed stable over time. n=4 for NHE1, n=3 for HIF1α, n=1 for HIF2 α, $p<0.05$, * *vs.* normoxic control, Student's t-test.

To check whether the increased expression of NHE1 in hypoxia was mediated by HIF, an siRNA approach was used. Figure 3-17 shows that application of specific siRNAs led to efficient downregulation of either HIF1α or HIF2α by approximately 85%. When HIF1α was downregulated, the hypoxia-induced NHE1 expression remained high (Figure 3-17). In contrast, downregulation of HIF2α prevented the effect of 72 h hypoxia on NHE1 expression suggesting that it was mediated by HIF2α. Interestingly, the accumulation of HIF1α and HIF2α seems to be interlinked. Upon knockdown of HIF2α, HIF1α levels significantly raised while HIF2α was moderately increased in cells where HIF1α was downregulated.

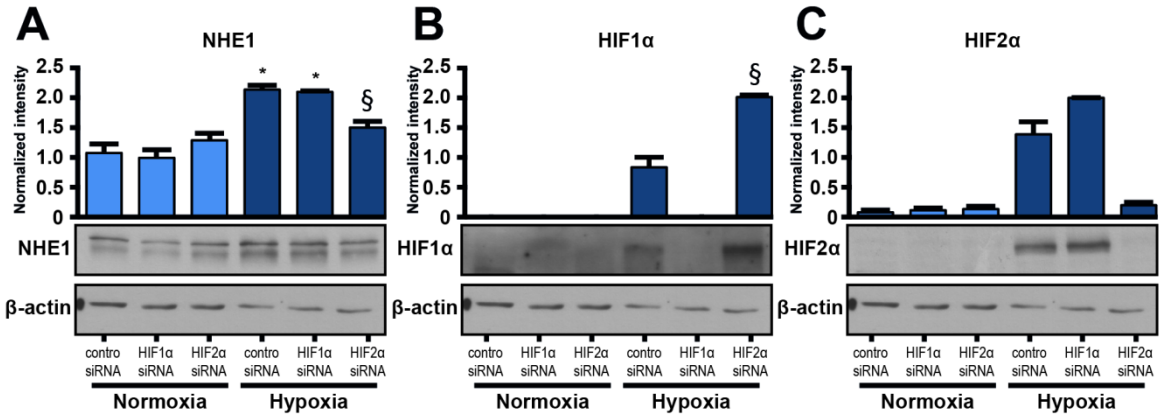

Figure 3-17: Expression of HIF1α, HIF2α and NHE1 in hypoxia
HUVEC incubated in hypoxia for 72 h double their NHE1 levels (A). This effect probably depends on HIF2α as its knockdown inhibits the increase in NHE1, whereas HIF1α knockdown has no effect. Additionally, HIF1α increases two fold if HIF2α is knocked down (B). n=4, $p<0.05$, * *vs.* normoxic control, § *vs.* CsiR and HIF2α siRNA hypoxia, Two Way RM ANOVA

To see whether induction of NHE1 in hypoxia is due to metabolites or proteins released into the medium upon hypoxia, cells were incubated in hypoxia or normoxia for 72 h and cell culture medium (preincubated for pH and O_2 adjustment) was refreshed every 24 h (Figure 3-18). The medium exchange was able to significantly inhibit the increase in NHE1 expression after 72 h in hypoxia suggesting HIF2α-mediated NHE1 expression may involve factors released into the medium.

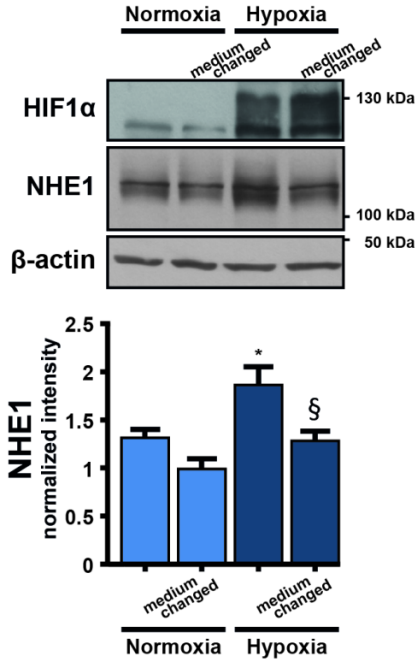

Figure 3-18: Effect of medium exchange on hypoxia-induced NHE1 expression

HUVEC were incubated for 72 h under hypoxic condition and medium (pre-incubated for pH and O_2 equilibration) was changed every 24 h. Under these conditions NHE1 levels remained comparable to normoxic controls while increased NHE1 abundance was seen in samples without medium change. n=4, $p<0.05$, * *vs*. normoxic control, § *vs*. hypoxic control, Two Way RM ANOVA.

3.6 The role of NHE1 for *in vivo* angiogenesis – Matrigel plug assay

Since, *in vitro* data suggested that NHE1 might be important for angiogenesis, a Matrigel plug assay was applied as an *in vivo* approach to study angiogenesis in wild type and constitutive *Nhe1*$^{-/-}$ mice. Ten to sixteen days old mice had to be used, because the constitutive *Nhe1*$^{-/-}$ mice die between two and four weeks. Seven days after subcutaneous injection of Matrigel with or without VEGF, the generated plugs were excized and analyzed for the formation of new blood vessels. The latter was done by immunofluorescence staining of the endothelial marker CD31 in Matrigel sections and quantified by normalizing CD31 positive pixels to the plug area. Due to the low weight of the young mice and smaller volume of injected Matrigel, however, some plugs were smaller than required in original protocols and did not reach the quality necessary for reliable quantification of vascular endothelium.

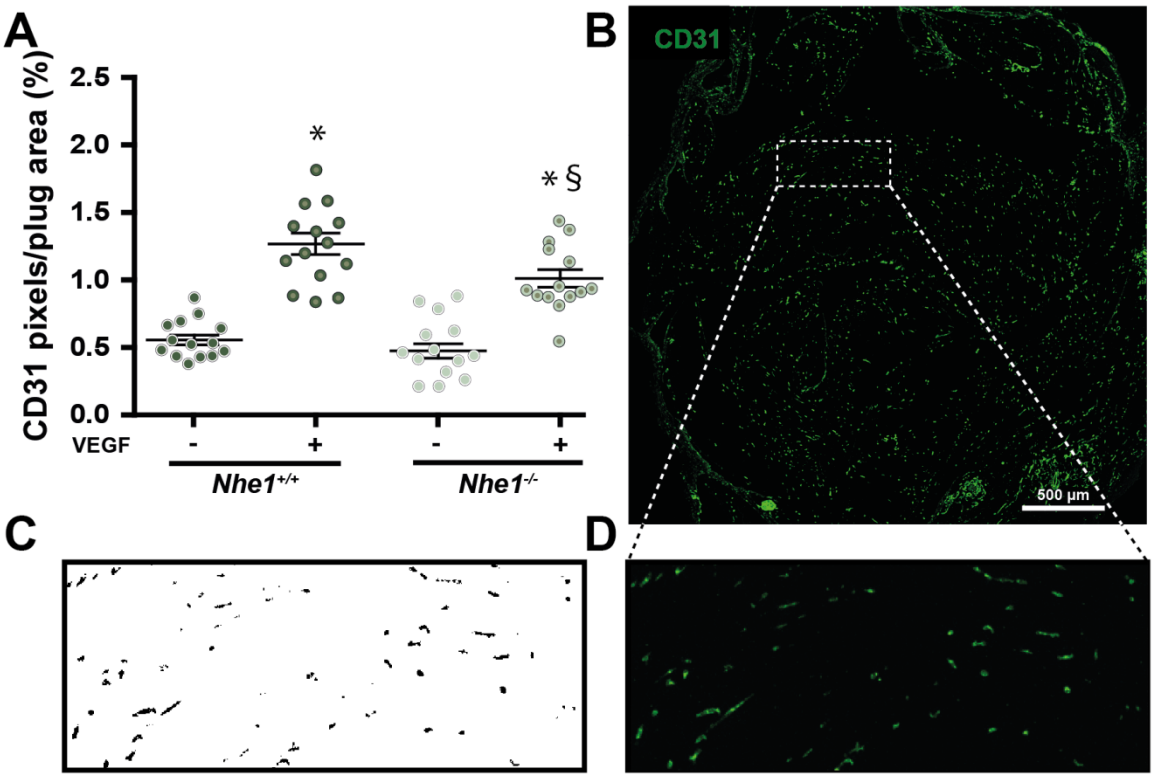

Figure 3-19: Matrigel plug assay in constitutive *Nhe1*$^{-/-}$ mice
For this experiment 10-16 days old *Nhe1*$^{+/+}$ (WT) and constitutive *Nhe1*$^{-/-}$ mice were used. 250 µl of Matrigel supplemented with or without VEGF (400 ng/ml) plus Heparin (400 µg/ml) was injected subcutaneously on either the right or the left flank, respectively. One week later, plugs were excised and angiogenesis was verified by immunofluorescence using an antibody against CD31. A representative figure of a whole plug is given in (B), while a thresholded example of a magnified plug part (D) is given in (C). Vessel formation was quantified by evaluating eight different sections deriving from four different levels of each plug using the ImageJ software. VEGF induced angiogenesis is lower in *Nhe1*$^{-/-}$ compared to WT mice. n=14, $p<0.05$, * *vs.* unstimulated, § *vs.* *Nhe1*$^{-/-}$ VEGF, Two Way RM ANOVA.

VEGF significantly induced around twofold higher vessel formation in WT mice (Figure 3-19). In *Nhe1*$^{-/-}$ mice significantly fewer vessels were formed in response to VEGF than in WT (22% less for plugs supplemented with VEGF). These data confirmed the results obtained in the *in vitro* spheroid assay and underline that NHE1 is likely to support the process of VEGF-induced angiogenesis.

3.7 The endothelial cell-specific *Nhe1*$^{-/-}$ mouse model

3.7.1 Generation and characterization of an endothelial cell-specific *Nhe1*$^{-/-}$ mouse model

Since constitutive *Nhe1*$^{-/-}$ mice display a severe neurological phenotype and die early, the model is unsuitable for more complex studies of angiogenesis *in vivo* such as the hind limb ischemia assay. Moreover, a constitutive *Nhe1*$^{-/-}$ model does not deliver specific information on the role of NHE1 in endothelial cells. For instance, angiogenesis is not only mediated by endothelial cells, but also by

mural or hematopoietic cells. Therefore, one aim of this study was to generate an endothelial-specific *Nhe1*$^{-/-}$ mouse and characterize endothelial function in these mice.

In order to knockout *Nhe1* specifically, two different Cre lines were tested, the *Tie2* [98] or the *VE-cadherin*-Cre line [97]. First, the efficiency and specificity of gene recombination was evaluated by mating *Tie2* and *VE-Cadherin*-Cre lines with a fluorescent reporter line, the Tomato mouse line [99]. Figure 3-20 shows that both Cre lines were able to specifically recombine the *Tomato*-knockin reporter allele in endothelial cells since tissue sections of several organs (heart, brain, liver, and kidney) showed the Tomato fluorescence at the CD31 positive sites.

Next, *Tie2* or the *VE-cadherin-Cre* line were mated with the *Nhe1*$^{flox/flox}$ mouse line. From the *Nhe1*$^{flox/flox}$;*Tie2-Cre*$^{+}$ (Tie2^{+}) mice and the *Nhe1*$^{flox/flox}$;*VE-Cadherin-Cre*$^{+}$ (VE-Cadherin^{+}) mice MLEC were prepared and compared to MLEC from *Nhe1*$^{flox/flox}$ mice without Cre recombinase (Cre^{-}). Western blot and flow cytometry analyses were applied since detection by immunofluorescence, which would have been the method of choice, was not possible due to a lack of an antibody that reliably stains NHE1 in mouse tissue sections.

For the Tie2^{+} line, western blot analysis suggested that recombination was inefficient, since the NHE1 protein level in MLEC lysates from Tie2^{+} and Cre^{-} mice was comparable (Figure 3-21A). Given that MLEC cultures also contain non-MLEC that may have a stronger expression of NHE1 and thus may cause false-positive NHE1 signals in combined cell lysates, NHE1 staining together with CD31 staining in flow cytometry was performed (Figure 3-21B). Here, NHE1 expression in cells that co-express CD31, *e.g.* endothelial cells, is distinguishable from NHE1 expression in CD31^{-} cells. Figure 3-21B shows that with this method a clear knockdown of NHE1 in endothelial cells from the constitutive *Nhe1*$^{-/-}$ mice was seen. However, fluorescence intensity for NHE1 in the CD31^{+} population from Tie2^{+} was only slightly lower than in CD31^{+} cells from Cre^{-} mice (Figure 3-21B). Therefore, it can be concluded that the *Tie2-Cre*$^{+}$ mouse line was not able to efficiently knockout *Nhe1* in MLEC and probably in other endothelial cells as well.

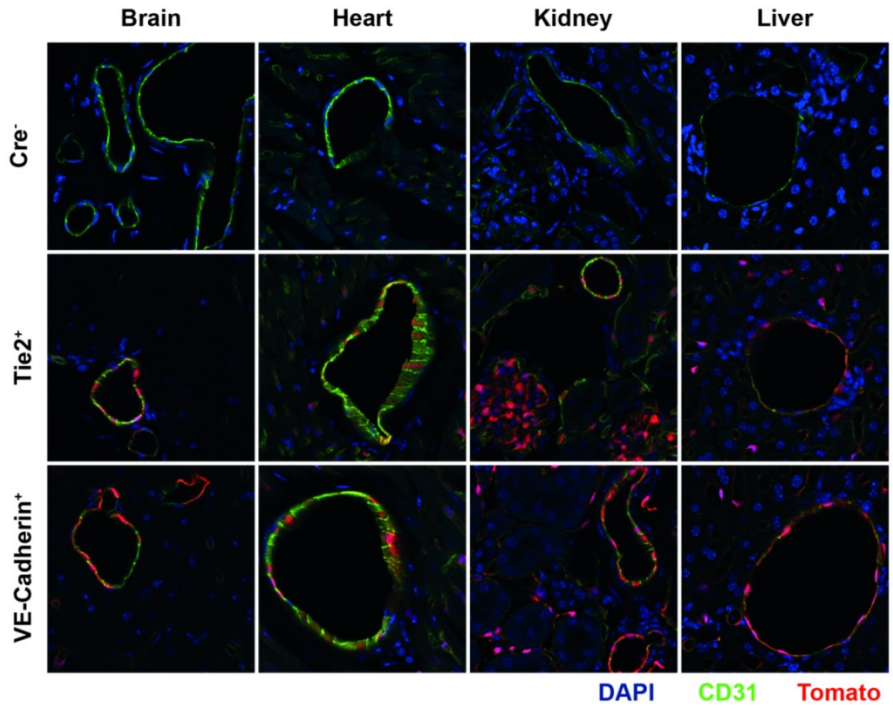

Figure 3-20: Immunohistochemistry of organs from *Tomato*$^{flox/flox}$ mated with *Tie2-Cre*$^{+}$ or *VE-Cadherin-Cre*$^{+}$

Several organs including brain, heart, kidney and liver were cryosectioned and stained for CD31. Tomato is a fluorescent protein and does not require staining. In sections from both Cre-lines, Tomato signal was localized at the CD31 positive sites, therefore both Cre-lines were able to recombine the *Tomato*-floxed allele. No Tomato signal was observed in Cre^{-} tissues.

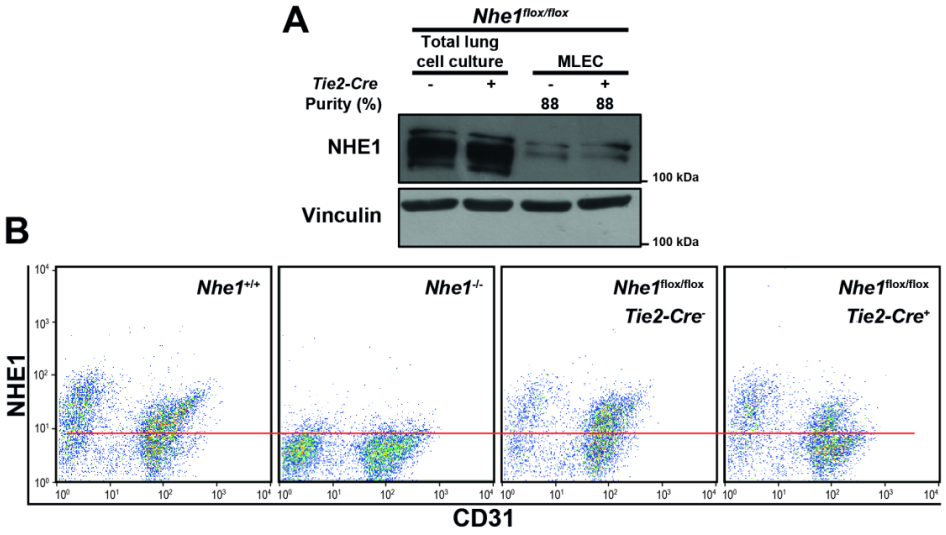

Figure 3-21: Detection of NHE1 in MLEC from the Tie2-Cre^{+} line

(A) Total lung cell lysates (prior to magnetic selection of MLEC) from Tie2-Cre^{+} mice and lysates from MLEC after magnetic separation were analyzed by SDS-PAGE and western blotting. (B) MLEC derived from constitutive *Nhe1*$^{-/-}$ mice or the Tie2-Cre^{+} mice were stained for CD31 (endothelial cell marker) and NHE1 and analyzed by flow cytometry. While a clear knockout of NHE1 was seen in constitutive knockout mice, *Tie2-Cre*$^{+}$ was unable to efficiently knockout *Nhe1* in MLEC. n=2 for flow cytometry, n=3 for western blot, n: is the number of mice.

In contrast, VE-cadherin$^+$ mice showed an efficient knockout of *Nhe1* in endothelial cells. No NHE1 protein was detected by western blot analysis of VE-Cadherin$^+$ MLEC (culture purity >95 %) (Figure 3-22A). Moreover, the CD31$^+$ population in VE-cadherin$^+$ samples did not show NHE1 expression similar to what was seen in MLEC from the constitutive *Nhe1*$^{-/-}$ mice (Figure 3-22B). MLEC from Cre$^-$ mice expressed NHE1 similar to WT mice. Additionally, NHE1 fluorescence of CD31 negative cells was similar between VE-Cadherin$^+$, Cre$^-$, and WT mice. This reassures the specificity of NHE1 knockout in VE-Cadherin$^+$ mice.

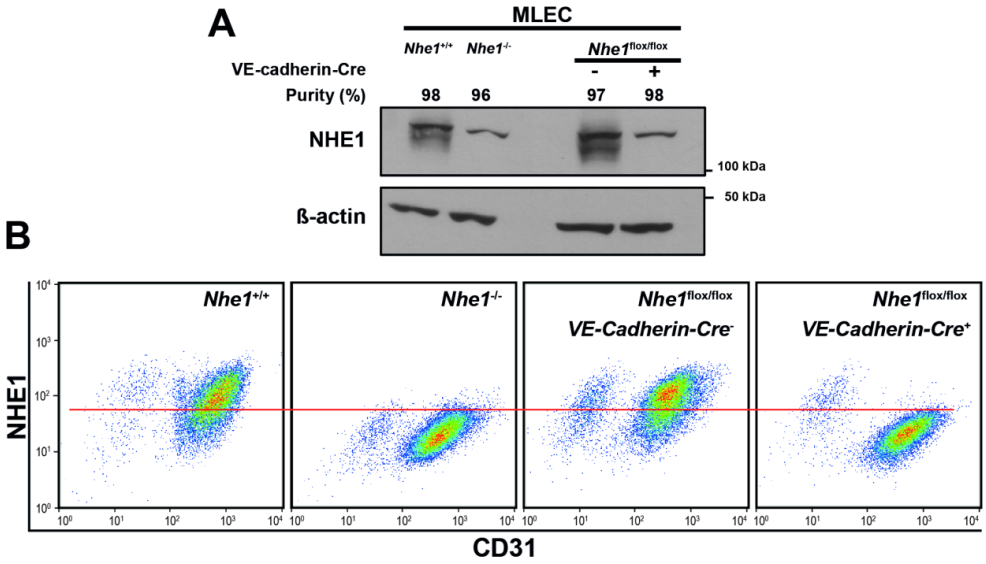

Figure 3-22: Detection of NHE1 in MLEC from the *Nhe1*$^{flox/flox}$;*VE-Cadherin-Cre*$^+$ (VE-Cadherin$^+$) line

(A) MLEC derived from constitutive *Nhe1*$^{-/-}$ mice or VE-Cadherin $^+$ mice were lysed and analyzed by SDS-PAGE and western blotting. (B) MLEC from both mice strains were stained for CD31 (endothelial cell marker) and NHE1 and analyzed by flow cytometry. VE-Cadherin $^+$ mice show an efficient knockout of *Nhe1* in MLEC, which is comparable to the one seen in MLEC from constitutive *Nhe1*$^{-/-}$ mice. The expression of NHE1 in CD31$^-$ cells is unaffected. n=5 flow cytometry, n=3 western blot; n: is the number of mice.

3.7.2 Functional characterization of MLEC from the endothelial cell-specific *Nhe1*$^{-/-}$ mice

To confirm knockout of *Nhe1* on a functional level, pH_i measurements were performed with MLEC from *Nhe1*$^{flox/flox}$;*VE-Cadherin*-Cre$^+$ (VE-Cadherin$^+$) and *Nhe1*$^{flox/flox}$ (Cre$^-$) mice (Figure 3-23). Measurements were performed in HEPES- or HCO_3^-/CO_2-buffered solutions to reveal effects of HCO_3^--dependent transporters. Figure 3-23C shows that in HEPES-buffered solutions basal pH_i was significantly lower in MLEC from VE-Cadherin$^+$ mice, in which NHE1 was not expressed, compared to cells from NHE1-containing Cre$^-$ mice (6.63±0.07 *vs.* 7.13±0.06, respectively). The difference was smaller in the presence of HCO_3^- (6.96±0.03 *vs.* 7.18±0.04, respectively). Cre$^-$ MLEC had similar basal pH_i in the presence and absence of HCO_3^-.

The pH_i of MLEC from VE-Cadherin$^+$ animals did almost not recover after an ammonium prepulse and Na^+-reintroduction in HEPES-buffered solutions. In the presence of HCO_3^-, the pH_i still recovered much slower in MLEC from VE-Cadherin$^+$ mice compared to cells from Cre$^-$ mice. In contrast, MLEC from Cre$^-$ animals recovered at a similar rate regardless of the presence of HCO_3^-.

Taken together, these data confirm the absence of NHE1 in endothelial cells via its function on pH_i regulation. They confirm results from HUVEC (see Figure 3-2) and are in agreement with a prominent role of NHE1 for the regulation of pH_i in endothelial cells. Moreover, it can be concluded that in MLEC NHE1 is the main contributor to pH_i recovery after acidification even in the presence of HCO_3^- .

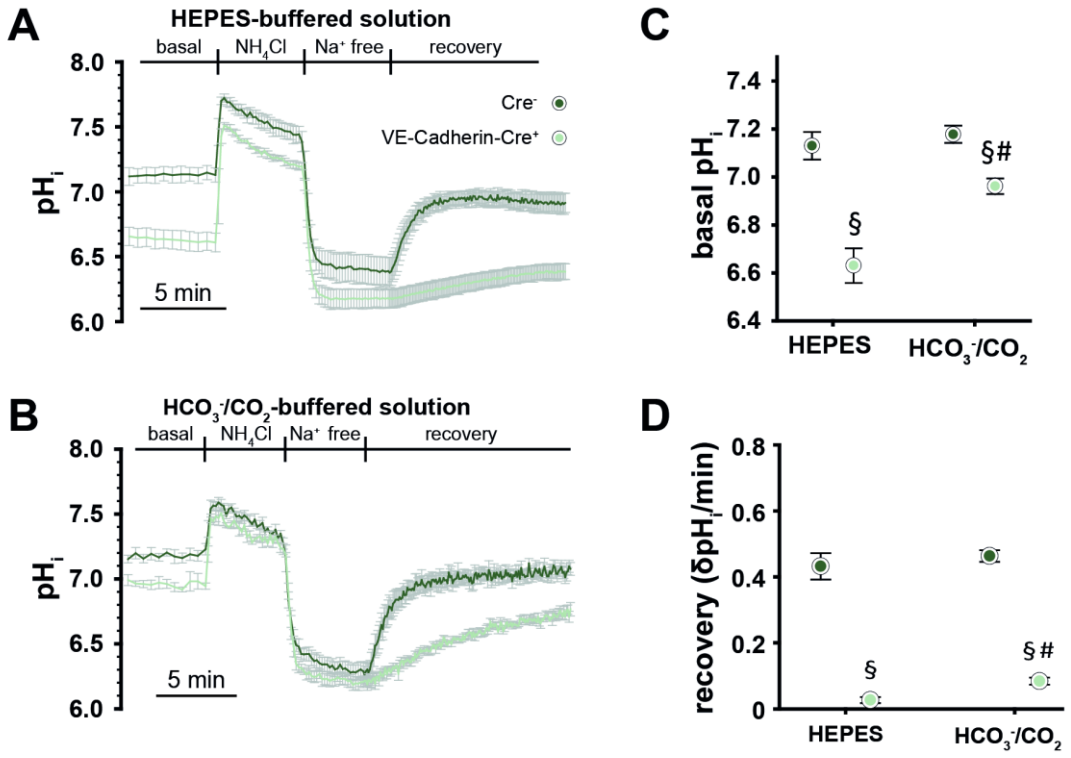

Figure 3-23: Endothelial cell-specific knockout of *Nhe1* affects intracellular pH regulation
Traces of pH_i mesurements over time using the ammonium prepulse protocol in HEPES- (A) and HCO_3^-/CO_2-buffered (B) solutions are demonstrated. The graphs show the values for basal pH_i (C) and the speed of recovery during the first 40 s after reintroducing Na^+ (D). NHE1 is important to maintain basal pH_i especially in the absence of HCO_3^-, and is crucial for pH_i recovery after acidification both in HEPES- and HCO_3^-/CO_2-buffered solutions. $n=6_{coverslips}/3_{mice}$ for Cre$^-$ in HEPES, n=5/3 for VE-Cadherin-Cre$^+$ in HEPES, n=4/2 for Cre$^-$ in HCO_3^-/CO_2, n=3/1 for VE-Cadherin-Cre$^+$ in HCO_3^-/CO_2, n: the number of coverslips/mice; Student's t-test, $p<0.05$, § *vs.* Cre$^-$, # *vs.* VE-Cadherin-Cre$^+$in HEPES.

3.7.3 *In vivo* angiogenesis in the endothelial cell-specific *Nhe1*$^{-/-}$ mice - Matrigel plug assay

After having demonstrated the specific knockdown of NHE1 in endothelial cells of *Nhe1*$^{flox/flox}$; *VE-Cadherin-Cre*$^+$ (VE-Cadherin$^+$) mice on a protein level and on a functional level, *in vivo* angiogenesis was evaluated applying the Matrigel plug assay. VE-Cadherin$^+$ and age-matched Cre$^-$ littermates at the

age of 12-15 weeks were used. 500 µl Matrigel with or without VEGF were injected and 7 days later plugs were excised and analyzed as described in section 3.6.

Figure 3-24 shows that in this series of experiments considerable angiogenesis was observed under basal conditions and VEGF had almost no additional effect on spouting regardless of whether NHE1 was expressed in endothelial cells or not. The high basal vessel formation may be due to a higher content of growth factors in this batch of Matrigel compared to experiments in 3.6. The absence of NHE1 had no effect on basal sprouting. Currently, it is not clear whether this result is due to technical issues or whether it contradicts the data obtained *in vitro* and in constitutive *Nhe1*$^{-/-}$ mice.

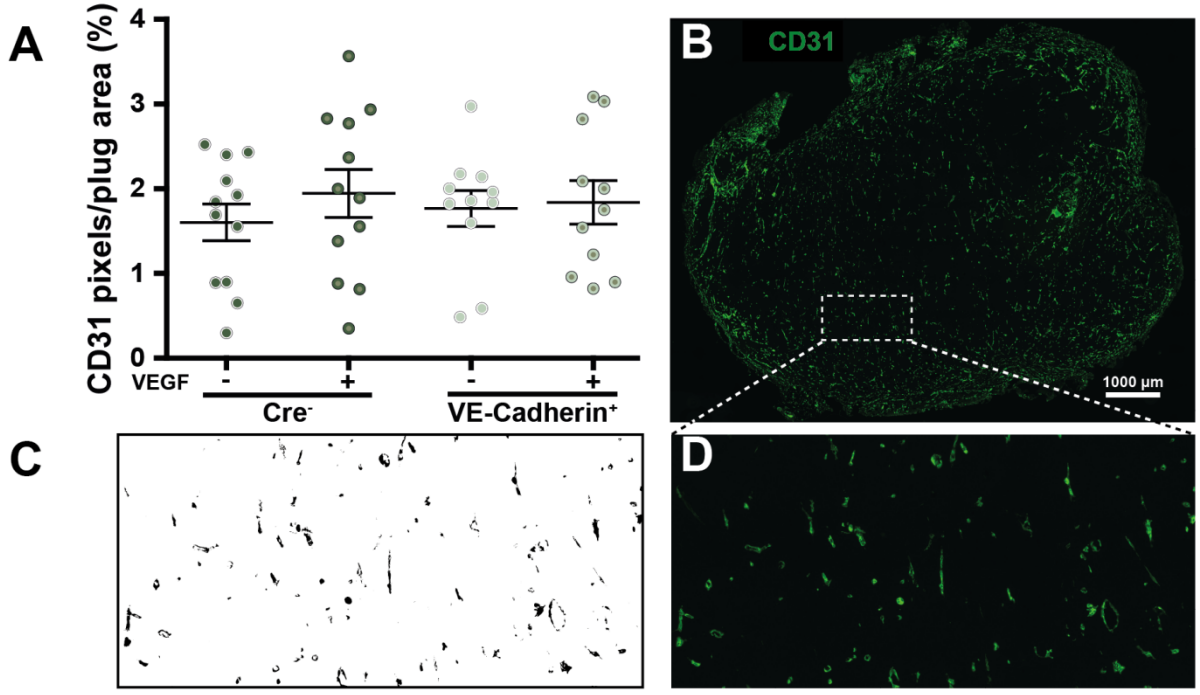

Figure 3-24: Matrigel plug assay in endothelialc cell-specific *Nhe1*$^{-/-}$ mice
For this experiment 12-15 weeks old *Nhe1*$^{flox/flox}$ (Cre^{-}) and *Nhe1*$^{flox/flox}$*;VE-Cadherin-Cre*$^{+}$ (VE-Cadherin^{+}) mice were used. 500 µl of Matrigel supplemented with or without VEGF (400 ng/ml) plus Heparin (400 µg/ml) was injected subcutaneously on either the right or the left flank, respectively. One week later, plugs were excised and angiogenesis was verified by immunofluorescence using an antibody against CD31. Quantification of vessel formation was done by evaluating eight different sections deriving from four different levels of each plug using the ImageJ software. A representative figure of a whole plug is given in (B), while a thresholded example of a magnified plug part (D) is given in (C). There was no VEGF-induced angiogenesis observed, and thus not difference between genotypes either. n=12 for *Nhe1*$^{flox/flox}$, n=11 for *Nhe1*$^{flox/flox}$*;VE-Cadherin-Cre*$^{+}$, $p<0.05$, * *vs.* unstimulated, § *vs. Nhe1*$^{-/-}$ VEGF, Two Way RM ANOVA.

4 Discussion

The Na^+/H^+ exchanger NHE1 is a ubiquitously expressed plasma membrane protein that mediates the exchange of intracellular H^+ for extracellular Na^+, anchors actin filaments and has a scaffold function. Besides the general role in regulating intracellular pH and cell volume, NHE1 was shown to be involved in different processes such as migration, proliferation and survival. Although previous *in vitro* and *in vivo* studies point to NHE1's importance in endothelial cells, its role in complex functions of the endothelium remains unexplored. This thesis was aimed at understanding NHE1 in endothelial cells; how it is regulated, its role in proliferation, survival, migration and in the complex process of angiogenesis. To this end, *in vitro* experiments were performed in mouse lung endothelial cells (MLEC) prepared from genetically modified mice and in primary human umbilical vein endothelial cells (HUVEC). Angiogenesis was also studied *in vivo* with constitutive *Nhe1*$^{-/-}$ and endothelial cell-specific *Nhe1*$^{-/-}$ mice. The latter was generated during the course of this thesis and will be a useful model for future studies.

The data of this thesis reveal that NHE1 is a major component of pH regulation in endothelial cells. It is involved in the regulation of growth factor-stimulated proliferation and migration and is regulated by hypoxia. NHE1 contributes to proangiogenic effects of VEGF *in vitro* and *in vivo* in constitutive *Nhe1*$^{-/-}$ mice but the final proof of an angiogenic role in endothelial cell-specific *Nhe1*$^{-/-}$ mice requires further experiments.

4.1 Downregulation of NHE1 in endothelial cells

In order to study the role of NHE1 in endothelial cells several tools had to be established. Downregulation of NHE1 in HUVEC by applying the RNAi technology was chosen as one approach to bypass the problems of specificity with pharmacological inhibitors and difficulties with overexpressing proteins in primary cells. A pool of four siRNA-sequences was selected, which allowed protein downregulation by approximately 75% and functional decline by 60% as detected by intracellular pH measurements, similar to what had been described previously [97]. The siRNA dose reaching maximal effects was lower (37 nM) than previously reported for the same siRNA pool [46, 97].

4.2 Generation and verification of the endothelial cell-specific *Nhe1*$^{-/-}$ mouse

Additional important tools to study the role of NHE1 in endothelial cells are mouse models, in which the protein is genetically ablated. In these mice, vascular phenotypes can be characterized under basal conditions and upon challenge. In addition, primary endothelial cells can be isolated and investigated with the advantage of a complete absence of the protein in comparison to protein downregulation via

RNAi strategies. The constitutive *Nhe1*$^{-/-}$ mouse, which was already available in the laboratory, has a short life span, which limits its usage for functional tests and preparation of cells. In addition, the data obtained in these mice are difficult to be attributed to endothelial NHE1. Thus, one aim of this study was to generate endothelial cell-specific *Nhe1*$^{-/-}$ mice to specifically investigate the function of NHE1 in endothelial cells.

In order to characterize specific knockout of the NHE1 protein in murine endothelial cells, methods to evaluate NHE1 expression were required. The detection of NHE1 in murine tissues was technically challenging. None of the antibodies tested (sc-136239 Santa Cruz; NHE11-A, Alpha Diagnostik; mab3140, Millipore; sc-28758, Santa Cruz) showed a specific staining for NHE1 in the mouse tissues when compared to the constitutive *Nhe1*$^{-/-}$ mouse tissues (brain, heart, kidney and liver; data not shown). Thus, gene knockout had to be verified in isolated MLEC. Here, the purity of the cultures revealed to be a critical point for western blot analyses. Contamination of MLEC with non-endothelial cells of more than 20% seemed sufficient to cause false positive NHE1 signals in western blots. Therefore, analyses of cells by flow cytometry was established, where the endothelial marker CD31 was additionally stained to determine NHE1 signal specifically from endothelial cells. Fortunately, one anti-NHE1 antibody (NHE11-A, Alpha Diagnostik) that failed to specifically stain the protein in the tissue, showed specific reactions in flow cytometry analysis of isolated cells. This was proven by a clear difference between MLEC from wild type mice and the constitutive *Nhe1*$^{-/-}$ mice.

At first, *Nhe1* gene-knockout in endothelial cells was attempted with a *Tie2-Cre-recombinase*$^{+}$ line, in which the expression of Cre-recombinase is driven by an endothelial-specific promoter/enhancer, which encodes the angiopoietin receptor Tie2 [98]. Experiments of this study had shown that this line successfully recombined a *Tomato*-floxed knockin gene [99]. However, the *Nhe1*-floxed gene was not efficiently recombined, probably because the *Nhe1* gene locus is more difficult to access than the Rosa26 locus, in which the gene for the Tomato fluorescent protein was inserted. Thus, western blot and flow cytometry analyses did not show differences in NHE1 expression between MLEC deriving from the *Nhe1*$^{flox/flox}$; *Tie2-Cre*$^{+}$ line and the *Nhe1*$^{flox/flox}$ line.

As a second attempt, another endothelial-specific Cre line, the *VE-Cadherin-Cre-recombinase*$^{+}$ line [97], was employed. Mating mice of this Cre line with mice from the *Nhe1*-floxed line led to the generation of a *Nhe1*$^{flox/flox}$;*VE-Cadherin-Cre*$^{+}$, in which the absence of NHE1 in isolated endothelial cells was clearly proven by different approaches. Flow cytometry analyses showed no NHE1 staining in CD31-positive cells whereas the CD31-negative cells expressed normal levels of the protein. This difference was not only shown in cells, which were cultured up to 12 days, but also in cells that were kept in culture shorter than two days. Thus, the possibility of recombination occurring *in vitro* during culturing was excluded. Gene knockout was also confirmed by western blot analysis of high purity (>95%) MLEC cultures, and functionally proven by intracellular pH measurements.

Taken together, mating the *Nhe1*-floxed line (generated by Dr. Christopher Hennings) with the *VE-Cadherin-Cre*$^{+}$ line, but not with the *Tie2-Cre*$^{+}$ line, enabled the generation of endothelial cell-specific *Nhe1*$^{-/-}$ mice. The mice were viable and grew normally without any of the obvious phenotypes described for the constitutive *Nhe1*$^{-/-}$ mice.

4.3 NHE1 is important in regulating endothelial cell intracellular pH

Measurements of intracellular pH in primary endothelial cells prepared from endothelial cell-specific *Nhe1*$^{-/-}$ mice as well as in HUVEC, in which NHE1 was downregulated, were performed in this study to understand the role of NHE1 in intracellular pH regulation. In addition, these experiments served to prove NHE1 knockout on a functional level (Figure 3-23).

The data obtained in primary murine *Nhe1*$^{-/-}$ endothelial cells suggest that NHE1 is the most important bicarbonate-independent acid extruder in endothelial cells. When NHE1 was knocked out, steady-state pH_i and recovery after cytoplasmic acidification were drastically reduced in bicarbonate-free buffered solutions. In the presence of bicarbonate, steady-state pH_i was only slightly reduced while recovery was still much slower, approximately fivefold. Therefore, whereas the bicarbonate-dependent transporters may play a role in the control of steady-state intracellular pH, NHE1 seems to be the prominent acid-extruder after acidification even in the presence of bicarbonate.

Similar results were observed after downregulation of NHE1 with siRNA in HUVEC, since the differences of intracellular pH and recovery rate compared to control cells with unchanged NHE1 levels were lower. NHE1-depleted cells recovered their pH_i at a 60% slower rate. The remaining ability to recover could be explained by maximal activation of residual NHE1 protein since downregulation was not complete. Given that the NHE1 inhibitor EIPA abolished pH_i recovery both in control siRNA- and NHE1-siRNA treated cells (Supplementary 1), it can be speculated that no other NHE isoform, especially NHE2, compensates for NHE1 in endothelial cells. The discrepancy between the effects of NHE1 knockout and knockdown underlines the importance of knockout models, in which the consequences of NHE1 depletion can be seen more clearly. This has also to be considered when interpreting the functional data obtained in cells, in which NHE1 is downregulated by siRNA.

The recovery rate of approximately 0.5 pH units/min that was observed in this study is similar to what has previously been reported in cultured endothelial cells [73]. Our findings are also in agreement with recent publications, in which regulation of intracellular pH was analyzed *in situ* on arteries from constitutive *Nhe1*$^{-/-}$ [17] and *Nbcn1*$^{-/-}$ [16] mice. Both studies identified NHE1 as the main bicarbonate-independent acid-extruding transporter in acidified endothelial cells even in the presence of bicarbonate while the Na^{+}/HCO_3^{-} cotransporter NBCn1 was the major bicarbonate-dependent mechanism. The steady-state pH_i values in these experiments seemed to be slightly higher [17] or lower [16] compared to the values seen in the current study (~ 7.2). This could be explained by the

different mouse strain used. As reported in the literature, the steady-state pH_i of endothelial cells ranges from 7.05 to 7.35 pH units depending on the genetic background of the mouse strains (NMRI, FVB, C57BL/6J) [107].

The contribution of NHE1 compared to NCBn1 in maintaining the steady-state pH_i is not uniformly discussed in the literature. In the two studies mentioned above [16, 17], NHE1 participation in the regulation of steady-state pH_i was small compared to bicarbonate-dependent transporters. In the current study, bicarbonate removal from the medium did not reduce the steady-state pH_i of endothelial cells that express NHE1 while *Nhe1*$^{-/-}$ MLEC had a lower steady-state pH_i even in the presence of bicarbonate. These findings highlight NHE1 as important in maintaining steady-state pH_i and contradict the hypothesis of a low contribution of NHE1 to steady-state pH_i regulation. Several hints from the literature support the finding of this study that NHE1 is active in the physiological range of steady-state pH_i. For instance, NHE1 was compensatory activated in NBCn1$^{-/-}$ endothelial cells [16, 17] and pharmacological inhibition of NHE1 prevented an increase of pH_i induced by bicarbonate removal [107]. However, besides the difference in mouse strains used, other variations in the experimental settings between the individual studies should also be considered. Whereas in this thesis cultured lung microvascular endothelial cells were used, the three publications mentioned above describe pH_i measurements *in situ* in mesenteric artery endothelial cells. Also, the methods of measuring recovery rates were different compared to the current work since *in situ* cells were acidified by superfusing with Na^+-free buffered solution, instead of ammonium prepulse technique.

In summary, our data together with literature data suggest that NHE1 and NBCn1 are the two important acid-extruding ion transporters in endothelial cells under steady-state conditions, while NHE1 mediates most of the proton extrusion at sub-physiological pH during the recovery of intracellular pH.

4.4 NHE1 supports endothelial cell proliferation without affecting survival

The ability of NHE1 to regulate global cytoplasmic pH and cell volume by exchanging hydrogen and sodium ions implicates it in homeostasis during cell proliferation. To test whether this applies to endothelial cells, NHE1 was silenced in HUVEC and proliferation was analyzed by monitoring cell numbers and cell cycle distribution. The effect of NHE1 downregulation was tested in two experimental settings, one was cell proliferation in growth factor-rich medium and the other one was VEGF-induced proliferation in serum-poor medium applying the same experimental schedule as in the spheroid assays. The obtained data show that NHE1 knockdown reduced endothelial cell proliferation by 35% in growth factor-rich medium, probably by blocking the cells in the G_0/G_1 phase of the cell cycle. Under this condition cell survival was not altered. Stimulation of control endothelial cells with VEGF led to only a moderate increase of proliferation, which is in line with previous observations from the laboratory and other groups [5, 108]. In contrast, VEGF had strong antiapoptotic effects.

When NHE1-depleted cells were stimulated with VEGF, proliferation was lower than in NHE1-containing cells. Basal and VEGF-induced survival were not affected by NHE1 knockdown, though.

So far, few studies indicate that NHE1 is important in endothelial cell proliferation. *Yu et al.* [109] showed that silencing NHE1 with siRNA inhibited human pulmonary artery endothelial and vascular smooth muscle cell proliferation by approximately 35%, probably as a consequence of cell arrest in G_0/G_1 phase, similarly to our observations. At least for smooth muscle cells, the authors suggested that the loss of NHE1 inhibits E2F1-dependent transcription of genes that control proliferation by increasing p27 (a cyclin-dependent kinase inhibitor). No information was provided on growth factors used, time frames and other experimental procedures though. Another study similarly showed that NHE1 siRNA reduced endothelial cell proliferation, whereas VEGF rescued the effect [88]. Endothelial proliferation is stimulated primarily via the ERK and PI3K/Akt pathways [110]. Since NHE1 has been reported to regulate MAPKs, NHE1 knockdown could inhibit proliferation by affecting MAPK-triggered proliferative pathways. The mechanisms linking NHE1 to MAPK regulation are not clear but may include roles of the transported ions and conformational coupling of NHE1 to enzymes or cytoskeletal elements and seem to be highly cell- and context-specific [111]. Regulation of MAPK by NHE1 has not been investigated in endothelial cells so far. The data of this study show that at least in response to VEGF, ERK1/2 phosphorylation is not altered in NHE1-depleted cells suggesting that ERK1/2 inhibition may not mediate the effects of NHE1 downregulation on proliferation. However, several proteins involved in the regulation of cell cyle and proliferation are pH sensitive and may contribute to the observed effects. One such example is ROCK, whose activity was decreased at low pH [16]. Therefore, since ROCK is known to be required for G_1-S phase transition of the cell cycle [112], a decrease in ROCK activity could be responsible for the observed cell cycle block in the G_0/G_1 phase.

NHE1 has also been shown to regulate the activation of the PI3K/AKT pathway and consequently cell survival. It has been reported that when renal proximal tubule epithelial cells were subjected to apoptotic stress, NHE1 acted as a scaffold for phosphorylated ezrin/radixin/moesin and phosphatidylinositol 4,5-bisphosphate [69] resulting in activation of the pro-survival kinase AKT [72]. However, in the current study neither VEGF-induced AKT phosphorylation nor VEGF-triggered survival was affected by NHE1 knockdown, which again may point to cell-specificity of NHE1 effects described in the literature.

In conclusion, the results of this study provide evidence that NHE1 supports endothelial cell proliferation probably by facilitating progression through the G_0/G_1 phase of the cell cycle, whereas it does not affect survival of endothelial cells. It remains to be clarified whether this is due to actin anchoring and scaffolding functions of NHE1 as well, or is limited to the ion exchange activity.

4.5 NHE1 supports endothelial cell chemotaxis

During angiogenesis, endothelial cells migrate in response to a cocktail of chemotactic factors, which trigger their invasion into the ischemic tissue. Although previously overexpression studies have shown overexpressed NHE1 to localize at the leading edge of migrating cells [39, 49], or native NHE1 in neocortical growth cones [113], the results of this study describe for the first time co-staining of native NHE1 and actin at cell protrusions of single endothelial cells migrating sporadically while NHE1 was localized at cell-cell contacts in confluent endothelial monolayers. Since localization in these plasma membrane domains pointed to a role of NHE1 in mediating cell migration, three different migration assays were employed in HUVEC: wound healing, transwell and chemotaxis assay. The chemotaxis assay mimics the conditions *in vivo* and allows real time tracking of cell movement towards the gradient of the stimulus.

In all the three assays, S1P strongly induced endothelial cell migration while VEGF failed to stimulate cell mobility under all conditions. Knockdown of NHE1 affected S1P-induced migration in the applied test systems. It reduced migration through transwell membranes and attenuated wound closure. Furthermore, NHE1-depleted cells moved slightly slower and could not properly orient in the parallel axis of the chemotactic gradient, which reduced the net movement towards S1P by 32% in the chemotaxis assay. Together, these data identify NHE1 as a pro-migratory factor in endothelial cells.

The exceptional potency of S1P as a migratory stimulus compared to VEGF is described in previous reports. *Liu et al.* [104] described S1P as four times more potent as VEGF in a transwell migration assay designed similarly to ours. Moreover, besides the argument that S1P is more potent than VEGF in inducing endothelial cell migration, the response to the stimulus might differ among endothelial cells from different tissue origin. For instance, VEGF stimulated-migration was sixfold higher in pulmonary artery endothelial cells than in lung microvascular endothelial cells [104].

Two publications directly involved NHE1 in endothelial cell migration. *Bussolino et al.* [34] evaluated the effect of pharmacological inhibition of NHE1 with EIPA on endothelial cell migration in response to granulocyte- and granulocyte-macrophage-colony-stimulating factor. In agreement with the current study the authors showed inhibitory effects of EIPA on endothelial migration although relatively high concentrations of EIPA were required (10 and 50 μM). In contrast, in the current study 0.5 μM EIPA were sufficient to completely block intracellular pH recovery after an ammonium prepulse (Supplementary 1). Pharmacological inhibition should only affect the ion exchange activity of NHE1 and not influence actin binding suggesting that NHE1 controls migration via pH_i regulation. The siRNA approach applied in the current study would affect all NHE1 functions and leave the question open of whether ion transport or cytoskeletal regulation are important for NHE1-mediated migration. In the study of *Mo et al.* [88], a pro-migratory role of NHE1 was also seen although under different conditions compared to the current experiments. The authors observed that overexpression of HIF1α

induced proliferation, migration and tube formation and that this was inhibited by NHE1 downregulation. The effect of NHE1 was attributed to maintaining calpain activity required for angiogenic processes probably by maintaining pH homeostasis.

NHE1 was extensively studied in migration of other cell types and the current results contribute to the few data on its involvement in endothelial cell migration. All three employed assays highlight a supportive role of NHE1 in S1P-induced migration of endothelial cells. It remains to be clarified whether this is a general effect on cell migration or specific to S1P stimulation. However, S1P is known to be a potent angiogenic signaling molecule and is involved in crosstalks with VEGF signaling pathways [9, 114]. For instance[114], an S1P1 receptor-selective antagonist inhibited VEGF-induced angiogenesis in a corneal model [9] and VEGF has been shown to upregulate S1P1 receptors in endothelial cells [115]. S1P has been shown to stimulate migration and angiogenesis mainly through S1P1 receptor and the activation of the small GTPase Rac [9]. The complete process of migration, however, requires coordinated actions of Rac and the Rho/ROCK system. Interestingly, tissue analysis from *Nhe1*$^{-/-}$ mice showed reduced protein and mRNA level of ROCK1 and ROCK2, which would be one explanation of how NHE1 could inhibit S1P-induced migration through Rho GTPase signaling [76]. In addition, ROCK activity is regulated by pH_i and was decreased at low pH [16]. NHE1 may also act downstream of RhoA to modulate initial steps in integrin signaling for the assembly of focal adhesions [116].

The current migration experiments were performed in 2D systems, in which important players of migratory response, the matrix metalloproteinases, are probably of minor importance. Proteolytic activity required for digestion of extracellular matrix, however, has been reported to be pH-dependent. In particular, localized NHE1 activity can decrease the extracellular pH near the plasma membrane and optimize matrix metalloproteinase digestive activity [56]. For instance, inhibiting the NHE1 or lowering extracellular pH has been shown to increase protease secretion and promote proteolysis in the peri-invadopodial microenvironment of tumor cells [56]. Therefore, NHE1 involvement in endothelial cell migration in an experimental 3D structure, for instance in Matrigel, or *in vivo* could be even more profound than the current *in vitro* data suggest [117, 118].

4.6 The role of NHE1 in angiogenesis

Proliferation and migration are two major processes required for angiogenesis. Since NHE1 was involved in the regulation of endothelial cell proliferation and chemotaxis, we expected its participation in the regulation of angiogenesis. Indeed, the results of this thesis suggest that NHE1 is a pro-angiogenic factor although unequivocal evidence is lacking.

In an *in vitro* approach, the spheroid assay, VEGF potently induced sprouting of HUVEC spheroids, although it had been a weak inducer of proliferation and did not affect HUVEC migration in the

current study. Probably, the simultaneous stimulation of several functional processes in a 3D system was required to induce a full angiogenic effect. Downregulation of NHE1 in HUVEC by siRNA inhibited VEGF-induced sprouting by 56%. Accordingly, *in vivo* studies in a Matrigel plug assay in constitutive *Nhe1*$^{-/-}$ mice showed an inhibition of VEGF-triggered vascularization. Both findings point to a pro-angiogenic function of NHE1, which could be attributed to mechanisms discussed above (see 1.4 and 1.5) and to additional effects on pH-sensitive pro-angiogenic molecules such as eNOS [16]. However, when the endothelial cell-specific *Nhe1*$^{-/-}$ mice became available and the Matrigel plug assay was repeated in these mice, the obtained result did not confirm the previous observation. This was mainly due to a lack of a proangiogenic VEGF effect in both, control and endothelial cell-specific *Nhe1*$^{-/-}$ mice.

The reason for the discrepancy of results between constitutive and endothelial-specific *Nhe1*$^{-/-}$ mice is not clear but two major differences between the two experimental series are apparent. Although all mice were of the C57BL/6J genetic background, endothelial cell-specific *Nhe1*$^{-/-}$ animals were 12-15 weeks old, whereas the assay with constitutive *Nhe1*$^{-/-}$ animals was performed with 10-16 days old mice due to the severe phenotype and early death of the animals. Also, as expected, constitutive *Nhe1*$^{-/-}$ mice exhibited growth retardation (data not shown) and it is not clear how this has affected the outcome of the assay. However, although the younger mice may have a better angiogenic potential in response to VEGF, the age difference would not explain the absence of VEGF effect in the older animals since our group has previously observed a robust VEGF-induced angiogenesis in mice of similar age [119].

Another variation between the two series of angiogenesis assays was that different Matrigel batches were used. Matrigel is an extract of extracellular matrix from mouse sarcomas, and despite processing to reduce its growth factor content, batches may differ and the remaining growth factors could cause high basal angiogenesis in the absence of VEGF. Indeed, in average, basal vascularization in the plugs from endothelial cell-specific *Nhe1*$^{-/-}$ mice seemed to be higher when compared to plugs from constitutive *Nhe1*$^{-/-}$ mice and VEGF was not able to induce further significant angiogenesis regardless of which mice were tested. Thus, to repeat the experiment with another Matrigel batch and/or to test angiogenesis in parallel in equally old constitutive and endothelial cell-specific *Nhe1*$^{-/-}$ mice could probably clarify how the discussed variables have influenced the outcome of the assay.

It is also possible that the effect of *Nhe1* knockout observed in the constitutive *Nhe1*$^{-/-}$ mice is not only dependent on the absence of NHE1 in endothelial cells. Angiogenesis is considerably affected by factors secreted from hematopoietic and mural cells suggesting that *Nhe1* knockout in these cells could play an additional role. In line with this NHE1 has been shown to promote VEGF secretion from leukemia cells [120]. Thus, the constitutive absence of NHE1 could alter the microenvironment of newly formed capillaries in a detrimental way. However, when staining cell nuclei in the plug

sections, almost all nuclei were co-stained with CD31 signal suggesting that only few non-endothelial cells were immigrated into the Matrigel plugs. Against this background, the suitability of the Matrigel assay for testing NHE1 functions *in vivo* could be questioned, since it uses an artificial matrix and provides limited options for physiologically important cell-cell interactions.

Taken together, *in vitro* and *in vivo* assays support the hypothesis that NHE1 in endothelial cells promotes angiogenesis. Studies in endothelial cell-specific *Nhe1*$^{-/-}$ mice were not conclusive since no pro-angiogenic effects in response to VEGF were seen, possibly due to methodological problems. Further studies, probably including more physiological angiogenesis assays, with endothelial cell-specific *Nhe1*$^{-/-}$ mice need to be performed.

4.7 Hypoxia induces NHE1 expression by HIF2α-dependent mechanisms

The results of this study show that endothelial cells exposed to hypoxia (1% O_2 experimentally) upregulate NHE1 expression. In parallel, the transcription factors HIF1α and HIF2α accumulated. Using RNAi technology to downregulate both hypoxia-induced transcriptions factors it could be demonstrated that HIF2α, but not HIF1α, was responsible for the induction of NHE1 protein. NHE1 expression was also increased in response to the chemical HIF inducer cobalt chloride.

Both HIF1α and HIF2α are co-expressed in a large number of cell types and exhibit overlapping functions but also unique and sometimes opposing activities [121]. HIF2α seems to be particularly abundant in blood vessels and may accumulate at higher levels of O_2 than HIF1α. Both transcription factors lead to expression of the glucose transporter GLUT1 and VEGF. HIF1α seems to specifically target genes encoding for glycolytic enzymes while HIF2α triggers expression of arginase, TGFα, angiopoietin 2 and delta-like protein 4, a ligand for the NOTCH receptor, to name a few. NHE1 has already been shown to be upregulated by hypoxia [73]. An involvement of HIF1α in NHE1 induction was suggested based on overexpression studies [88, 89] but no detailed analyses on the involvement of endogenously expressed HIF1α or HIF2α were performed. The current study suggests that NHE1 gene- or protein-regulating factors may represent targets of HIF2α. How this fits into the general pattern of HIF2α target genes and how it may help to understand the angiogenic role of NHE1 remains to be investigated.

The pathophysiological reason for the induction of NHE1 in endothelial cells is not clear but may be related to an upregulation of glycolysis in endothelial cells under hypoxic/ischemic conditions. The higher rate of glucose consumption would lead to an increase of the production of acid equivalents similar to ischemia and require higher NHE1 activity. Interestingly, results of this thesis show that hypoxia induction of NHE1 was diminished when changing medium every 24 h. Since the new medium was preincubated for pH, O_2 and temperature equilibration, the effect could have either

resulted from the removal of secreted factors into the supernatant or supplementation of the supernatant for the degraded factors. Therefore, HIF2α may directly act as a transcriptional factor on the NHE1 promoter, but it may also indirectly influence NHE1 protein expression or degradation.

Cutaia et al. [73] has shown that hypoxia induced NHE1 protein levels in endothelial cells after 72 h, whereas mRNA levels remained comparable to the normoxic control. Therefore it is possible that HIF2α regulates NHE1 expression post-translationally by promoting factors, which negatively regulate NHE1 degradation. For instance, one study on breast cancer showed that EGF increased NHE1 expression by inhibiting protein degradation [122]. ROS have also been linked to NHE1 regulation whereby O^{2-} increased expression and H_2O_2 decreased its expression [87]. Thus, it is possible that hypoxia-induced ROS could affect NHE1 protein levels. Given that different ROS could have opposing effects, such experiments would need to be carefully designed the more so that ROS such as H_2O_2 were shown to inhibit NHE1 activity in endothelial cells [75].

In conclusion, the results of this study show that NHE1 protein levels increase during hypoxia via HIF2α-dependent mechanisms. Future studies should test whether increased expression is paralleled by enhanced NHE1 activity. These findings should be considered in terms of NHE1's role in endothelial cells during angiogenesis and wound healing, vascular tone [17], atherosclerosis [31, 32], and ischemia/reoxygenation induced tissue damage.

5 Conclusions and Outlook

Angiogenesis is a complex process controlled by various intracellular mechanisms, growth factors and changes in the tissue microenvironment. The current study suggests a proangiogenic role for the Na^+/H^+ exchanger NHE1, which adds to our understanding of its importance in endothelial cells and the vasculature. However, several limitations have to be considered. Firstly, the angiogenesis assay employed during this study, the matrigel plug assay, does not sufficiently mimic changes in the microenvironment that occur in the ischemic tissue during angiogenesis. Moreover, the constitutive *Nhe1*$^{-/-}$ mice, in which the effect of NHE1 on VEGF-induced angiogenesis was observed, have a severe phenotype that could potentially influence the outcome of the *in vivo* results. And finally, the ultimate evidence from the endothelial cell-specific *Nhe1*$^{-/-}$ mice is still lacking. In any case, given that the differences of VEGF-induced angiogenesis between constitutive *Nhe1*$^{-/-}$ and wild type mice was moderate, NHE1 may belong to permissive proangiogenic factors rather than being an essential one.

The efficient *Nhe1* knockout in the endothelial cell-specific Nhe1$^{-/-}$ mice is, however, very encouraging to further discern the role of NHE1 in the endothelium. Hypoxia-induced NHE1 expression may potentiate its proangiogenic role in the acidic and hypoxic microenvironment during ischemia-induced angiogenesis. This may be relevant during tumor angiogenesis, the more so that NHE1 inhibitors were shown to inhibit tumor growth [123] and may impair inflammatory processes [86, 93, 124-126]. Pharmacological inhibition of NHE1 could be beneficial by synergistically targeting several cell types. Therefore, other models better mimicking physiological and pathophysiological angiogenesis, like the hind limb ischemia model and tumor angiogenesis models could provide clearer insights into the role of NHE1 in this process.

Besides angiogenesis, the newly generated endothelial cell-specific *Nhe1*$^{-/-}$ mice could be useful in analyzing NHE1´s role in other vascular functions. As described in *Boedtkjer et al.* [17], the artery walls of the constitutive *Nhe1*$^{-/-}$ mice were thinner and mice had low arterial blood pressure compared to the wild type littermates. Since this phenotype could also be related to *Nhe1* knockout in vascular smooth muscle cells it would be interesting to analyze whether the endothelial cell-specific *Nhe1*$^{-/-}$ mice show the same phenotype. These mice could be used in stroke models as well, where NHE1 inhibition preserved the endothelial cell barrier, which reduced brain edema and tissue damage. Our preliminary results show that NHE1 downregulation in endothelial cells reduced PAI-1 expression. This might be an interesting finding since clinical trials to treat cardiomyopathies with NHE1 inhibitors were stopped as a result of increased incidence of thromboembolic strokes [82, 127].

Finally, a lot of effort has been made to develop specific pharmacological inhibitors of NHE1. Many of them have been studied in clinical trials and valuable experience on their pharmacokinetic and toxicological properties is available. Therefore, understanding the role of NHE1 in vascular tissue is of

potential clinical significance. For instance, NHE1 inhibitors seem to be promising anticancer agents in a wide array of malignant tumors and leukemias. Against this background, their influences on the vasculature and their potential vascular side effects have to be clarified. However, translating mouse studies with genetic deletion of *Nhe1* into pharmacological inhibition in the clinics needs to be done cautiously, since the pharmacological inhibition mainly affects the ion exchange activity, whereas the knockout of NHE1 in mice affects all the functions of the protein.

6 Acknowledgements

My deepest gratitude to both my supervisors, Prof. Dr. Regine Heller and Prof. Dr. Christian Hübner, for sharing their precious experience and knowledge with me, and continuously boosting my motivation. I am thankful to them for guiding me through the challenges of the experimental work and their input for my personal growth.

Furthermore, I want to thank Prof. Dr. Regine Heller for the opportunity to participate in the summer school of molecular medicine and be given the chance to do my PhD in Jena. Also, I want to thank Prof. Dr. Otto Witte and the IZKF for the financial support during the first three years, and Prof. Dr. Christian Hübner for financing the fourth year of my PhD.

I want to thank Prof. Dr. Reinhard Bauer and Prof. Dr. Regine Heller for helping me with the Matrigel plug assay, Silke for her help with the spheroid assay, Elke for making the work in cell culture easier, and Rose for teaching me how to handle histological preparations. I sincerely thank both of my groups for the continuous assistance in the lab work. I am also thankful to David Böhm for his help with cryosections and staining.

Especially, I want to thank Christopher for all the interesting things I have learned from him, his continuous help and his patients, and for providing me with the precious *Nhe1*-floxed mouse line.

I want to thank my friends in CMB and Human Genetics for the friendly working environment and bringing fun to the leisure time.

Special thanks to my lovely family, to my parents for giving me a piece of their heart everytime we said goodbye at the airport, and my brother and sister for providing a shoulder to lean on.

Finally, I want to thank Matthias for the cookies and Govind´s open access drawer with chocolates for taking care of the hunger during late evenings in the lab.

7 Supplementary

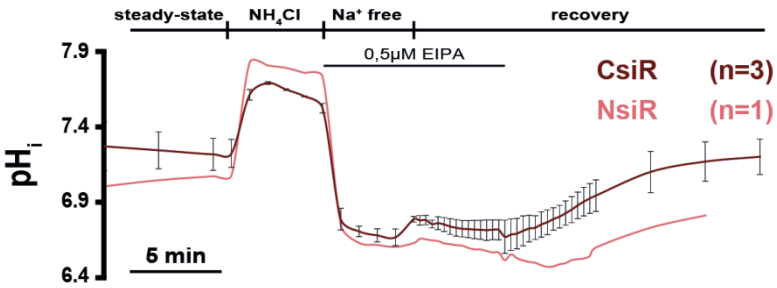

Supplementary 1: Intracellular pH measurements in HUVEC after inhibition with EIPA
Traces of pH_i measurements in HEPES-buffered solutions after inhibition with 0.5 µM EIPA show inhibition of pH_i recovery after acidification with ammonium prepulse protocol in both CsiR and NsiR HUVEC. n=3 for CsiR (scRNA transfected HUVEC), n=1 for NsiR (NHE1 siRNA transfected HUVEC)

8 List of figures

9 List of tables

10 References

1. Bravo-Cordero, J.J., et al., *Functions of cofilin in cell locomotion and invasion.* Nat Rev Mol Cell Biol, 2013. **14**(7): p. 405-15.
2. Adair, T.H. and J.P. Montani, in *Angiogenesis*. 2010: San Rafael (CA).
3. Feletou, M., in *The Endothelium: Part 1: Multiple Functions of the Endothelial Cells-Focus on Endothelium-Derived Vasoactive Mediators*. 2011: San Rafael (CA).
4. Lamalice, L., F. Le Boeuf, and J. Huot, *Endothelial cell migration during angiogenesis.* Circ Res, 2007. **100**(6): p. 782-94.
5. Olsson, A.K., et al., *VEGF receptor signalling - in control of vascular function.* Nat Rev Mol Cell Biol, 2006. **7**(5): p. 359-71.
6. Costa, C., R. Soares, and F. Schmitt, *Angiogenesis: now and then.* APMIS, 2004. **112**(7-8): p. 402-12.
7. Lee, M.J., et al., *Vascular endothelial cell adherens junction assembly and morphogenesis induced by sphingosine-1-phosphate.* Cell, 1999. **99**(3): p. 301-12.
8. Spiegel, S. and S. Milstien, *Sphingosine-1-phosphate: an enigmatic signalling lipid.* Nat Rev Mol Cell Biol, 2003. **4**(5): p. 397-407.
9. Takuwa, Y., et al., *Roles of sphingosine-1-phosphate signaling in angiogenesis.* World J Biol Chem, 2010. **1**(10): p. 298-306.
10. English, D., et al., *Sphingosine 1-phosphate released from platelets during clotting accounts for the potent endothelial cell chemotactic activity of blood serum and provides a novel link between hemostasis and angiogenesis.* FASEB J, 2000. **14**(14): p. 2255-65.
11. Whitten, S.T., E.B. Garcia-Moreno, and V.J. Hilser, *Local conformational fluctuations can modulate the coupling between proton binding and global structural transitions in proteins.* Proc Natl Acad Sci U S A, 2005. **102**(12): p. 4282-7.
12. Trivedi, B. and W.H. Danforth, *Effect of pH on the kinetics of frog muscle phosphofructokinase.* J Biol Chem, 1966. **241**(17): p. 4110-2.
13. Fidelman, M.L., et al., *Intracellular pH mediates action of insulin on glycolysis in frog skeletal muscle.* Am J Physiol, 1982. **242**(1): p. C87-93.
14. Boedtkjer, E. and C. Aalkjaer, *Intracellular pH in the resistance vasculature: regulation and functional implications.* J Vasc Res, 2012. **49**(6): p. 479-96.
15. Fleming, I., M. Hecker, and R. Busse, *Intracellular alkalinization induced by bradykinin sustains activation of the constitutive nitric oxide synthase in endothelial cells.* Circ Res, 1994. **74**(6): p. 1220-6.
16. Boedtkjer, E., et al., *Disruption of Na+,HCO(3)(-) cotransporter NBCn1 (slc4a7) inhibits NO-mediated vasorelaxation, smooth muscle Ca(2)(+) sensitivity, and hypertension development in mice.* Circulation, 2011. **124**(17): p. 1819-29.
17. Boedtkjer, E., H.H. Damkier, and C. Aalkjaer, *NHE1 knockout reduces blood pressure and arterial media/lumen ratio with no effect on resting pH(i) in the vascular wall.* J Physiol, 2012. **590**(Pt 8): p. 1895-906.
18. Ahn, K., et al., *The endothelin-converting enzyme from human umbilical vein is a membrane-bound metalloprotease similar to that from bovine aortic endothelial cells.* Proc Natl Acad Sci U S A, 1992. **89**(18): p. 8606-10.
19. Ohgaki, R., et al., *Organellar Na+/H+ exchangers: novel players in organelle pH regulation and their emerging functions.* Biochemistry, 2011. **50**(4): p. 443-50.
20. Yan, G.X. and A.G. Kleber, *Changes in extracellular and intracellular pH in ischemic rabbit papillary muscle.* Circ Res, 1992. **71**(2): p. 460-70.
21. Cardone, R.A., V. Casavola, and S.J. Reshkin, *The role of disturbed pH dynamics and the Na+/H+ exchanger in metastasis.* Nat Rev Cancer, 2005. **5**(10): p. 786-95.

22. Boron, W.F., *Regulation of intracellular pH.* Adv Physiol Educ, 2004. **28**(1-4): p. 160-79.
23. Austin, C. and S. Wray, *Extracellular pH signals affect rat vascular tone by rapid transduction into intracellular pH changes.* J Physiol, 1993. **466**: p. 1-8.
24. Peng, H.L., et al., *Effect of acidosis on tension and [Ca2+]i in rat cerebral arteries: is there a role for membrane potential?* Am J Physiol, 1998. **274**(2 Pt 2): p. H655-62.
25. Rohra, D.K., S.Y. Saito, and Y. Ohizumi, *Low extracellular Cl- environment attenuates changes in intracellular pH and contraction following extracellular acidosis in Wistar Kyoto rat aorta.* Pharmacology, 2005. **75**(1): p. 30-6.
26. Wakabayashi, S., M. Shigekawa, and J. Pouyssegur, *Molecular physiology of vertebrate Na+/H+ exchangers.* Physiol Rev, 1997. **77**(1): p. 51-74.
27. Casey, J.R., S. Grinstein, and J. Orlowski, *Sensors and regulators of intracellular pH.* Nat Rev Mol Cell Biol, 2010. **11**(1): p. 50-61.
28. Okada, Y., *Ion channels and transporters involved in cell volume regulation and sensor mechanisms.* Cell Biochem Biophys, 2004. **41**(2): p. 233-58.
29. Okada, Y., et al., *Receptor-mediated control of regulatory volume decrease (RVD) and apoptotic volume decrease (AVD).* J Physiol, 2001. **532**(Pt 1): p. 3-16.
30. Putney, L.K., S.P. Denker, and D.L. Barber, *The changing face of the Na+/H+ exchanger, NHE1: structure, regulation, and cellular actions.* Annu Rev Pharmacol Toxicol, 2002. **42**: p. 527-52.
31. Madonna, R. and R. De Caterina, *Aquaporin-1 and sodium-hydrogen exchangers as pharmacological targets in diabetic atherosclerosis.* Curr Drug Targets, 2015. **16**(4): p. 361-5.
32. Sarigianni, M., et al., *Na+ H+ exchanger-1: a link with atherogenesis?* Expert Opin Investig Drugs, 2010. **19**(12): p. 1545-56.
33. Reshkin, S.J., R.A. Cardone, and S. Harguindey, *Na+-H+ exchanger, pH regulation and cancer.* Recent Pat Anticancer Drug Discov, 2013. **8**(1): p. 85-99.
34. Bussolino, F., et al., *Stimulation of the Na+/H+ exchanger in human endothelial cells activated by granulocyte- and granulocyte-macrophage-colony-stimulating factor. Evidence for a role in proliferation and migration.* J Biol Chem, 1989. **264**(31): p. 18284-7.
35. Orlowski, J. and S. Grinstein, *Diversity of the mammalian sodium/proton exchanger SLC9 gene family.* Pflugers Arch, 2004. **447**(5): p. 549-65.
36. Fuster, D.G. and R.T. Alexander, *Traditional and emerging roles for the SLC9 Na+/H+ exchangers.* Pflugers Arch, 2014. **466**(1): p. 61-76.
37. Slepkov, E.R., et al., *Structural and functional analysis of the Na+/H+ exchanger.* Biochem J, 2007. **401**(3): p. 623-33.
38. Baumgartner, M., H. Patel, and D.L. Barber, *Na(+)/H(+) exchanger NHE1 as plasma membrane scaffold in the assembly of signaling complexes.* Am J Physiol Cell Physiol, 2004. **287**(4): p. C844-50.
39. Denker, S.P., et al., *Direct binding of the Na--H exchanger NHE1 to ERM proteins regulates the cortical cytoskeleton and cell shape independently of H(+) translocation.* Mol Cell, 2000. **6**(6): p. 1425-36.
40. Amith, S.R. and L. Fliegel, *Regulation of the Na+/H+ Exchanger (NHE1) in Breast Cancer Metastasis.* Cancer Res, 2013. **73**(4): p. 1259-64.
41. Yan, W., et al., *The Nck-interacting kinase (NIK) phosphorylates the Na+-H+ exchanger NHE1 and regulates NHE1 activation by platelet-derived growth factor.* J Biol Chem, 2001. **276**(33): p. 31349-56.
42. Takahashi, E., et al., *p90(RSK) is a serum-stimulated Na+/H+ exchanger isoform-1 kinase. Regulatory phosphorylation of serine 703 of Na+/H+ exchanger isoform-1.* J Biol Chem, 1999. **274**(29): p. 20206-14.
43. Tominaga, T., et al., *p160ROCK mediates RhoA activation of Na-H exchange.* EMBO J, 1998. **17**(16): p. 4712-22.
44. Cardone, R.A., et al., *Protein kinase A gating of a pseudopodial-located RhoA/ROCK/p38/NHE1 signal module regulates invasion in breast cancer cell lines.* Mol Biol Cell, 2005. **16**(7): p. 3117-27.

45. Hisamitsu, T., et al., *Dimerization is crucial for the function of the Na+/H+ exchanger NHE1.* Biochemistry, 2006. **45**(44): p. 13346-55.
46. Li, S., N.F. Huang, and S. Hsu, *Mechanotransduction in endothelial cell migration.* J Cell Biochem, 2005. **96**(6): p. 1110-26.
47. Lauffenburger, D.A. and A.F. Horwitz, *Cell migration: a physically integrated molecular process.* Cell, 1996. **84**(3): p. 359-69.
48. Denker, S.P. and D.L. Barber, *Ion transport proteins anchor and regulate the cytoskeleton.* Curr Opin Cell Biol, 2002. **14**(2): p. 214-20.
49. Denker, S.P. and D.L. Barber, *Cell migration requires both ion translocation and cytoskeletal anchoring by the Na-H exchanger NHE1.* J Cell Biol, 2002. **159**(6): p. 1087-96.
50. Borisy, G.G. and T.M. Svitkina, *Actin machinery: pushing the envelope.* Curr Opin Cell Biol, 2000. **12**(1): p. 104-12.
51. Carlier, M.F., F. Ressad, and D. Pantaloni, *Control of actin dynamics in cell motility. Role of ADF/cofilin.* J Biol Chem, 1999. **274**(48): p. 33827-30.
52. Ludwig, F.T., A. Schwab, and C. Stock, *The Na+ /H+ -exchanger (NHE1) generates pH nanodomains at focal adhesions.* J Cell Physiol, 2013. **228**(6): p. 1351-8.
53. Ritter, M., *Cell volume regulatory ion transport in cell migration.* Contrib Nephrol, 1998. **123**: p. 135-57.
54. Oster, G.F. and A.S. Perelson, *The physics of cell motility.* J Cell Sci Suppl, 1987. **8**: p. 35-54.
55. Stock, C., et al., *pH nanoenvironment at the surface of single melanoma cells.* Cell Physiol Biochem, 2007. **20**(5): p. 679-86.
56. Busco, G., et al., *NHE1 promotes invadopodial ECM proteolysis through acidification of the peri-invadopodial space.* FASEB J, 2010. **24**(10): p. 3903-15.
57. Meima, M.E., et al., *The sodium-hydrogen exchanger NHE1 is an Akt substrate necessary for actin filament reorganization by growth factors.* J Biol Chem, 2009. **284**(39): p. 26666-75.
58. Stewart, A.K., C.A. Boyd, and R.D. Vaughan-Jones, *A novel role for carbonic anhydrase: cytoplasmic pH gradient dissipation in mouse small intestinal enterocytes.* J Physiol, 1999. **516 (Pt 1)**: p. 209-17.
59. Martin, C., et al., *Intracellular pH gradients in migrating cells.* Am J Physiol Cell Physiol, 2011. **300**(3): p. C490-5.
60. Simchowitz, L. and E.J. Cragoe, Jr., *Inhibition of chemotactic factor-activated Na+/H+ exchange in human neutrophils by analogues of amiloride: structure-activity relationships in the amiloride series.* Mol Pharmacol, 1986. **30**(2): p. 112-20.
61. Coelho, C.M. and S.J. Leevers, *Do growth and cell division rates determine cell size in multicellular organisms?* J Cell Sci, 2000. **113 (Pt 17)**: p. 2927-34.
62. Putney, L.K. and D.L. Barber, *Na-H exchange-dependent increase in intracellular pH times G2/M entry and transition.* J Biol Chem, 2003. **278**(45): p. 44645-9.
63. Wu, D., H. Doods, and J.M. Stassen, *Inhibition of human pulmonary artery smooth muscle cell proliferation and migration by sabiporide, a new specific NHE-1 inhibitor.* J Cardiovasc Pharmacol, 2006. **48**(2): p. 34-40.
64. Kapus, A., et al., *Functional characterization of three isoforms of the Na+/H+ exchanger stably expressed in Chinese hamster ovary cells. ATP dependence, osmotic sensitivity, and role in cell proliferation.* J Biol Chem, 1994. **269**(38): p. 23544-52.
65. Pouyssegur, J., et al., *A specific mutation abolishing Na+/H+ antiport activity in hamster fibroblasts precludes growth at neutral and acidic pH.* Proc Natl Acad Sci U S A, 1984. **81**(15): p. 4833-7.
66. Delvaux, M., et al., *Amiloride and analogues inhibit Na(+)-H+ exchange and cell proliferation in AR42J pancreatic cell line.* Am J Physiol, 1990. **259**(5 Pt 1): p. G842-9.
67. Horvat, B., S. Taheri, and A. Salihagic, *Tumour cell proliferation is abolished by inhibitors of Na+/H+ and HCO3-/Cl- exchange.* Eur J Cancer, 1992. **29A**(1): p. 132-7.

68. Benedetti, A., et al., *Inhibition of the NA(+)/H(+) exchanger reduces rat hepatic stellate cell activity and liver fibrosis: an in vitro and in vivo study.* Gastroenterology, 2001. **120**(2): p. 545-56.
69. Schelling, J.R. and B.G. Abu Jawdeh, *Regulation of cell survival by Na+/H+ exchanger-1.* Am J Physiol Renal Physiol, 2008. **295**(3): p. F625-32.
70. Lang, F., et al., *Cell volume in the regulation of cell proliferation and apoptotic cell death.* Cell Physiol Biochem, 2000. **10**(5-6): p. 417-28.
71. Bortner, C.D. and J.A. Cidlowski, *Absence of volume regulatory mechanisms contributes to the rapid activation of apoptosis in thymocytes.* Am J Physiol, 1996. **271**(3 Pt 1): p. C950-61.
72. Wu, K.L., et al., *The NHE1 Na+/H+ exchanger recruits ezrin/radixin/moesin proteins to regulate Akt-dependent cell survival.* J Biol Chem, 2004. **279**(25): p. 26280-6.
73. Cutaia, M.V., et al., *Effect of hypoxic exposure on Na+/H+ antiport activity, isoform expression, and localization in endothelial cells.* Am J Physiol, 1998. **275**(3 Pt 1): p. L442-51.
74. Rimmer, S.J., et al., *Corrigendum to: 'Demonstration of a Na(+)/H(+) exchanger NHE1 in fresh bovine corneal endothelial cell basolateral plasma membrane'.* Biochim Biophys Acta, 2000. **1463**(1): p. 196.
75. Boedtkjer, E. and C. Aalkjaer, *Insulin inhibits Na+/H+ exchange in vascular smooth muscle and endothelial cells in situ: involvement of H2O2 and tyrosine phosphatase SHP-2.* Am J Physiol Heart Circ Physiol, 2009. **296**(2): p. H247-55.
76. Yu, L., et al., *Deficiency of the NHE1 gene prevents hypoxia-induced pulmonary hypertension and vascular remodeling.* Am J Respir Crit Care Med, 2008. **177**(11): p. 1276-84.
77. Karmazyn, M., A. Kilic, and S. Javadov, *The role of NHE-1 in myocardial hypertrophy and remodelling.* J Mol Cell Cardiol, 2008. **44**(4): p. 647-53.
78. Symons, J.D. and S. Schaefer, *Na(+)/H(+) exchange subtype 1 inhibition reduces endothelial dysfunction in vessels from stunned myocardium.* Am J Physiol Heart Circ Physiol, 2001. **281**(4): p. H1575-82.
79. Hileeto, D., et al., *Contributions of endothelin-1 and sodium hydrogen exchanger-1 in the diabetic myocardium.* Diabetes Metab Res Rev, 2002. **18**(5): p. 386-94.
80. Vial, G., et al., *Na+/H+ exchange inhibition with cariporide prevents alterations of coronary endothelial function in streptozotocin-induced diabetes.* Mol Cell Biochem, 2008. **310**(1-2): p. 93-102.
81. Klatte, K., et al., *Increased mortality after coronary artery bypass graft surgery is associated with increased levels of postoperative creatine kinase-myocardial band isoenzyme release: results from the GUARDIAN trial.* J Am Coll Cardiol, 2001. **38**(4): p. 1070-7.
82. Mentzer, R.M., Jr., et al., *Sodium-hydrogen exchange inhibition by cariporide to reduce the risk of ischemic cardiac events in patients undergoing coronary artery bypass grafting: results of the EXPEDITION study.* Ann Thorac Surg, 2008. **85**(4): p. 1261-70.
83. Teiwes, J. and R.D. Toto, *Epithelial sodium channel inhibition in cardiovascular disease. A potential role for amiloride.* Am J Hypertens, 2007. **20**(1): p. 109-17.
84. Tardif, J.C., et al., *Effect of inhibition of the Na+/H+ exchanger with cariporide on left ventricular function in acute coronary syndromes: results from the echocardiographic substudy of the GUARDIAN trial.* Can J Cardiol, 2004. **20**(3): p. 317-22.
85. Hendrikx, M., et al., *New Na(+)-H+ exchange inhibitor HOE 694 improves postischemic function and high-energy phosphate resynthesis and reduces Ca2+ overload in isolated perfused rabbit heart.* Circulation, 1994. **89**(6): p. 2787-98.
86. Hattori, R., et al., *NHE and ICAM-1 expression in hypoxic/reoxygenated coronary microvascular endothelial cells.* Am J Physiol Heart Circ Physiol, 2001. **280**(6): p. H2796-803.
87. Akram, S., et al., *Reactive oxygen species-mediated regulation of the Na+-H+ exchanger 1 gene expression connects intracellular redox status with cells' sensitivity to death triggers.* Cell Death Differ, 2006. **13**(4): p. 628-41.
88. Mo, X.G., et al., *Suppression of NHE1 by small interfering RNA inhibits HIF-1alpha-induced angiogenesis in vitro via modulation of calpain activity.* Microvasc Res, 2011. **81**(2): p. 160-8.

89. Shimoda, L.A., et al., *HIF-1 regulates hypoxic induction of NHE1 expression and alkalinization of intracellular pH in pulmonary arterial myocytes.* Am J Physiol Lung Cell Mol Physiol, 2006. **291**(5): p. L941-9.
90. Park, S.L., et al., *The effect of Na(+)/H(+) exchanger-1 inhibition by sabiporide on blood-brain barrier dysfunction after ischemia/hypoxia in vivo and in vitro.* Brain Res, 2010. **1366**: p. 189-96.
91. Lam, T.I., P.M. Wise, and M.E. O'Donnell, *Cerebral microvascular endothelial cell Na/H exchange: evidence for the presence of NHE1 and NHE2 isoforms and regulation by arginine vasopressin.* Am J Physiol Cell Physiol, 2009. **297**(2): p. C278-89.
92. Wang, Y., et al., *Gene inactivation of Na+/H+ exchanger isoform 1 attenuates apoptosis and mitochondrial damage following transient focal cerebral ischemia.* Eur J Neurosci, 2008. **28**(1): p. 51-61.
93. Qadri, S.M., et al., *Endothelial Na+/H+ exchanger NHE1 participates in redox-sensitive leukocyte recruitment triggered by methylglyoxal.* Cardiovasc Diabetol, 2014. **13**: p. 134.
94. Bell, S.M., et al., *Targeted disruption of the murine Nhe1 locus induces ataxia, growth retardation, and seizures.* Am J Physiol, 1999. **276**(4 Pt 1): p. C788-95.
95. Zengel, P., et al., *mu-Slide Chemotaxis: a new chamber for long-term chemotaxis studies.* BMC Cell Biol, 2011. **12**: p. 21.
96. Schwenk, F., U. Baron, and K. Rajewsky, *A cre-transgenic mouse strain for the ubiquitous deletion of loxP-flanked gene segments including deletion in germ cells.* Nucleic Acids Res, 1995. **23**(24): p. 5080-1.
97. Alva, J.A., et al., *VE-Cadherin-Cre-recombinase transgenic mouse: a tool for lineage analysis and gene deletion in endothelial cells.* Dev Dyn, 2006. **235**(3): p. 759-67.
98. Kisanuki, Y.Y., et al., *Tie2-Cre transgenic mice: a new model for endothelial cell-lineage analysis in vivo.* Dev Biol, 2001. **230**(2): p. 230-42.
99. Madisen, L., et al., *A robust and high-throughput Cre reporting and characterization system for the whole mouse brain.* Nat Neurosci, 2010. **13**(1): p. 133-40.
100. Rink, T.J., R.Y. Tsien, and T. Pozzan, *Cytoplasmic pH and free Mg2+ in lymphocytes.* J Cell Biol, 1982. **95**(1): p. 189-96.
101. Boyarsky, G., et al., *pH regulation in single glomerular mesangial cells. I. Acid extrusion in absence and presence of HCO3.* Am J Physiol, 1988. **255**(6 Pt 1): p. C844-56.
102. Boron, W.F. and P. De Weer, *Intracellular pH transients in squid giant axons caused by CO2, NH3, and metabolic inhibitors.* J Gen Physiol, 1976. **67**(1): p. 91-112.
103. Clement, D.L., et al., *PDGFRα signaling in the primary cilium regulates NHE1-dependent fibroblast migration via coordinated differential activity of MEK1/2–ERK1/2–p90(RSK) and AKT signaling pathways.* Journal of Cell Science, 2013. **126**(4): p. 953-965.
104. Liu, F., et al., *Differential regulation of sphingosine-1-phosphate- and VEGF-induced endothelial cell chemotaxis. Involvement of G(ialpha2)-linked Rho kinase activity.* Am J Respir Cell Mol Biol, 2001. **24**(6): p. 711-9.
105. Favot, L., et al., *VEGF-induced HUVEC migration and proliferation are decreased by PDE2 and PDE4 inhibitors.* Thromb Haemost, 2003. **90**(2): p. 334-43.
106. Suehiro, J., et al., *Vascular endothelial growth factor activation of endothelial cells is mediated by early growth response-3.* Blood, 2010. **115**(12): p. 2520-32.
107. Boedtkjer, E., S. Kim, and C. Aalkjaer, *Endothelial alkalinisation inhibits gap junction communication and endothelium-derived hyperpolarisations in mouse mesenteric arteries.* J Physiol, 2013. **591**(Pt 6): p. 1447-61.
108. Ashikari-Hada, S., et al., *Heparin regulates vascular endothelial growth factor165-dependent mitogenic activity, tube formation, and its receptor phosphorylation of human endothelial cells. Comparison of the effects of heparin and modified heparins.* J Biol Chem, 2005. **280**(36): p. 31508-15.

109. Yu, L. and C.A. Hales, *Silencing of sodium-hydrogen exchanger 1 attenuates the proliferation, hypertrophy, and migration of pulmonary artery smooth muscle cells via E2F1.* Am J Respir Cell Mol Biol, 2011. **45**(5): p. 923-30.
110. Claesson-Welsh, L. and M. Welsh, *VEGFA and tumour angiogenesis.* J Intern Med, 2013. **273**(2): p. 114-27.
111. Pedersen, S.F., et al., *Regulation of mitogen-activated protein kinase pathways by the plasma membrane Na+/H+ exchanger, NHE1.* Arch Biochem Biophys, 2007. **462**(2): p. 195-201.
112. Wozniak, M.A. and C.S. Chen, *Mechanotransduction in development: a growing role for contractility.* Nat Rev Mol Cell Biol, 2009. **10**(1): p. 34-43.
113. Sin, W.C., et al., *Regulation of early neurite morphogenesis by the Na+/H+ exchanger NHE1.* J Neurosci, 2009. **29**(28): p. 8946-59.
114. Yonesu, K., et al., *Involvement of sphingosine-1-phosphate and S1P1 in angiogenesis: analyses using a new S1P1 antagonist of non-sphingosine-1-phosphate analog.* Biochem Pharmacol, 2009. **77**(6): p. 1011-20.
115. Igarashi, J., et al., *VEGF induces S1P1 receptors in endothelial cells: Implications for cross-talk between sphingolipid and growth factor receptors.* Proc Natl Acad Sci U S A, 2003. **100**(19): p. 10664-9.
116. Tominaga, T. and D.L. Barber, *Na–H Exchange Acts Downstream of RhoA to Regulate Integrin-induced Cell Adhesion and Spreading.* Molecular Biology of the Cell, 1998. **9**(8): p. 2287-2303.
117. Takuwa, Y., *Subtype-specific differential regulation of Rho family G proteins and cell migration by the Edg family sphingosine-1-phosphate receptors.* Biochim Biophys Acta, 2002. **1582**(1-3): p. 112-20.
118. Ryu, Y., et al., *Sphingosine-1-phosphate, a platelet-derived lysophospholipid mediator, negatively regulates cellular Rac activity and cell migration in vascular smooth muscle cells.* Circ Res, 2002. **90**(3): p. 325-32.
119. Stahmann, N., et al., *Activation of AMP-activated protein kinase by vascular endothelial growth factor mediates endothelial angiogenesis independently of nitric-oxide synthase.* J Biol Chem, 2010. **285**(14): p. 10638-52.
120. Gao, W., et al., *Inhibition of K562 leukemia angiogenesis and growth by selective Na+/H+ exchanger inhibitor cariporide through down-regulation of pro-angiogenesis factor VEGF.* Leuk Res, 2011. **35**(11): p. 1506-11.
121. Keith, B., R.S. Johnson, and M.C. Simon, *HIF1alpha and HIF2alpha: sibling rivalry in hypoxic tumour growth and progression.* Nat Rev Cancer, 2012. **12**(1): p. 9-22.
122. Chiang, Y., et al., *EGF upregulates Na+/H+ exchanger NHE1 by post-translational regulation that is important for cervical cancer cell invasiveness.* J Cell Physiol, 2008. **214**(3): p. 810-9.
123. Harguindey, S., et al., *Cariporide and other new and powerful NHE1 inhibitors as potentially selective anticancer drugs – an integral molecular/biochemical/metabolic/clinical approach after one hundred years of cancer research.* Journal of Translational Medicine, 2013. **11**: p. 282-282.
124. Shi, Y., et al., *The role of Na(+)/h (+) exchanger isoform 1 in inflammatory responses: maintaining H(+) homeostasis of immune cells.* Adv Exp Med Biol, 2013. **961**: p. 411-8.
125. Hayashi, H., et al., *Na+/H+ exchange and pH regulation in the control of neutrophil chemokinesis and chemotaxis.* Am J Physiol Cell Physiol, 2008. **294**(2): p. C526-34.
126. De Vito, P., *The sodium/hydrogen exchanger: a possible mediator of immunity.* Cell Immunol, 2006. **240**(2): p. 69-85.
127. Karmazyn, M., *NHE-1: still a viable therapeutic target.* J Mol Cell Cardiol, 2013. **61**: p. 77-82.

Nderim Kryeziu – Curriculum Vitae

E-mail	nderim_kryeziu@hotmail.com
Nationality	Kosovo
Date of birth	03.05.1987
Gender	Male

Education and training

Dates	10.2005 – 12.2011
	Master of Pharmacy, Pharmacy, University of Prishtina, Kosova
Dates	27.08.2011 – 29.09.2011
	Summer School of Molecular Medicine Friedrich Schiller University of Jena
Dates	01.09.2010 – 30.06.2011
	Pharmaceutical Sciences Exchange student at the University of Graz, Austria
	Erasmus Mundus External Cooperation Window – JoinEu-See Project scholarship
Dates	01.03.2010-30.06.2010
	Exchange student at the University of Graz, Austria
	Experience at the NMR laboratory, and German language courses
	CEEPUS scholarship
Dates	24.02.2009 – 20.09.2009
	Exchange student at the University of Zagreb, Croatia
	Pharmaceutical Sciences
	Erasmus Mundus External Cooperation Window – Basileus Project scholarship
Dates	01.09.2001-01.09.2005
	Diploma
	Pharmacy Technician
	Secondary Medical School, Prishtina, Kosova

Certificates and Awards

Distinguished student of the University of Prishtina, 2010
Interdisziplinäres Zentrum für Klinische Forschung (IZKF) scholar – University Clinic, Jena
Eberhard-Betz-Preis for the Best poster, 2015, German Atherosclerosis Society

Scientific publications

Characterization of coxcackievirus B3 replication in human umbilical vein endothelial cells
Distinguished student of the University of Prishtina, 2010
Kühn A. Rien C, Spengler K, Kryeziu N, Sauerbrei A, Heller R, Henke A
Med. Microbiol Immunol. 2015 Aug;203(4):217-29

Languages

Albanian (mother tongue), English, German, Serbo-croatian

Ehrenwörtliche Erklärung

Hiermit versichere ich,

(1) dass mir die Promotionsordnung der Fakultät bekannt ist,

(2) dass ich die vorliegende Dissertation selbständig angefertigt habe, und alle verwendeten Quellen, Hilfsmittel und persönlichen Informationen als solche gekennzeichnet habe,

(3) dass mich Prof. Dr. R. Heller sowie Prof. Dr. C. Hübner bei der Auswahl und Anfertigung des Materials sowie Manuskriptes unterstützt haben,

(4) dass ich weder die Hilfe eines Promotionsberaters in Anspruch genommen habe, noch andere Personen unmittelbare oder mittelbare geldwerte Leistungen von mir erhalten haben, die im Zusammenhang mit dem Inhalt der vorgelegten Dissertation stehen,

(5) dass ich die Dissertation noch nicht als Prüfungsarbeit für eine staatliche oder andere wissenschaftliche Prüfung eingereicht habe

(6) dass ich zu keinem Zeitpunkt die gleiche, eine in wesentlichen Teilen ähnliche oder eine andere Abhandlung als Dissertation an einer anderen Hochschule eingereicht habe.

Jena, Februar 2016